CHAPTER II NATURAL ENVIRONMENT

CHAPTER II NATURAL ENVIRONMENT

II-1 Geography of the Country

(1) General

The country of Chile stretches from north to south along the southwest coastal zone of the South American continent facing the Pacific Ocean. It encompasses an area of approx. 740 thousand sq. km from latitude 17°30'S to 55°59'S and from longitude 66°30'W to 75°40'W.[1] The country stretches approx. 4,300 km from north to south but only an average of 180 km from east to west.

This country is located on the Pacific Ocean side of the Andes Mountain Range that runs down the western side of the South American continent. About 600 thousand sq. km or 80% of the total land area of Chile is mountainous. Chile has a rich variety of land form owing to its geographic features. The Andes Mountain Range constitutes a belt of volcanic activity. Because of the tectonic plate of the Pacific slipping under the plate of the South American continent from the west, the country of Chile lies in an earthquake belt.

(2) Geography

The two main mountain ranges in Chile are the Andes (La Cordillera de los Andes) and the coastal mountain range (La Cordillera de Costa) running longitudinally from north to south through the country. These two mountain ranges divide the country into four distinctive geographical regions, the Andes Mountains, the Ceneral Basin, the Coastal Mountains and the Coastal Plain.

The Andes Mountain range runs along the western edge of the South American continent stretching over 8,500 km. Within Chilean territory, there are more than 20 high mountains ranging from 5,000 to 6,000 m in height in the northern and central sections of the country while the southern part of the country is characterized by lower mountains, 3,000 to 4,000 m in height. Moreover, the Chilian side of the Andes has at least 55 active volcanoes.

The Central Basin, a concave belt of land running north to south, is bounded on the east by the Andes and on the west by the Coastal Mountain range. The northern part of this zone is a desert belt that is famous for

---

1) Source: Republic of Chile ; Catin America Association Japan

the production of copper and Chilean saltpeter. On the other hand, the southern part is a fertile agricultural belt for production of crops and livestock. The majority of the country's population lives in the central zone of the country.

The Coastal Mountain range runs along the coast from about 20 km south of Arica city in the north to the Taitao Peninsula. The slightly round mountains are 1,000 to 2,000 m in height. This mountainous belt significantly effects on the weather of Chile.

The prominent feature of the Coastal Plain is the presence of large urban areas. Major Chilean ports are developed at places where the coastal plain is relatively wide. This can be seen at such cities as Antofagasta, La Serena, Valparaiso and Lota.

(3) Climate

The major factor of climate change in Chile is latitude with a variety of climates from north to south as follows:

① North Country: desert zone having little rainfall, extending from the Peruvian border to the latitude of 30° S.

② Central: area of mediterranean climate with a warm, dry summer season and rain falling mostly in the winter season.

③ South Country: mild climate area with heavy rainfall, forming a grassland belt

④ South Extremity: area of steppe or tundra climate having low temperatures and much rain.

The geography of the country plays an important role in determining the climate. This is manifested in two ways: (i) the mountainous terrain distributed over a wide area of the country limits the influence of the oceanic climate and (ii) the Andes act as a "weather screen" which protects the country except for the Patagonian region from the influence of continental climates.

1) Rainfall

There is a trend of a sharp increase in rainfall towards the south while, at the same latitude, rainfall is higher on the coastal side than on the Andes side. The desert region in the north of Chile is extremely dry with practically no rainfall. The south regions have much rainfall, and particularly the archipelago in southern Chile is an area of heavy rain.

2) Temperature

The annual mean temperature is rather uniform despite Chile being a long and narrow country stretching from north to south. The annual mean is 18.8°C at Arica and 5.8°C at Navari, for instance. In general, the inland areas exhibit a large difference between diurnal and nocturnal temperatures.

3) Winds

North of latitude 30°C, southerly winds including southwesterly and southeasterly winds are more frequent throughout the year. But in the coastal areas, both sea and land breezes play important roles in the local wind patterns. In the area from 35°S to 40°S, the dominant southerly winds withdraw in the winter season of June and July and northerly winds become predominant. South of 40°S, northwesterly winds prevail in the winter season from June to August, but westerly winds are most frequent during the rest of the year.

4) Fog and Visibility over the Sea

Fog at sea is most frequent in April and May between Lats. 30°S and 15°S. Fig. II-1-1 illustrates the average frequency of fog at sea (visibility less than 1,100 yards at sea) in the months of April and October. These months shows the highest and lowest frequency for the region.

(4) Currents and Tidal Streams

Near the Chilian coast from Isla Chiloé northward, the general trend of the Peru current is northerly along the coast. The strength of the Peru current does not vary appreciably throughout the year. The speed of the northerly current is from half a knot to three-quarters of a knot.

Along the greater part of the western coast of South America, which is fairly steep and free from major obstruction to the water flow, the tidal streams are weak, and in general, negligible compared with the currents previously described.

(5) Earthquake

The country lies in part of the eastern region of the Pan Pacific Earthquake Belt of volcanic activities. In Chile, 55 volcanoes are supposed to be active at present.

Since 1543, Chile has experienced some 15 thousand earthquakes. Althogh the majority of these were imperceptible, about 90 earthquakes of strong intensity have been recorded. In this century, 24 earthquakes have been recorded.

The secondary influences of earthquakes are the huge waves known as tsunami. One which brought large-scale devastation to the coast of Chile occurred on May 22, 1960, and destroyed all the ports between Conceptión and Aisén.

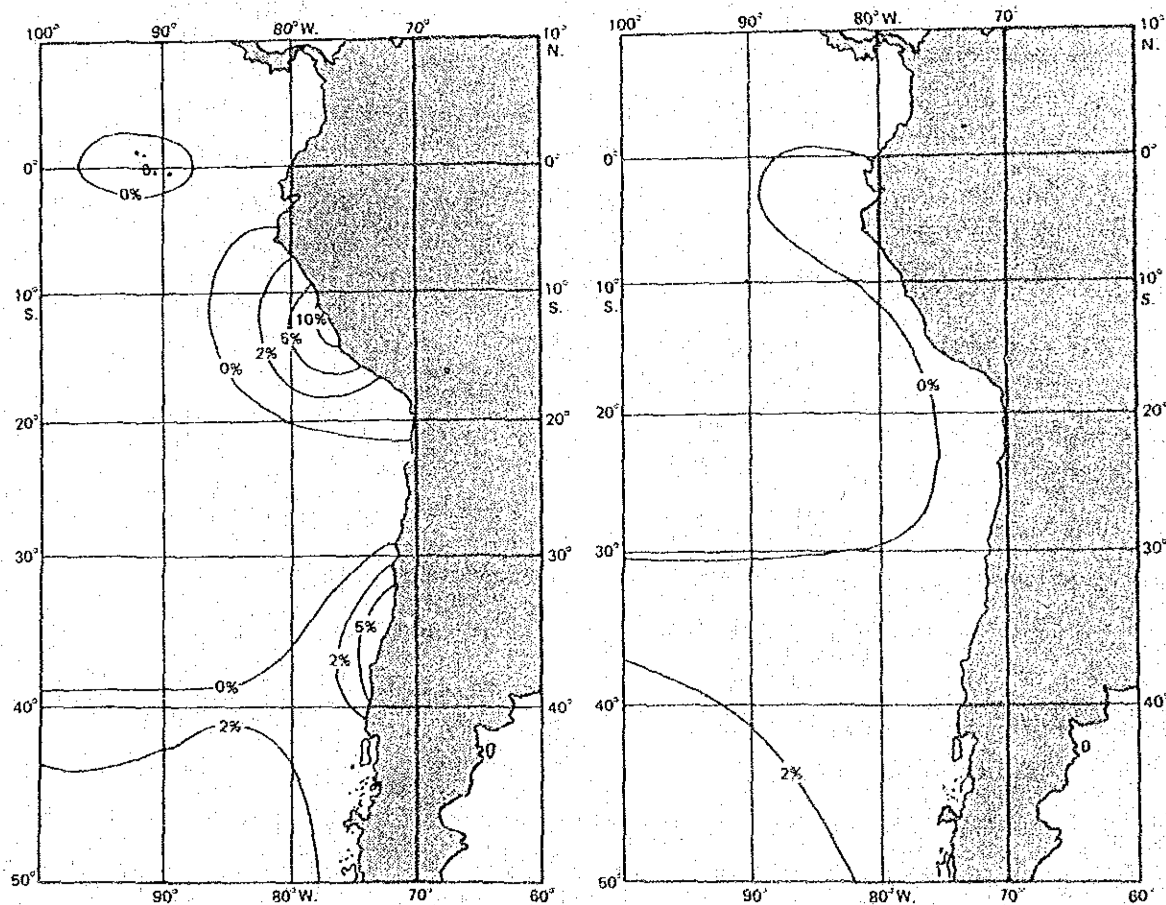

Percentage frequency of fog (1100 yards) – April

Percentage frequency of fog (1100 yards) – October

Source: South America Pilot

Fig. II-1-1 Frequency of Fog Occurrence

II-2 Natural Conditions Surrounding the Ports

(1) General

Existing data and information on the natural conditions surrounding the ports were collected by the JICA team. Also, the JICA study team carried out field surveys on topography, meteorological conditions, subsoil and geological profiles for the port areas. Table II-2-1 lists the items of the field survey works carried out by the team.

All the field works as well as laboratory tests on subsoil samples were entrusted to local firms under the supervision of the team specialists. The work schedule of the field surveys was determined under consultation with the JICA Technical Advisers together with the counterparts of the Ministry of Public Works of Chile. An outline of the field surveys is presented below.

① Topographic Survey

The topographic features of the ports of Valparaiso and San Antonio as well as the closely related back-of-port areas were surveyed by a plane survey based on existing geographic data and aerophotos. The results of the topographic survey are plotted on a map with a scale of 1 to 2,000.

② Current

The current observation was carried out with 25 hours of continuous readings using the current meter supplemented by float tracking conducted for 2 to 3 hours during flood and ebb tides. Within the harbour, two points and three points for the current reading and the float tracking, respectively, were observed at both ports.

③ Bathymetry

The bathymetry in the water area of the ports was checked using an echo sounder. The survey was conducted along the survey lines arranged for geological exploration adopting the continuous sonic profiling method.

④ Subsoil Investigation

The subsoil investigations on land and geological exploration in the water area using the continuous sonic profiling method were carried out as follows.

- 5 boring holes at the port of Valparaiso and 4 holes at San Antonio with standard penetration tests (SPT) and subsoil samplings
- laboratory tests on the subsoil samples taken from the bored holes
- P.S. prospecting using 3 bored holes at each port
- Geological exploration using a Geo-Soner 19CE (sparker type) along nine and six lines at the ports of Valparaiso and San Antonio respectively.

Table II-2-1 Field Investigation on Natural Conditions

Part \ Item	Investigation Item	Method	Port	
			Valparaiso	San Antonio
Natural Conditions I (Topographic and Meteorological Conditions)	1) Topography	° Plane Survey	150 ha	60 ha
	2) Current	° Float Tracking ° Current Observation	3 points/2 times 2 points/25 hours	3 points/2 times 2 points/25 hours
	3) Tide	° Data Collection	-	-
	4) Waves	° Data Collection and Hindcasting	-	-
	5) Meteorological Conditions	° Data Collection	-	-
	6) Bathymetry	° Echo Sounding	9 lines	6 lines
Natural Conditions II (Subsoil Conditions)	1) Soil Conditions	° Boring ° SPT ° PS Prospecting ° Laboratory test	5 points 59 points 3 points 22 samples	4 points 58 points 3 points 31 samples
	2) Geology	° Acoustic Profiling	9 lines	6 lines
Natural Conditions III (Present Condition of Port Facilities)	1) Underwater Inspection	° Visual Inspection ° Underwater photography ° Underwater measurement	10 berths	7 berths
	2) Port Facilities Inspection on land	° Quaywall ° Rail Condition ° Others	10 berths 10 berths	7 berths 7 berths
	3) Backfilled Condition	° Observation by excavation	1 point	1 point
	4) Deterioration of Concrete	° Core Sampling for testing ° Visual inspection	6 samples 10 berths	- 7 berths
	5) Inspection of steel Materials	° Sampling for tension test ° Paco Meter ° Visual Inspection	3 Samples	-

(2) The Port of Valparaiso

1) Topography

Fig. II-2-1 shows the port of Valparaiso developed at the southern tip of Valparaiso Bay between Punta Angeles and Punta Concón. The waterfront area of about 3 km from Punta Angels on the west to the Baron district on the east is used as the port area. The bay is widely open to the Pacific to the northwest along the 15 km coastline between Punta Angeles and Punta Concón. The Punta Angeles naturally shelters the port of Valparaiso from offshore waves except for northerly and north-westerly waves that are mostly predominant in the winter season.

Fig. II-2-2 is a topographic map prepared by the team through field surveys of the port area and its hinterland.

2) Seabed Topography

Fig. II-2-3 is a cross section of the seabed topography of Valparaiso Bay. The seabed features show a steep slope in the water depths between approx. 10 m to 30 m which then slopes gently offshore until it becomes almost flat at a water depth of around 40 m. The gradient of the slope is approximately 1:10 at the steepest and becomes 1:50 to 1:60 in the deeper water area. The existing berth no. 7 was constructed at an area of 35 m original water depth while the breakwater (Mole de Abrigo) upon the rock mound was placed in extremely deep water, 45 m in original depth.

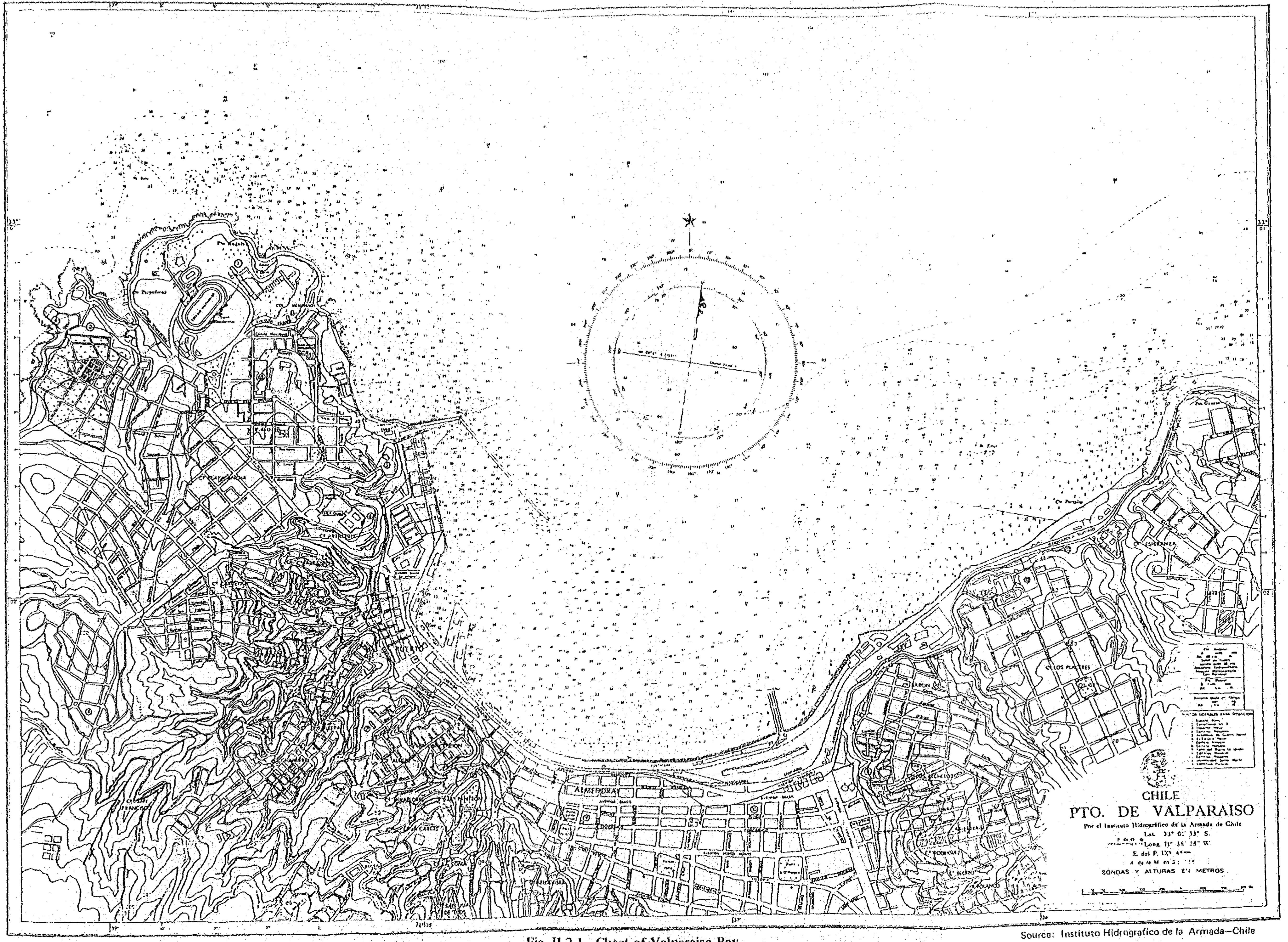

Source: Instituto Hidrografico de la Armada—Chile

Fig. II-2-1 Chart of Valparaiso Bay

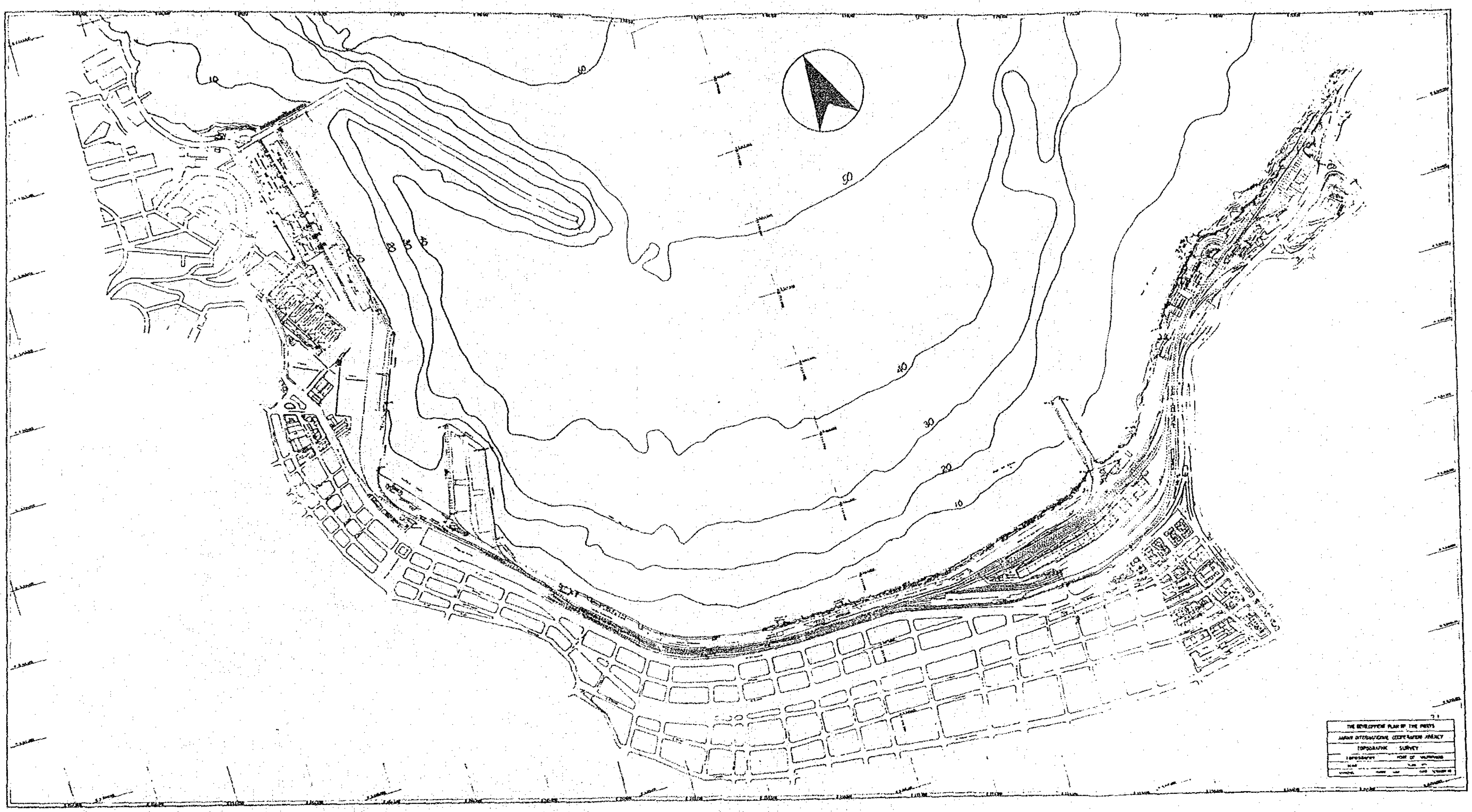

Fig. II-2-2 Topographic Survey Map of the Port of Valparaiso

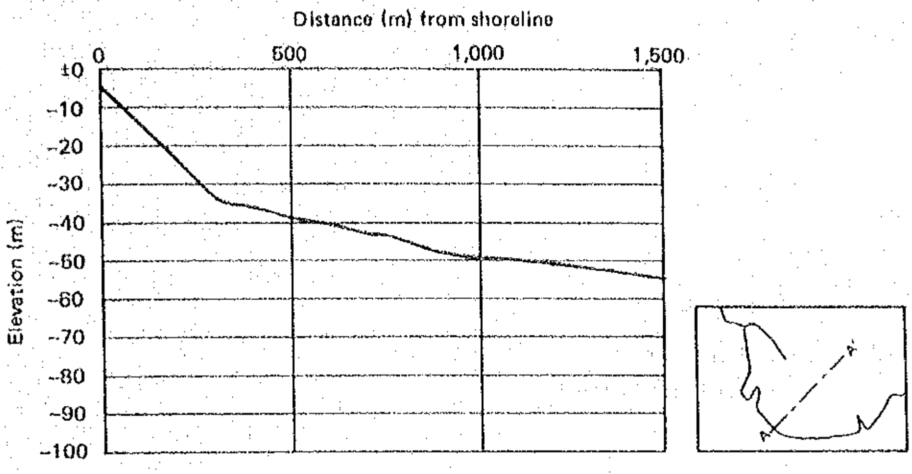

Cross Section A-A'

Fig. II-2-3 Seabed Cross Section at Valparaiso

3) Climate

(i) Temperature and Rainfall

The climate at Valparaiso is a warm, dry summer and a wet winter. Due to the influence of the Peru Current (cool), the annual mean temperature is 14.2°C while the annual mean maximum and minimum are 19.0°C and 10.6°C, respectively. The monthly mean temperature and rainfall are shown in Table II-2-2 and Fig. II-2-4.

The monthly mean temperatures are 11.8°C minimum and 18°C maximum, which gives a small annual difference of only 6.2°C. This is very different from those at Santiago where the monthly means are 20°C maximum and 8.1°C minimum with a difference of 11.9°C.

Valparaiso has a relatively large rainfall. The monthly mean rainfall is largest in June being 126.3 mm, but it drops to 1.2 mm in February. The total annual rainfall is 441.3 mm.

Table II-2-2 Monthly Temperature and Rainfall at Valparaiso

	Jan.	Feb.	Mar.	Apr.	May	Jun.	Jul.	Aug.	Sep.	Oct.	Nov.	Dec.
(°C) Max. Temperature	22.4	22.4	21.2	19.3	17.3	15.8	15.6	16.1	16.9	18.3	20.4	21.8
(°C) Mean Temperature	18.0	17.9	16.7	14.9	13.5	12.3	11.8	12.1	12.9	14.1	15.8	17.3
(°C) Min. Temperature	13.3	13.3	12.3	10.9	10.1	8.9	8.4	8.4	9.0	10.0	11.1	12.4
Rainfall (mm)	1.6	1.2	6.9	17.5	88.5	126.3	95.6	65.2	25.1	12.3	5.6	2.9

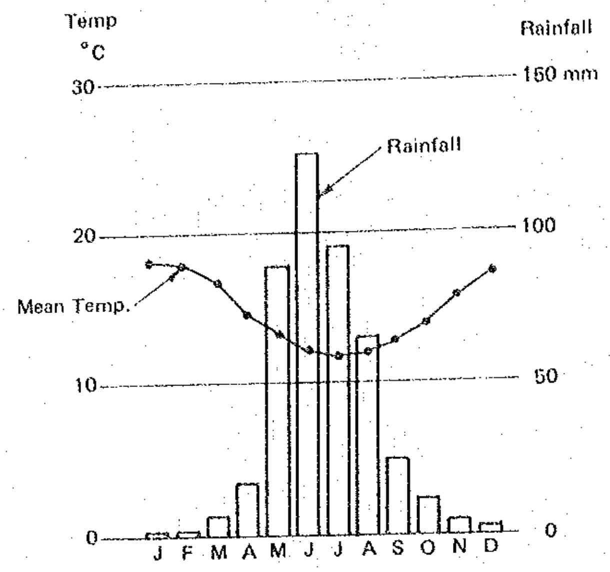

Fig. II-2-4 Mean Temperature and Rainfall at Valparaiso

Source: Instituto Hidrografico de la Armada-Chile

(ii) Winds

i) On-land Winds

The section of the Chilean coast in which Valparaiso is located is sandwiched between the South Pacific and the South Atlantic high pressure zones which causes pressure throughs to develop, resulting in the southwesterly winds which predominate throughout the year. Particularly in the summer season, the South Pacific high pressure zones generate in the further south and causes lower pressure zones on the South American continent. This pressure distribution gives rise to sea breezes and the relatively frequent occurrence of southwesterly winds.

Table II-2-3 (monthly frequency of wind directions) and Fig. II-2-5 (monthly wind roses) show the statistics on winds observed on-land at Valparaiso. As can be seen, winds from the southwest occur at a frequency of approx. 30% in May to August and 40 - 50% in other months. Winds from other directions occur mostly from May to July when the northerly and northeasterly winds are somewhat frequent. This is due to the more frequent passing of low-pressure troughs. The annual mean wind velocity is SW 3 (3.4 - 5.5 m/sec), but there is a fairly large daily variation due to the generation of sea

Table II-2-3 Wind Data at Valparaiso compiled from Observation Over 30 Years

Month	Percentage of Wind Direction (%)									Mean Wind Speed (Knots)			Max. Wind Speed (Knots)	Number of Days	
	N	NE	E	SE	S	SW	W	NW	Calm	12Z	18Z	24 Z		V ≤ 6	V ≥ 8
January	4	8	2	3	7	49	4	2	21	calm	S 16	SW 12	SW 40	2.7	0.4
February	3	6	3	4	8	46	4	2	24	calm	SW 16	SW 12	SW 40	2.3	0.2
March	4	5	4	5	7	39	4	2	30	calm	SW 18	SW 9	SW 34	1.7	0.2
April	4	6	6	6	7	39	7	1	24	calm	SW 11	SW 8	W 30 SW 30	0.4	0.2
May	13	8	7	8	5	30	2	1	26	calm	SW 10	SW 6	N 25 NE 25	0.4	0.2
June	11	12	9	15	9	23	2	1	18	SE 4	SW 11	SW 8	N 37	0.8	0.4
July	12	12	9	11	8	23	3	3	19	calm	SW 11	SW 8	S 37	0.3	0.2
August	7	8	7	12	9	34	5	2	16	calm	SW 13	SW 9	SW 38	0.8	0.1
September	7	7	5	8	9	40	3	2	19	calm	SW 15	SW 10	SW 39	1.3	0.0
October	5	8	5	5	7	47	3	2	18	SW 6	SW 18	SW 10	SW 44	2.0	0.1
November	6	4	4	3	6	55	3	2	17	SW 6	SW 18	SW 10	SW 44	4.5	0.6
December	4	5	4	3	9	54	3	2	16	calm SW 9	SW 19	SW 11	SW 44	3.7	1.0

Z: G.M.T, V = Beaufort Scale 6: (10.8 13.9 m/sec), The past Max. Record : Beaufort Scale 10 (24.5 285.m/sec)

8: (17.2 20.8 m/sec)

Source: Instituto Hidrografic de la Armada-Chile

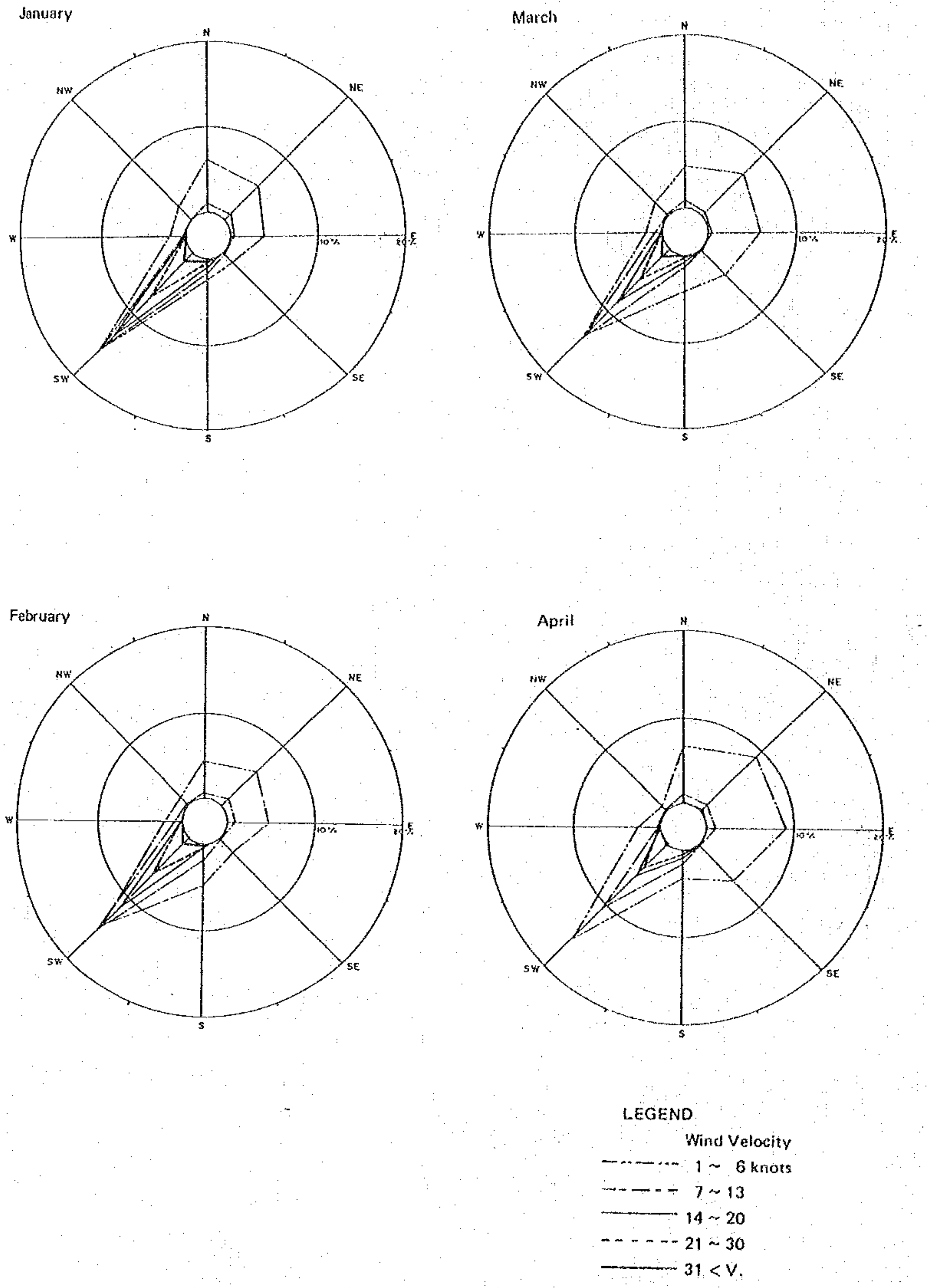

Fig. II-2-5 (1) Monthly Wind Rose of Valparaiso (1968 ~ 1982)

Source: Institute Hidrografico de la Armada – Chile.

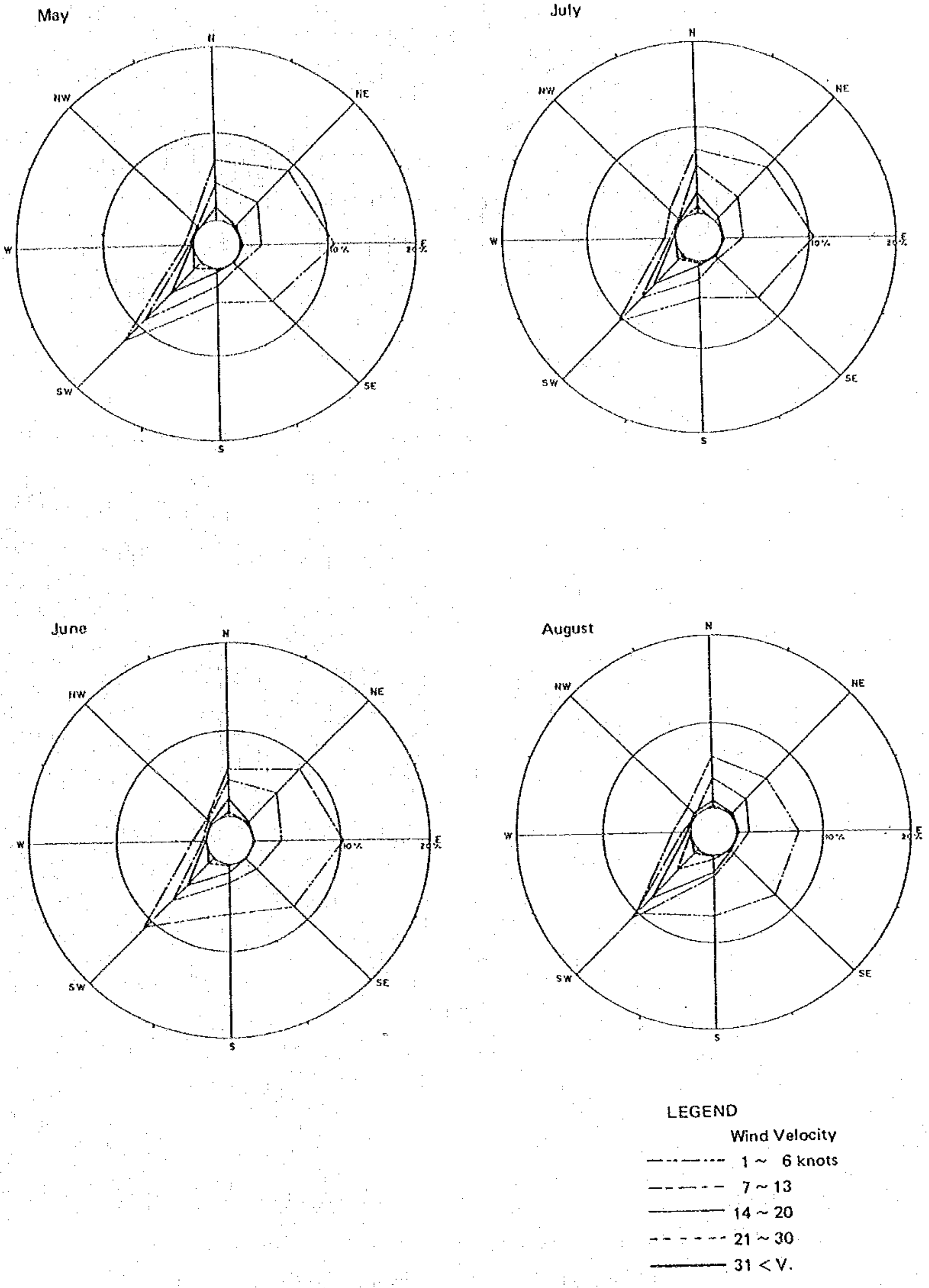

Fig. II-2-5 (2) Monthly Wind Rose of Valparaiso (1968 ~ 1982)

Source: Institute Hidrografico de la Armada – Chile.

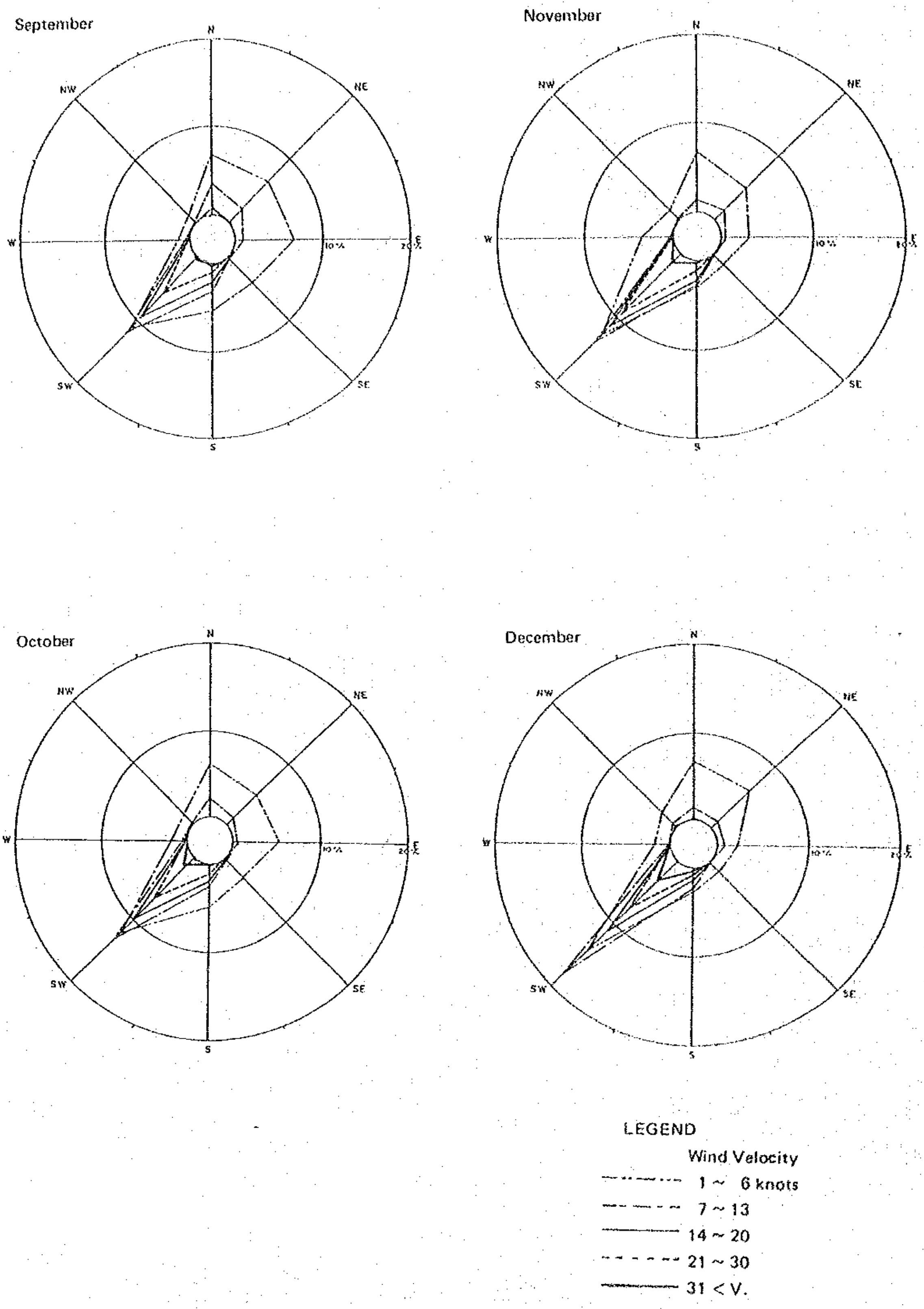

Fig. II-2-5 (3) Monthly Wind Rose of Valparaiso (1968 ~ 1982)

Source: Institute Hidrografico de la Armada – Chile.

breezes. The winds in the morning are weak but strengthen throughout the day to become about 5 - 6 m/sec in winter and 8 - 9m/sec in summer.

Mostly southwesterly winds prevail. The frequency of gales is remarkable in summer but rare in winter, and their direction is mainly southwest. Since strong gales are generated by the passing of extremely low-pressure troughs, the frequency of strong gales is relatively low. But, when they do occur, northerly or northwesterly winds become extremely strong.

Extremely low-pressure troughs generally occur from the end of autumn until the spring when the prevailing westerly surface winds move to the north and become stronger. Along with the eastward progression of these low-pressure troughs comes the northeasterly movement of cold fronts. When these cold fronts approach, strong winds from the north to northwest blow over the coastal region around Valparaiso. The southwesterly winds prevail generally after this cold front passes by. It is not unusual for these winds to blow for over 2,000 km.

It is also noted in Table II-2-3 that the maximum velocity winds usually come from the southwest, but they come from the north in May and June. The maximum wind velocity is SW 44 knots (22.6 m/sec) and N37 knots (19 m/sec).

ii) Winds over sea areas

The wind data observed at the lighthouse on the breakwater are available to study the wind patterns over the sea. The wind records of maximum monthly velocity for the period 1980 - 1983 are shown in Table II-2-4. Extremely high velocities of 70 - 80 knots have been recorded from the north to west. Although these winds last for only a short period of time during the approach of cold fronts, they are relatively strong compared with the southwesterly winds.

Moreover, southwesterly winds also blow due to pressure troughs which are easily formed along the coast of Chile and, therefore, strong southwesterly winds tend to develop frequently over the offshore area of the coast.

The winds that affect the port of Valparaiso are mostly south-

Table II-2-4 Wind Data at Breakwater of Valparaiso

EN EL FARO DUPHAT MOLO DE ABRIGO (VALPARAISO)

AÑO 1980

MES	DIA	DIREC.	FZA. NDS.	HORA
ENERO	NO SE HABIA	INSTALADO	ANEMOGRAFO EN	EL MOLO
FEBRERO	NO SE HABIA	INSTALADO	ANEMOGRAFO EN	EL MOLO
MARZO	NO SE HABIA	INSTALADO	ANEMOGRAFO EN	EL MOLO
ABRIL	10	NORTE	70/80 NDS.	0000/0600
MAYO	10	NORTE	20 NDS.	0300/0600
JUNIO	07	N/NE	20 NDS.	1200/1600
JULIO	23/18	N/NW	35 NDS.	1300/1500
AGOSTO	18	SURWESTE	20 NDS.	1300/1400
SEPT.	29	NORTE	38 NDS.	0600/0800
OCTUBRE	21	SW/SE	20 NDS.	1500/2030
NOVIEMBRE	22	SE	22 NDS.	1300/1600
DICIEMBRE	24	SW	30 NDS.	1700/2000

AÑO 1981

MES	DIA	DIREC.	FZA. NDS.	HORA
ENERO	20	SE.	18 NDS.	1400/1700
FEBRERO	FALLA EL	REGISTRADOR DE	INTENSIDAD DEL	VIENTO
MARZO	04	W/NW	35 NDS.	0800/2400
ABRIL	02	SE/S	24 NDS.	1500/1800
MAYO	11	W	30 NDS.	0900/1600
JUNIO	20	W	18 NDS.	0700/1100
JULIO	13	W	18 NDS.	1500/1800
AGOSTO	22	NW	15 NDS.	1100/1500
SEPT.	14	SE	20 NDS.	1300/1400
OCTUBRE	11	SE	24 NDS.	1400/1600
NOVIEMBRE	29	SW	20 NDS.	1400/1800
DICIEMBRE	23	SW	16 NDS.	1000/1300

AÑO 1982

MES	DIA	DIREC.	FZA. NDS.	HORA
ENERO	20	NE/N	20 NDS.	1300/1600
FEBRERO	02	NE	20 NDS.	1400/1700
MARZO	16	NE/E	16 NDS.	1300/1400
APRIL	SE CORTAN LOS CABLES DE ALIMENTACION			
MAYO	SIGE MALA LA LINEA DE ALIMENTACION DEL FARO			
JUNIO	SE CAMBIA LA LINEA DE ALIMENTACION COMPLETA			
JULIO	23	E.	20 NDS.	1500/1900
AGOSTO	12	W.	80 NDS.	0300/0345
SEPT.	13 CORTAN LOS CABLES DE CHILECTRA ALIMENTACION			
OCTUBRE	23	SW	18 NDS	1200/1400
NOVIEMBRE	26	NW	19 NDS.	0900/2000
DICIEMBRE	19	SW	20 NDS.	1000/1200

AÑO 1983

MES	DIA	DIREC.	FZA NDS.	HORA
ENERO	13	SW	20 NDS.	1600/1800
FEBRERO	18	NW	18 NDS.	1400/1700
MARZO	17	W/SW	14 NDS.	1100/1400
ABRIL	28	S/SW	16 NDS.	1500/1600
MAYO	18/19	W.	30 NDS.	1500/2000
MAYO	19	W.	30 NDS.	0200/0400
JUNIO	20	NORTE	60 NDS.	1000/1400
JULIO	06	NW	60 NDS.	1500/1900
AGOSTO	10	NW	30 NDS.	0400/0800
AGOSTO	12	NW	30 NDS.	1000/1200
SEPT.	25	W/NW	18 NDS.	1100/1700
OCTUBRE	-	-	-	-
NOVIEMBRE	-	-	-	-
DICIEMBRE	-	-	-	-

Source: Instituto Hidrografico de la Armada-Chile westerly, but strong winds from the north to northwest are the most important in formation of extremely high waves.

iii) Fog

At Valparaiso, fog days with visibility less than 1100 yds are most frequent (about 6 days per month) in April and May and least frequent (between 1 and 2 days) in November and December. Table II-2-5 summarizes the frequency of fog at the port of Valparaiso.

Table II-2-5 Average Frequency of Fog (Number of Days) at Valparaiso

Month	Jan.	Feb.	Mar.	Apr.	May	Jun.	July	Aug.	Sep.	Oct.	Nov.	Dec.	Total
No. of days with visibility less than 1100 yds	2	3	4	6	6	4	2	2	3	3	1	1	37

Source: South America Pilot

4) Sea Conditions

(i) Offshore Waves

i) Wave Data

Table II-2-6 summarizes the wave data for a 19 year period recorded offshore of Valparaiso where the water depth is approximately 100 m. The frequency of northwesterly waves is less than the actual frequency due to the effects of Punta Craumilla and Punta Angeles. Waves up to 1.5 m high constitute 81% of all waves and waves of a 4.0 - 16.0 second period comprise 85.1%. Although wave periods are widely distributed, they are centered in the range of 8.0 - 10.0 sec.

The offshore high waves which affect the port of Valparaiso are principally generated by the northerly to northwesterly winds due to the shelter of Punta Angeles.

ii) Hindcasting of Offshore Waves

The maximum offshore waves at the port of Valparaiso are hindcast using the relationship between the fetch and continuation time of wind blow by Wilson's diagram for the period from 1980 to 1983

Table II-2-6 Deep Water Wave Distribution at the Port of Valparaiso

Wave Height (m) / Wave Period (Sec)	0.0 ~ 0.5	0.5 ~ 1.0	1.0 ~ 1.5	1.5 ~ 2.0	2.0 ~ 2.5	2.5 ~ 3.0	3.0 ~ 3.5	3.5 ~ 4.0	4.0 ~ 4.5	4.5 ~ 5.0	5.0 ~ 5.5	5.5 ~ 6.0	6.0 ~ 6.5	6.5 ~ 7.0	7.0 ~ 7.5	7.5 ~ 8.0	8.0 ~ 8.5	8.5 ~ 9.0	Total	Percentage to Total (%)
0.0 ~ 2.0	152	145	96	29	16	6	2	0	0	0	0	0	0	0	0	0	0	-	446	0.8
2.0 ~ 4.0	892	1063	581	240	111	41	16	7	7	1	0	0	1	0	0	0	0	-	2960	5.4
4.0 ~ 6.0	1727	2444	1439	581	252	116	48	17	11	4	1	0	0	0	0	0	0	-	6642	12.2
6.0 ~ 8.0	2306	3345	1912	905	366	163	72	31	9	4	1	0	0	0	0	0	0	-	9122	17.0
8.0 ~ 10.0	2236	3354	2105	1032	428	184	69	29	16	6	2	1	1	0	0	0	0	-	9463	17.3
10.0 ~ 12.0	1994	3012	1969	978	397	167	80	37	16	7	1	2	0	3	1	0	1	-	8665	15.9
12.0 ~ 14.0	1621	2528	1645	888	424	201	73	34	14	0	3	1	1	0	0	0	0	-	7439	13.6
14.0 ~ 16.0	1148	1625	1172	647	291	133	62	21	7	6	4	1	1	0	0	0	0	-	5118	9.4
16.0 ~ 18.0	657	954	686	413	175	88	28	11	9	6	3	0	1	0	0	0	0	-	3031	5.6
18.0 ~ 20.0	268	389	276	169	78	24	23	7	2	1	0	0	0	0	0	0	0	-	1237	2.3
20.0 ~ 22.0	81	121	82	38	20	13	7	5	1	2	0	0	0	0	0	0	0	-	370	0.4
22.0 ~ 24.0	18	32	18	9	6	2	0	1	0	0	0	0	0	0	0	0	0	-	86	0.08
24.0 ~ 26.0	4	5	2	2	1	0	1	0	0	0	0	0	0	0	0	0	0	-	15	0.015
26.0 ~ 28.0	0	0	0	0	0	0	0	0	0	0	0	0	0	0	0	0	0	-	0	0
28.0 ~ 30.0	2	0	0	0	0	0	0	0	0	0	0	0	0	0	0	0	0	-	2	0.005
Total	13106	19025	11983	5931	2565	1138	480	201	92	43	16	6	5	3	1	0	1	-	54596	100
Percent to Total (%)	24.0	34.8	21.9	10.9	4.7	2.1	0.9	0.3	0.17	0.08	0.03	0.04	0.04	0.02	0.01	0	0.01	-	100	

Source: Instituto Hidrografico de la Armada-Chile based on Table II-2-4.

Based on Table II-2-6, the maximum wave height with respect of the return period is determined on Gumbel extreme probalility paper as shown in Fig. II-2-6. It is shown that waves of 9.2 m in height may occur once in 50 years. The wave period of the maximum wave can be considered to be 11.0 sec. from the wind data at Valparaiso. The design waves for the port facilities at Valparaiso are governed by those from the north to north-northwest. The waves are refracted and diffracted as they approach the shore. Fig. II-2-7 indicates the wave refraction and diffraction in the case of norhterly and north-northwesterly waves of 11.0 sec. period.

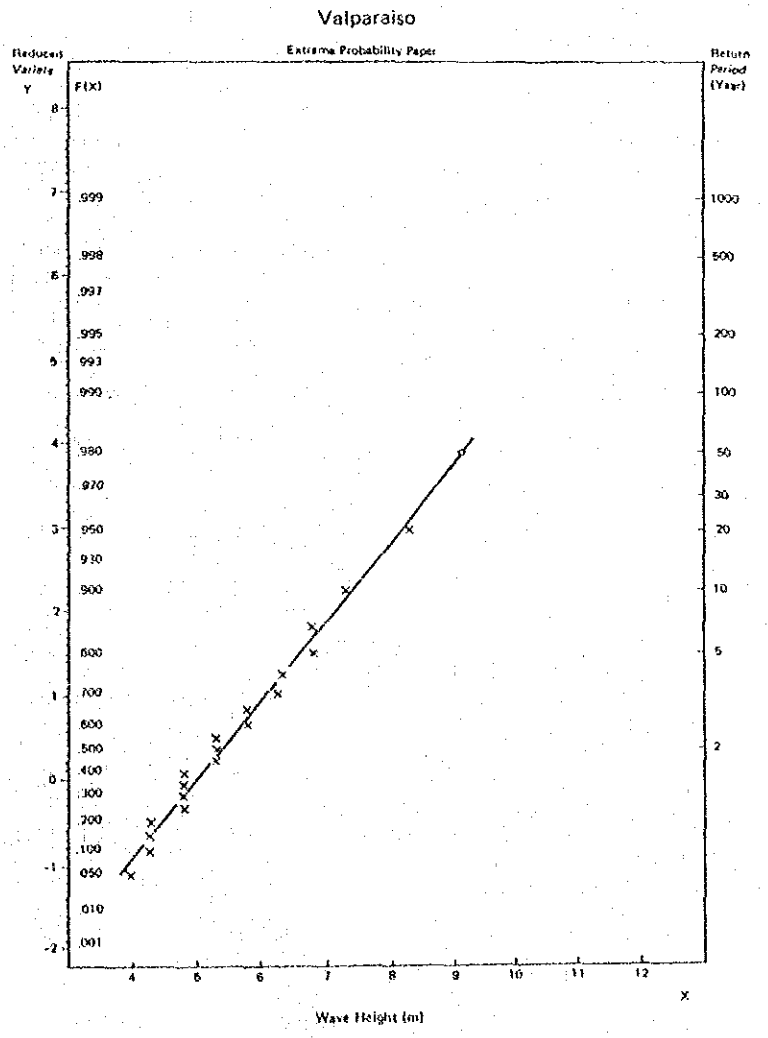

Fig. II-2-6 Max. Wave Height and Return Period at Valparaiso

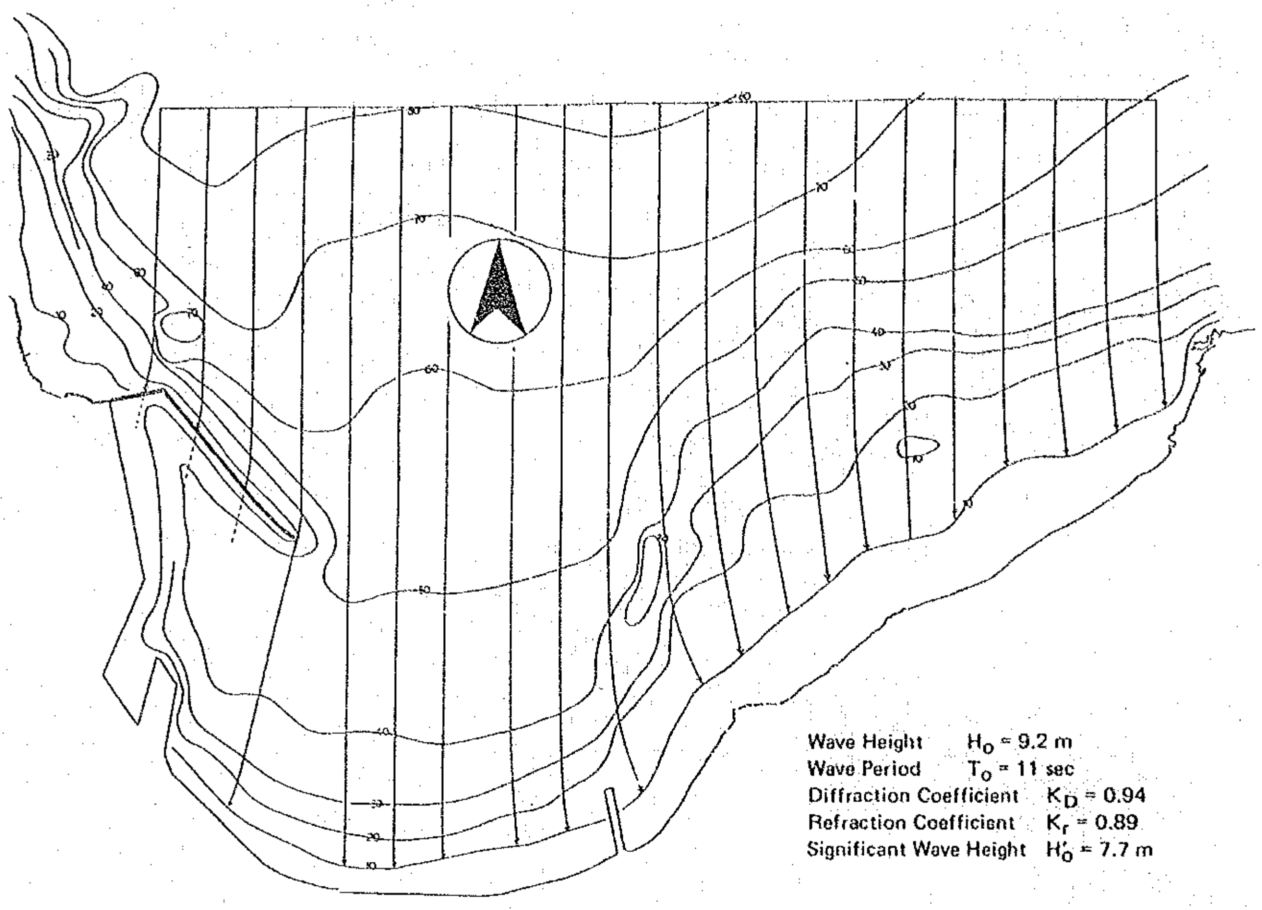

(1) North T = 11 sec

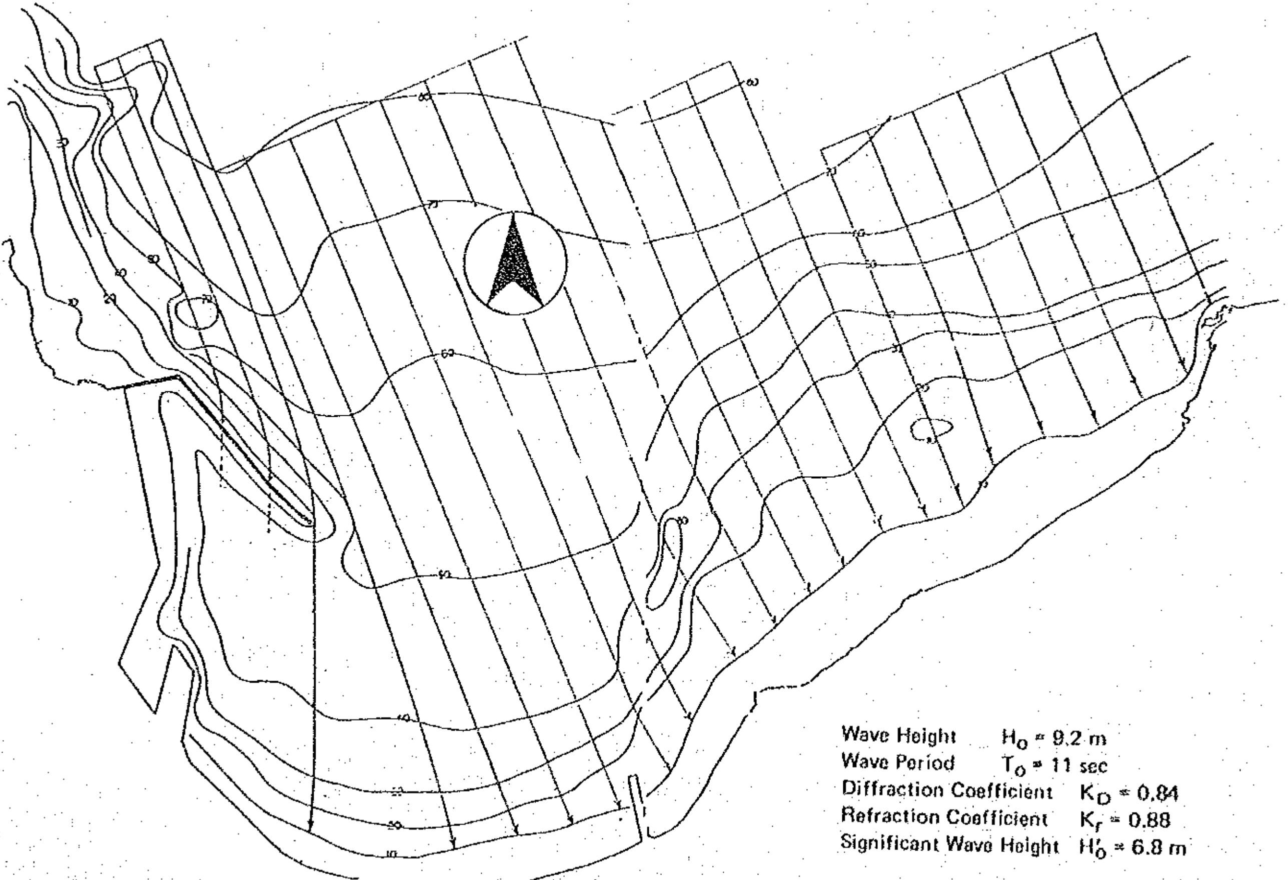

(2) N.N.W. T = 11 sec

Fig. II-2-7 Wave Refraction and Diffraction Diagram at Valparaiso

(ii) Tide Levels

The datum and tide levels for the port are summarized as follows based on the Tide Table.1)

- Highest High Water (recorded in 1958 at Valparaiso)	+ 2.07 m
- Mean High Water	+ 1.90
- Mean Water	+ 0.91
- Mean Low Water	+ 0.15
- Lowest Low Water (port datum of tide table)	+ 0.00

(iii) Current

Accodingly to available data, the current movements outside the port area vary in direction by location and time but are generally in line with the shoreline at a velocity of 0.10 - 0.25 knots, although they are largely related to waves, tides, winds and offshore currents.

Fig. II-2-8 shows the current observation carried out at two locations for the current meter survey and three locations for the float tracking during the 27th to 29th October, 1985. The observation was made during the spring tides of the port. The observation by current meter with automatic recorder was performed in two layers near the water surface and the sea bottom for a period of 25 hours continuously.

Fig. II-2-9 show northerly and easterly velocity components of the current observed at 3 m water depth at station 1 and 3 respectively. The westerly and southerly components are dominant during flood tide while the easterly and northerly components are stronger during ebb tide. The current is not so strong, being 23 cm/s (0.45 knots) and 15 cm/s (0.29 knots) maximum, at location 1 and 3 respectively. The surface flows are stronger in the port area as compared with those near the sea bottom.

On the other hand, the results of the current observation by float tracking show that northeasterly current at a velocity of 0.11 - 0.34 knots is remarkable at station 1 during ebb tide while

---

1) Source: Insititute Hidrografico de la Armada-Chile, Tables de Mareas de la Costa de Chile 1985

stations 2 and 3 show a trend of northerly to easterly current at a velocity of approx. 0.10 - 0.30 knots. The difference with the results by current meter observation may be due to the stronger effects of diurnal winds and waves which generally intensify the float movement toward the shore.

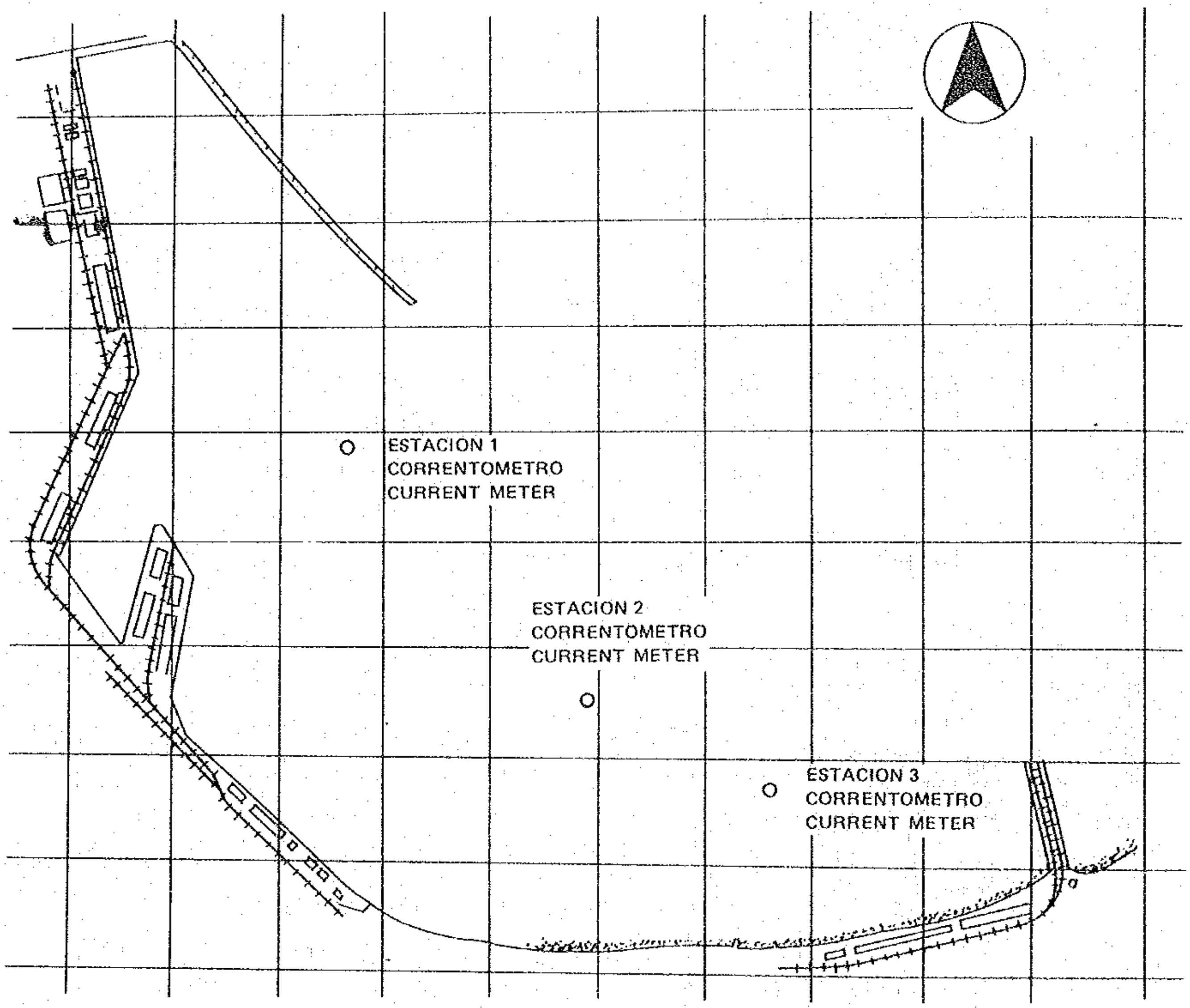

Fig. II-2-8 Location of Current Observation at Valparaiso

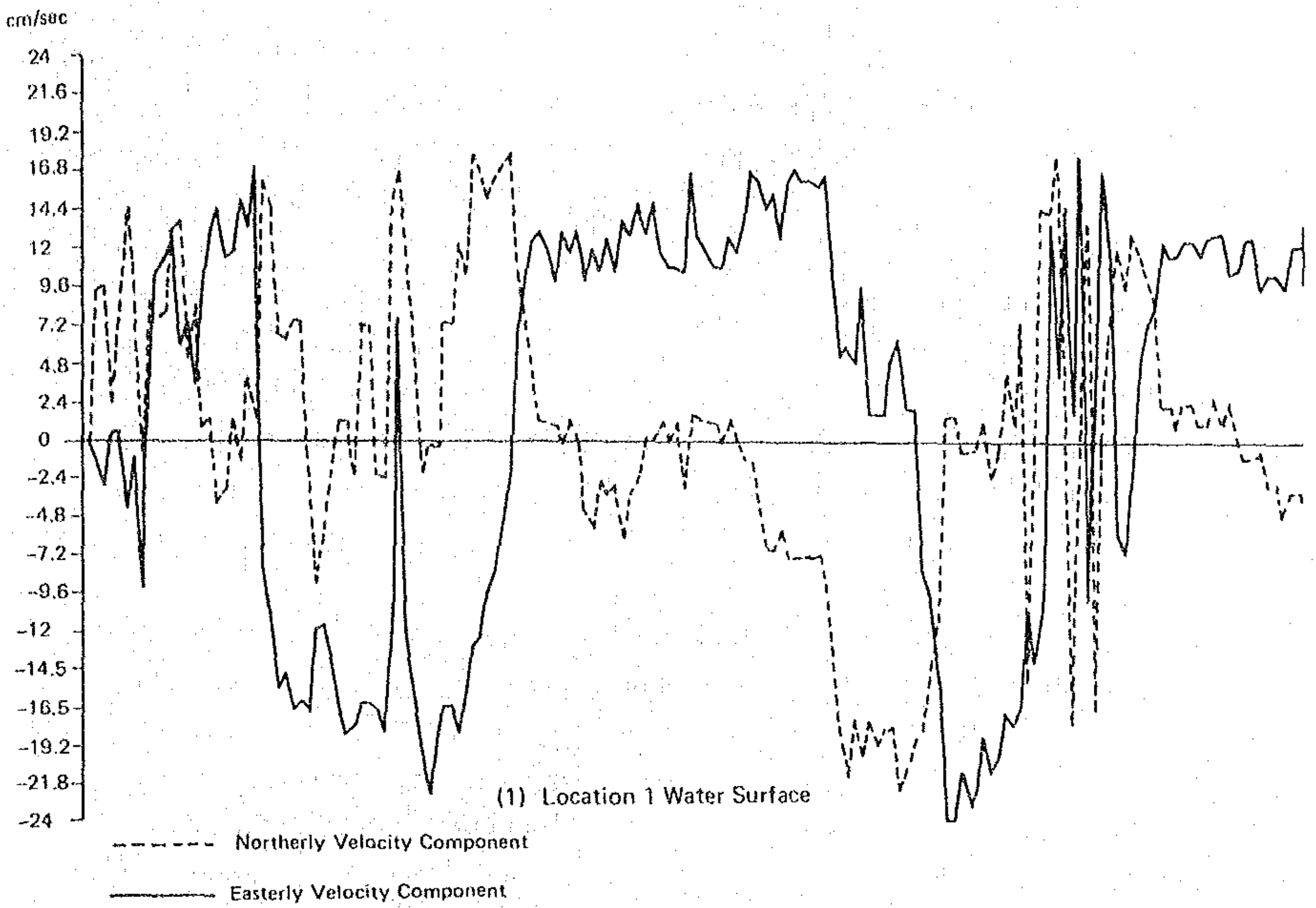

(1) Location 1 Water Surface

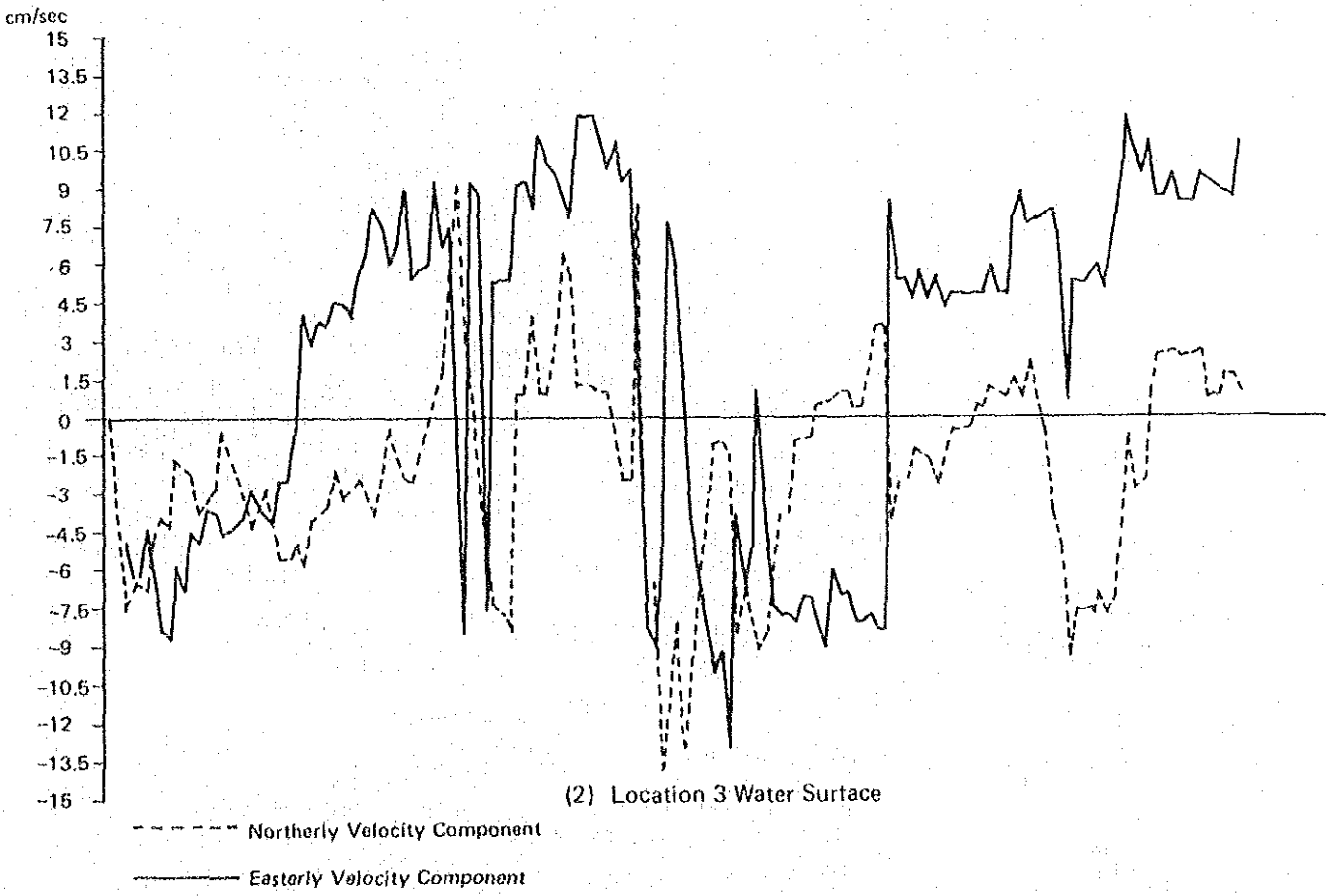

(2) Location 3 Water Surface

Fig. II-2-9 Nortnerly and Easterly Current Velocity Component at Valparaiso

5) Geological and Subsoil Conditions

(i) Geological Features Surrounding the Port

Fig. II-2-10 is a geological map of the Valparaiso zone. Valpariso and its adjacent area is generally characterized by topographic features that indicate a typical regressive coast. The remarkable geological features are the marine abrasion terrace and its sediments, the cliff and the deep valley. The cliff along the coastline is partly interrupted by the marine deposits forming sand beaches. The present coastal area of Valparaiso city and most of the valley behind the urban area is developed upon marine sand deposits and artificial fill. These marine deposits are supposed to be the sediments of the quarternary to the present. The coastal deposits at Valparaiso city are embraced by the lamellar amphibole of the Precambrian. In the western zone of Valparaiso, granitic graise of the Precambrian and granite of biotite of the Paleozoic are widely extended up to the Marga-Marga fault running northwesterly to Vinã-del-mar which is developed upon marine and fluvial sand deposits.

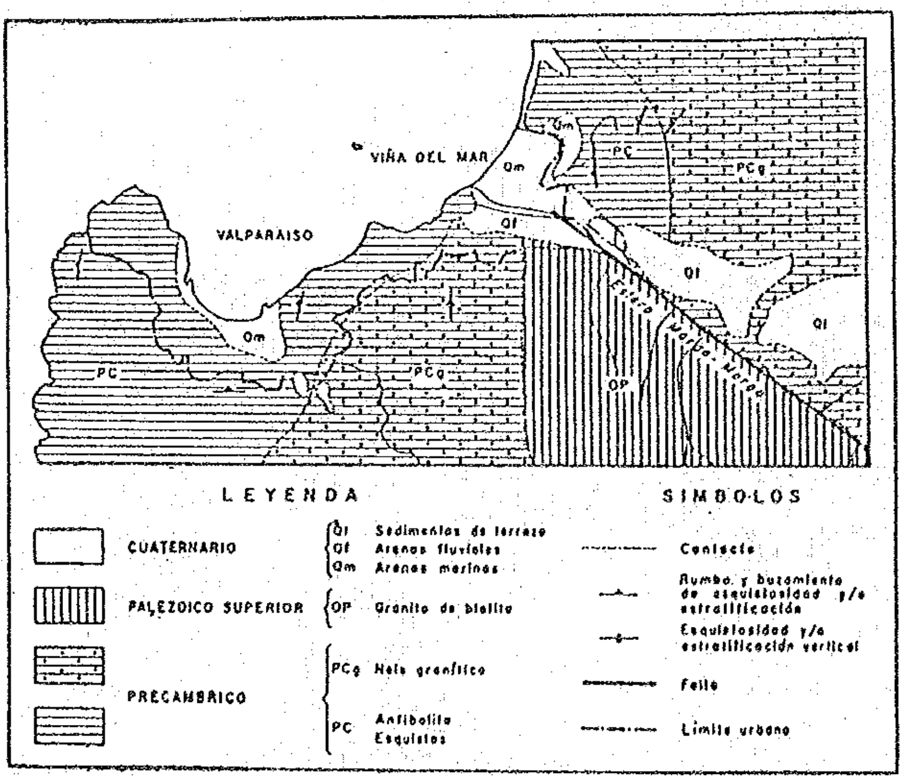

Fig. II-2-10 Geological Map at Valparaiso

Source: Instituto de Investigaciones Geológicas, Edades Radiométricas de rocas Intrusivas y Metamórficas de la Hoja Valparaiso – San Antonio (Boletín Nº 28)

(ii) *Geological and Subsoil Conditions of the Port*

Our boring works with SPT and soil sampling were executed at five locations on land, principally up to the depth of 25m. The onland boring works were supplemented by a geological exploration on the water area of the port adopting the continuous sonic profiling method. The locations of the investigation are shown in Fig. II-2-11.

Geological formations in the port are of Valparaiso are generally classified into the following three major strata.

Table II-2-7 Geology in the Port of Valparaiso

Symbol	Geological Period		Subsoil Classification	Description
S_1	Quarternary	Recent Stage	Sandy or Silty Soil	4-15m depth soft silty deposit or medium dense sands, marine formation and artificial filling
S_2		Pleistocene Stage	Sand or Gravel	7-20m depth very dense deposit, sediments from the terraces by marine formation
B	Precambrian		Rock	Lamellar amphibole produced by local metamorphism from andesite lava

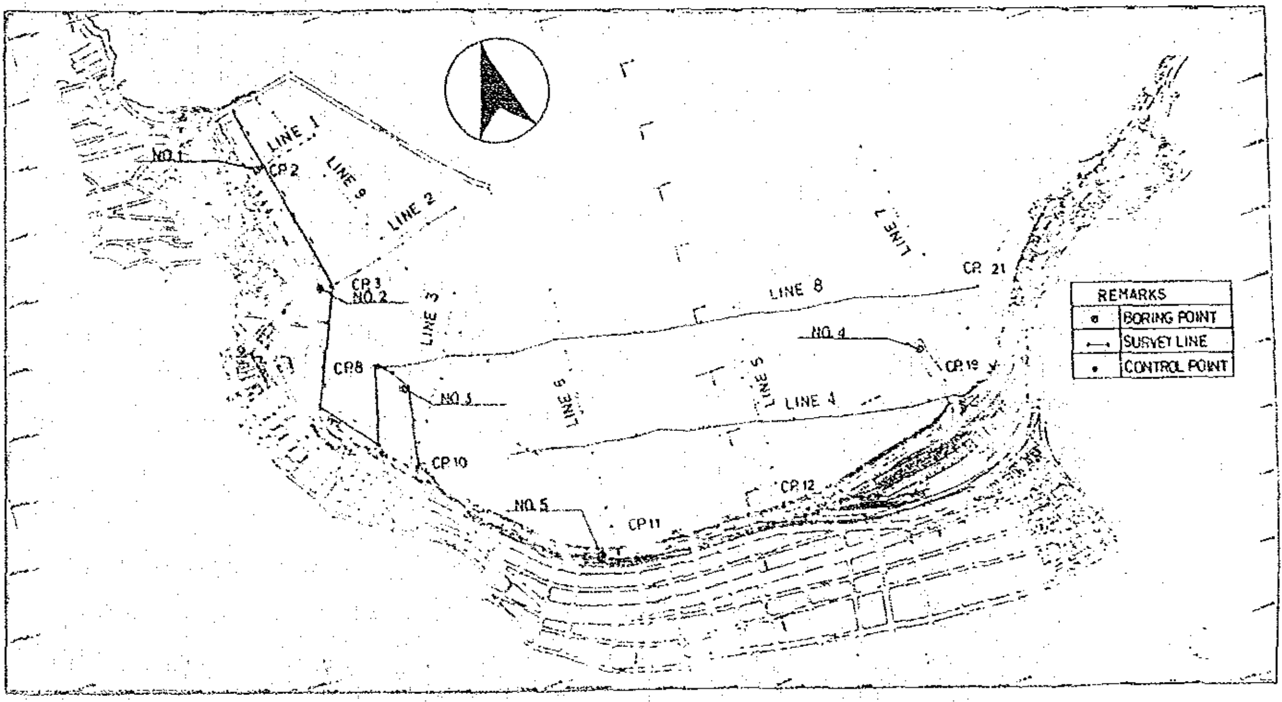

Fig. II-2-11 Location of Soil Investigation at the Port of Valparaiso

The subsurface layer (S_1) is almost uniformly distributed over the whole area of the port. The layer deposits at the water area of the port are around 5 m deep, but near the shoreline become thicker up to 10 m deep in front of berths nos. 1 to 3 and the Baron pier. Basically, this layer is medium dense fine sand of more or less 20 N-value in SPT.

But, at the area around Baron pier, the layer (S_1) is classified into very soft silty soils of about 5 m depth as shown in the boring log of hole no.4. Fig. II-2-12 shows the subsoil profile obtained through our boring works supplemented with those carried out by Direccion de Obras Portuarias, Ministerio de Obras Publicas. Soft subsurface clays of considerable thickness are observed in the water area between berths 4 to 6.

The sand formation of artificial fill is located in the subsurface layer (S_1) at the land area. Sand or gravel deposits (S_2) exist under the subsurface layer (S_1) in a thickness of 7 - 20 m, although its lower boundary with the rock formation (B) is not so clearly indicated by the recorded geo-sonar profiles.

The layer(S_2) shows a high degree of hardness being not less than 40 in N-value of SPT and is technically regarded to be a reliable bearing stratum for port facilities. This layer is deeper at offshore areas, but is found at the depth of -10 m at berths Nos. 1 to 3 (Br. 1 and 2), -8.5 m at Br. 5 and -20.0 m at the water area of the Baron pier (Br. 4).

By boring works, the base rock formation (B) is found at -16 m (Br. 1) and -17 m (Br. 2). This base rock may be distributed over the offshore area of the port in a steep slope of 1/10 to 1/20 towards the offshore, although it is not clearly indicated in the offshore area partly due to the weak reflection pattern showed in the recorded profiles.

Fig. II-2-13 shows the geological profile of the port area by section along the investigated lines for the continuous sonic profiling. The boring logs with the results of the laboratory tests on subsoil samples and PS prospecting at boreholes Nos. 1 to 3 are also shown in Fig. II-2-14.

Disturbed backfilled sands taken from boreholes Nos. 1 and 2 were used to the cyclic triaxial tests of which results are shown in Table II-2-8.

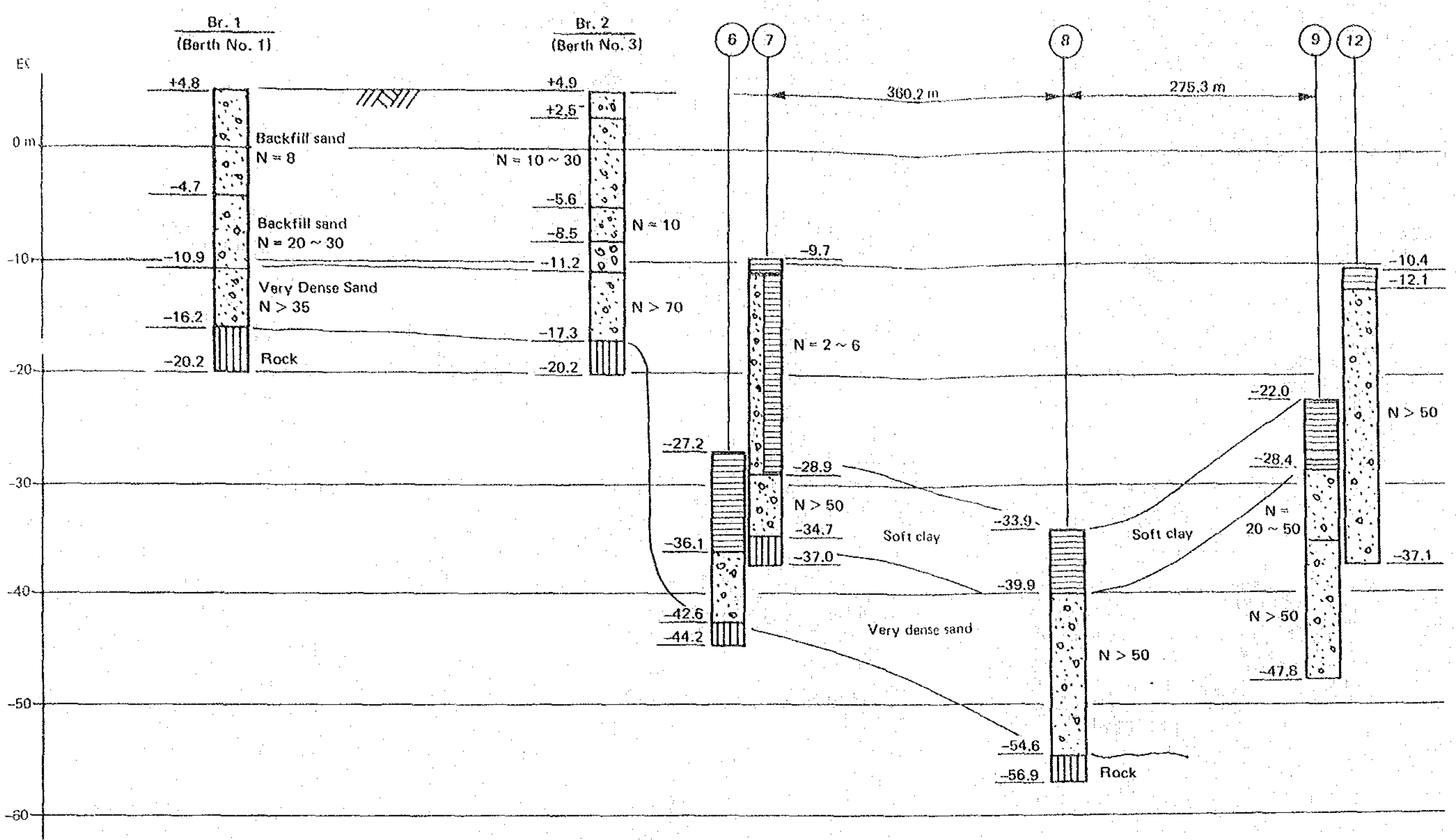

SECTION A-A

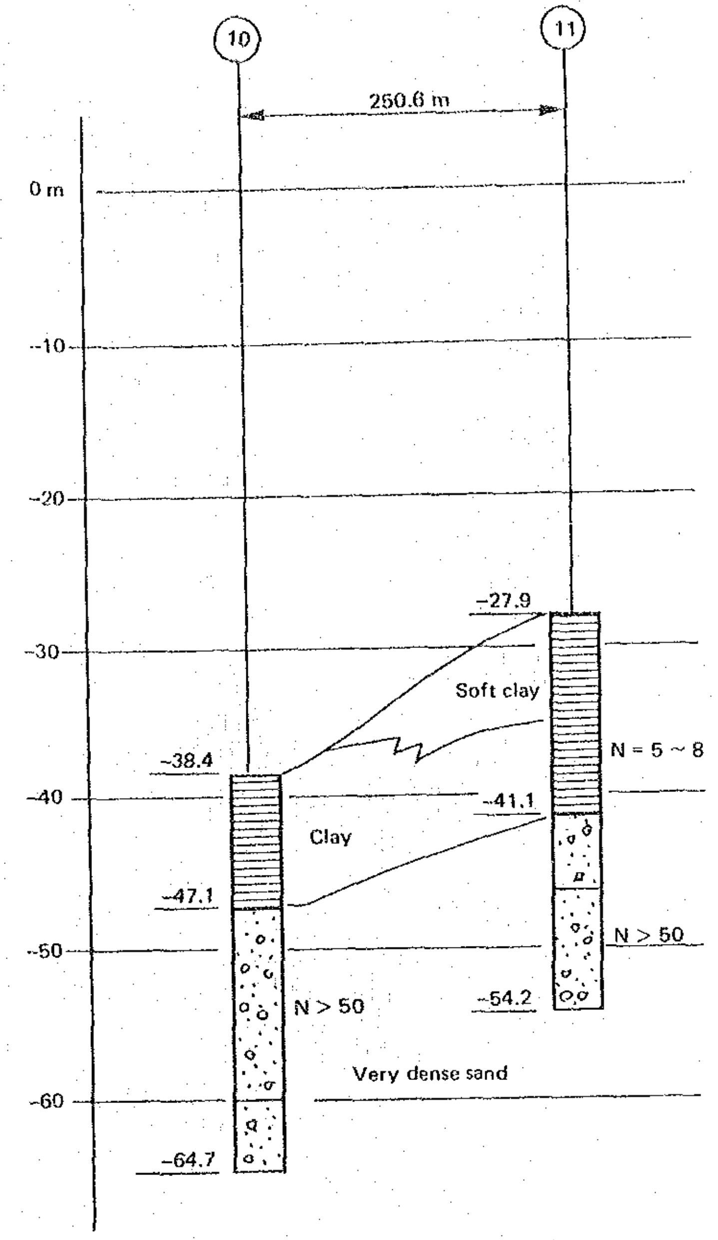

SECTION B-B

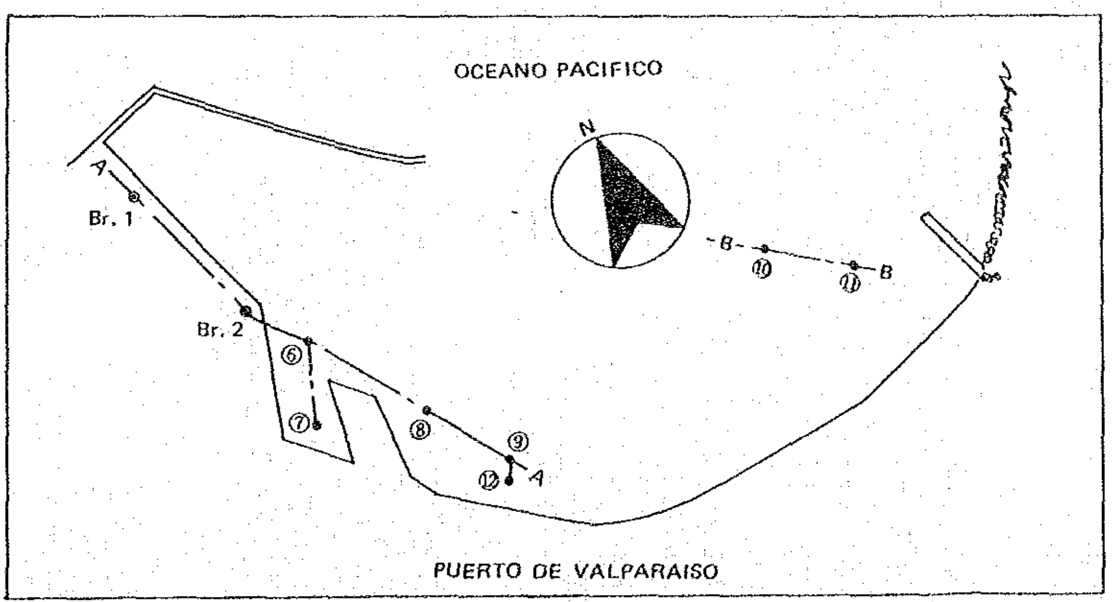

Location Map of Borings

Source: Our Boring Works supplemented with data from the report of "Proyecto Reparacion y Peposicion, Puerto de Valparaiso – VI Parte Sondeos Geotecnicos"; Direccion de Obras Portuarias, Ministerio de Obras Publicas, Julio – 1986

Fig. II-2-12 Subsoil Profiles at the Port of Valparaiso

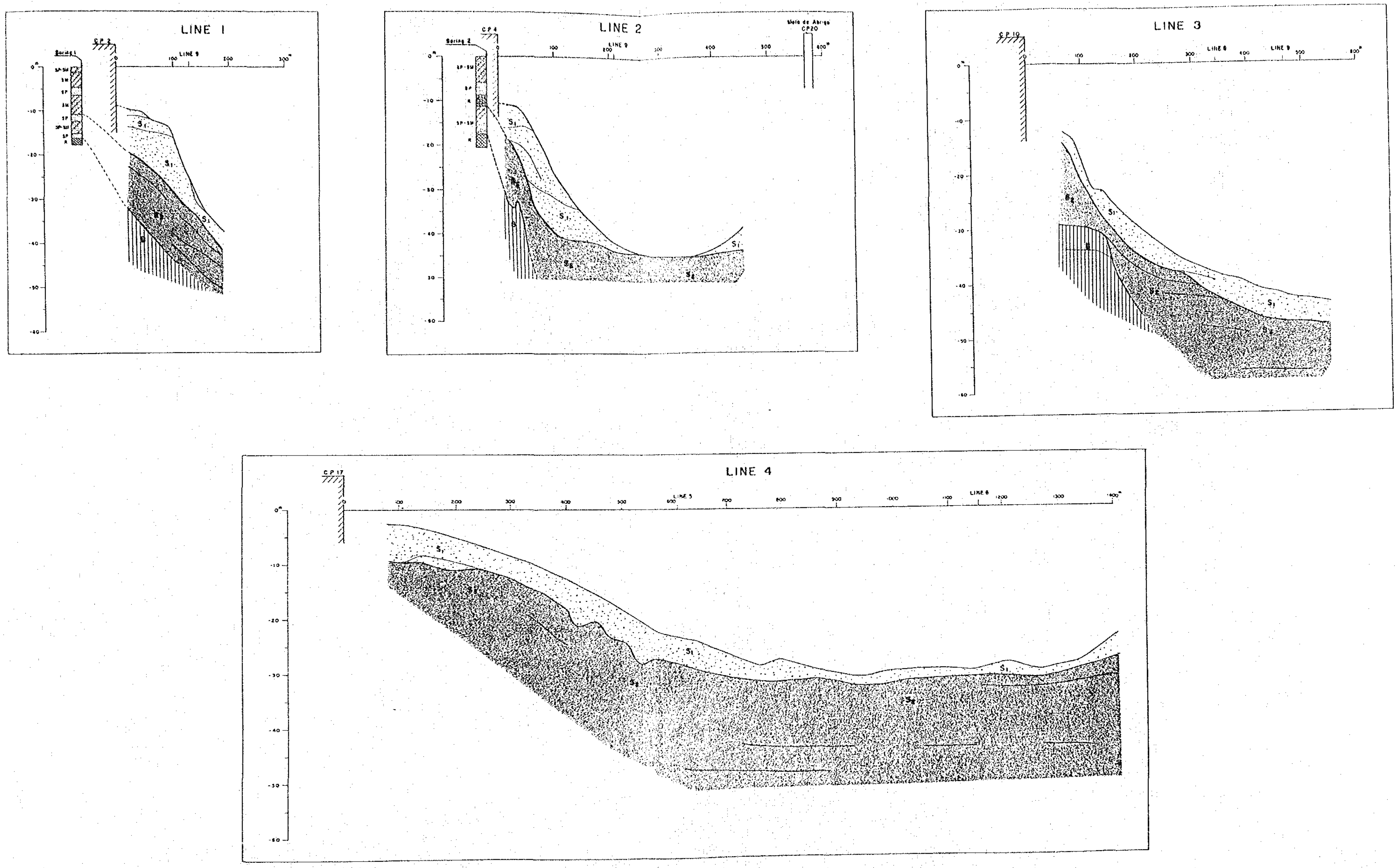

Fig. II-2-13 (1)   Cross Section of Geological Profiles in the Port Area of Valparaiso

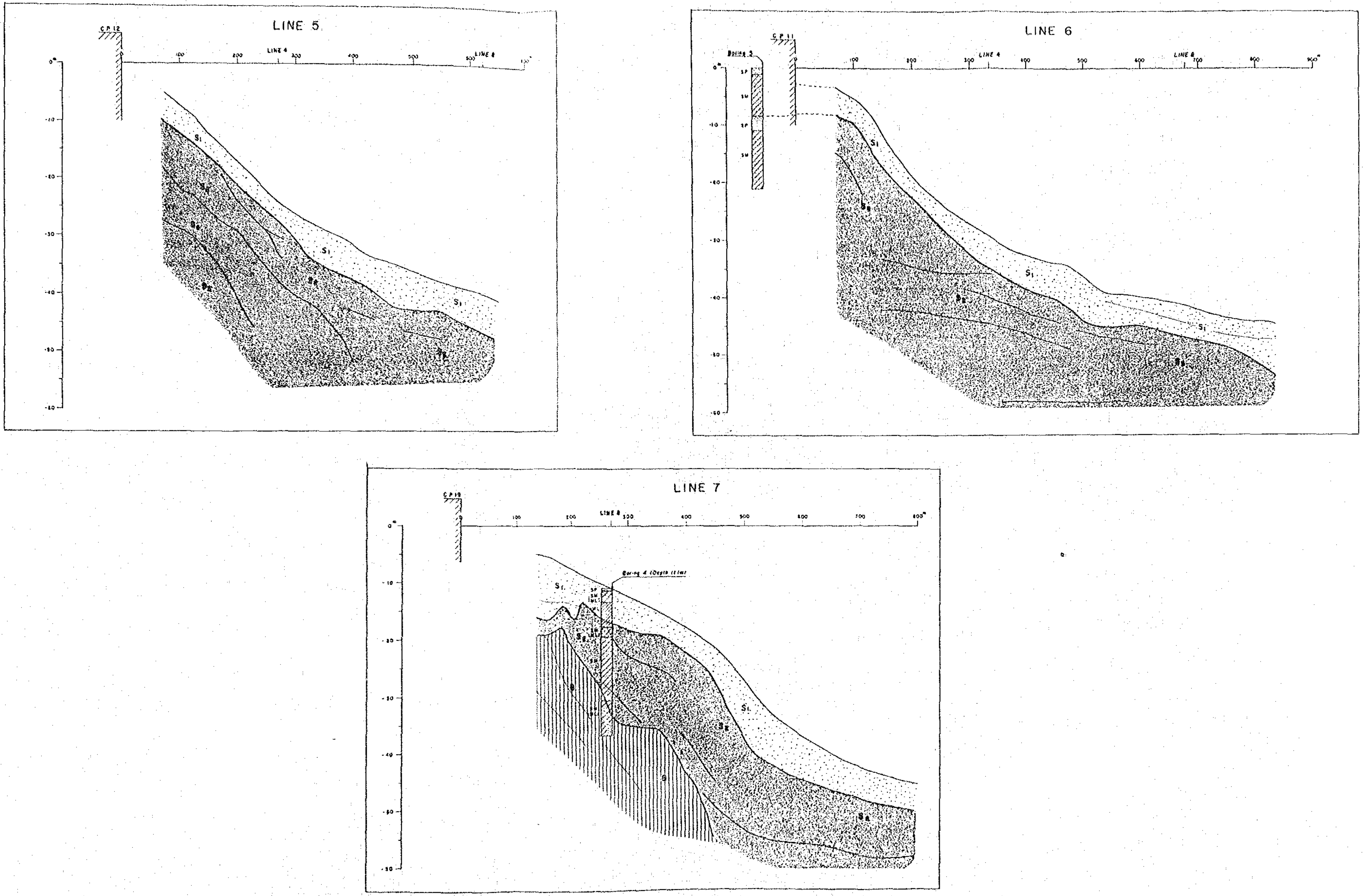

Fig. II-2-13 (2) Cross Section of Geological Profiles in the Port Area of Valparaiso

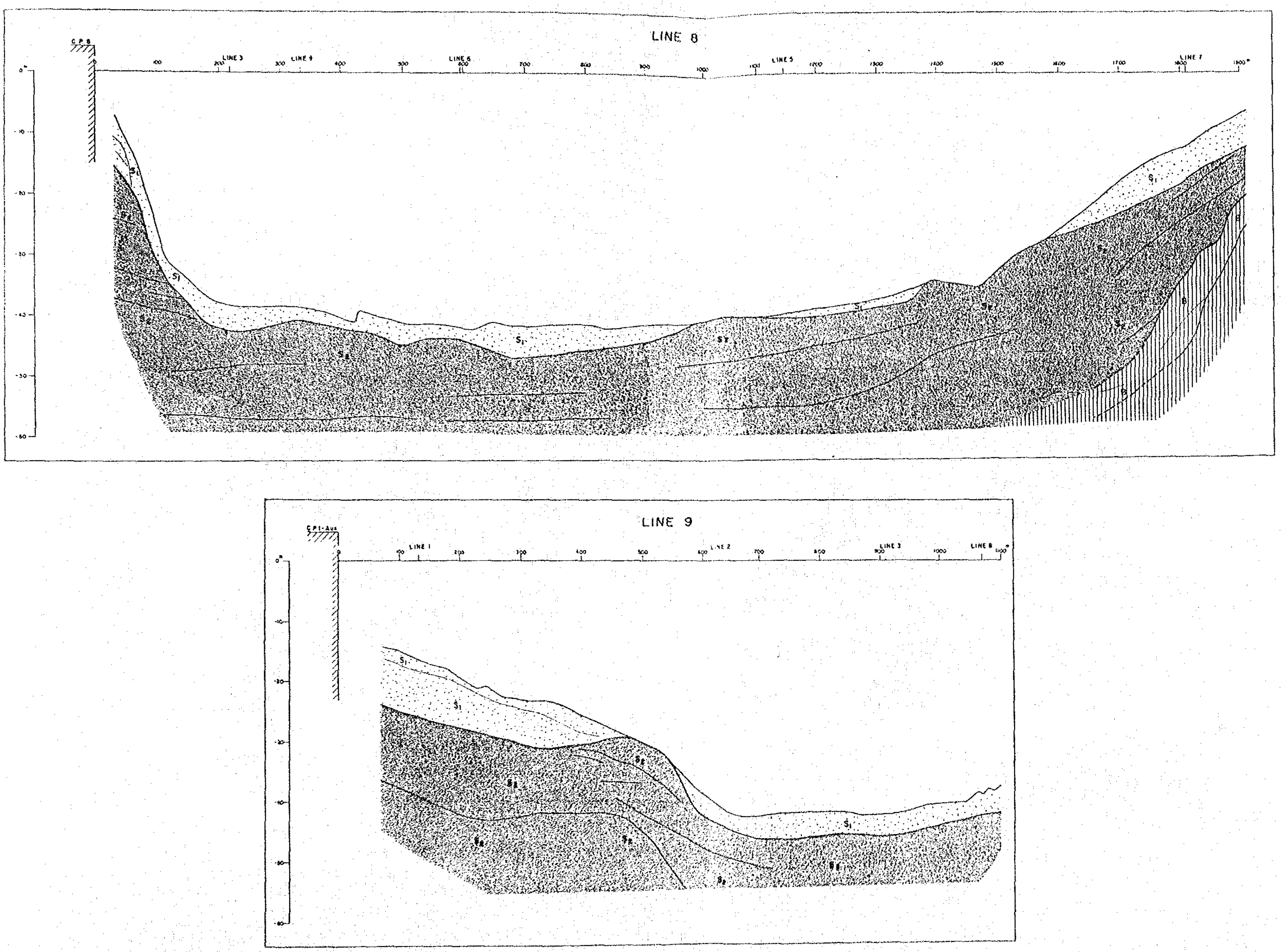

Fig. II-2-13 (3) Cross Section of Geological Profiles in the Port Area of Valparaiso

Valparaiso: Boring No. 1

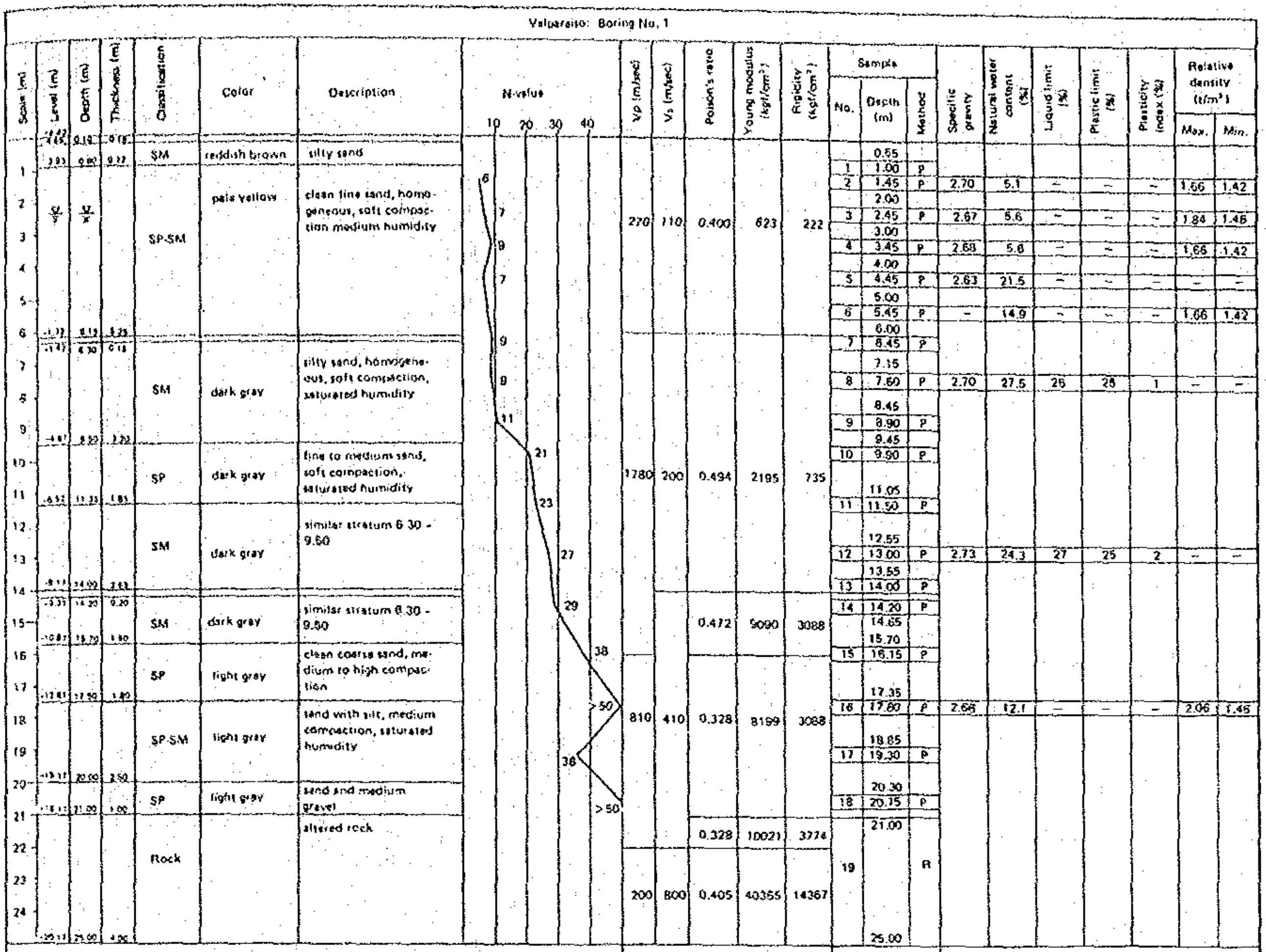

Level (m)	Depth (m)	Thickness (m)	Classification	Color	Description
4.65	0.18	0.18			
3.93	0.90	0.72	SM	reddish brown	silty sand
-1.32	6.15	5.25	SP-SM	pale yellow	clean fine sand, homogeneous, soft compaction medium humidity
-1.47	6.30	0.15			
-4.67	9.50	3.20	SM	dark gray	silty sand, homogeneous, soft compaction, saturated humidity
-6.52	11.35	1.85	SP	dark gray	fine to medium sand, soft compaction, saturated humidity
-9.17	14.00	2.65	SM	dark gray	similar stratum 6.30 - 9.60
-9.37	14.20	0.20			
-10.87	15.70	1.50	SM	dark gray	similar stratum 6.30 - 9.60
-12.67	17.50	1.80	SP	light gray	clean coarse sand, medium to high compaction
-15.17	20.00	2.50	SP-SM	light gray	sand with silt, medium compaction, saturated humidity
-16.17	21.00	1.00	SP	light gray	sand and medium gravel
-20.17	25.00	4.00	Rock		altered rock

Vp (m/sec)	Vs (m/sec)	Poison's ratio	Young modulus (kgf/cm²)	Rigidity (kgf/cm²)
270	110	0.400	623	222
1780	200	0.494	2195	735
		0.472	9090	3088
810	410	0.328	8199	3088
		0.328	10021	3774
200	800	0.405	40355	14367

Sample No.	Sample Depth (m)	Sample Method	Specific gravity	Natural water content (%)	Liquid limit (%)	Plastic limit (%)	Plasticity index (%)	Relative density (t/m³) Max.	Relative density (t/m³) Min.
	0.55								
1	1.00	P							
2	1.45	P	2.70	5.1	–	–	–	1.66	1.42
	2.00								
3	2.45	P	2.67	5.6	–	–	–	1.84	1.46
	3.00								
4	3.45	P	2.68	5.8	–	–	–	1.66	1.42
	4.00								
5	4.45	P	2.63	21.5	–	–	–	–	–
	5.00								
6	5.45	P	–	14.9	–	–	–	1.66	1.42
	6.00								
7	6.45	P							
	7.15								
8	7.60	P	2.70	27.5	26	25	1	–	–
	8.45								
9	8.90	P							
	9.45								
10	9.90	P							
	11.05								
11	11.50	P							
	12.55								
12	13.00	P	2.73	24.3	27	25	2	–	–
	13.55								
13	14.00	P							
14	14.20	P							
	14.65								
	15.70								
15	16.15	P							
	17.35								
16	17.80	P	2.66	12.1	–	–	–	2.06	1.46
	18.85								
17	19.30	P							
	20.30								
18	20.75	P							
	21.00								
19		R							
	25.00								

Note:

0.00 ~ 0.18	:	cement soil base
0.18 ~ 0.90	:	medium compaction, medium humidity
6.15 ~ 6.30	:	clean coarse sand, pale yellow, soft compaction, saturated
14.00 ~ 14.20	:	lens of transition materials, clean medium gravel

P. sand ...... 1.8 g/cm³
natural rock ...... 2.2 g/cm³

P: SPT
R: Rock

Fig. II-2-14 (1) Boring Log at the Port of Valparaiso

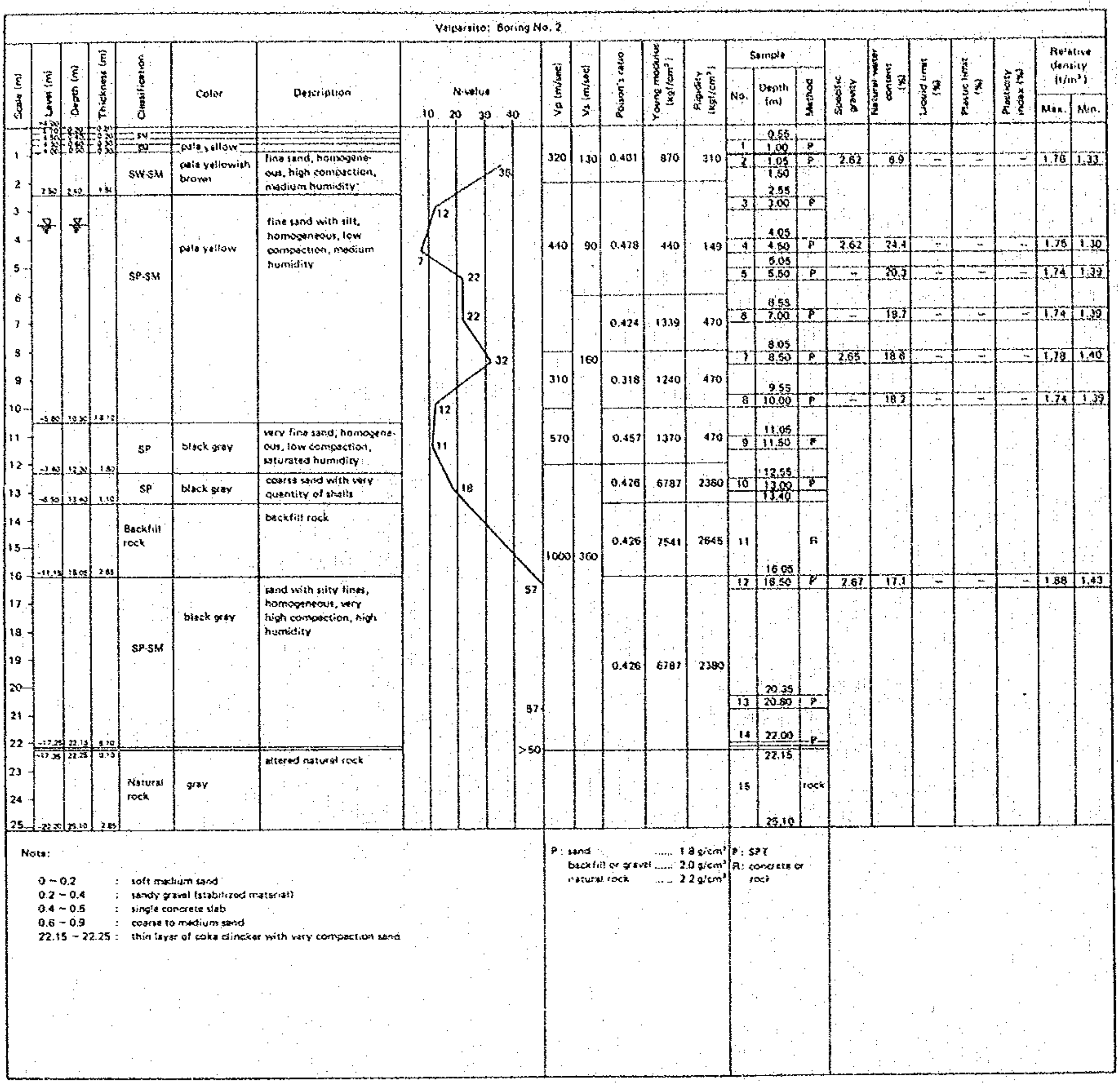

Valparaiso; Boring No. 2

Level (m)	Depth (m)	Thickness (m)	Classification	Color	Description
2.50	2.50	1.50	SW-SM	pale yellowish brown	fine sand, homogeneous, high compaction, medium humidity
-5.80	10.30	7.80	SP-SM	pale yellow	fine sand with silt, homogeneous, low compaction, medium humidity
-7.80	12.30	1.80	SP	black gray	very fine sand, homogeneous, low compaction, saturated humidity
-8.90	13.40	1.10	SP	black gray	coarse sand with very quantity of shells
-11.55	16.05	2.65	Backfill rock		backfill rock
-17.65	22.15	6.10	SP-SM	black gray	sand with silty fines, homogeneous, very high compaction, high humidity
-17.75	22.25	0.10			
-20.60	25.10	2.85	Natural rock	gray	altered natural rock

Vp (m/sec)	Vs (m/sec)	Poison's ratio	Young modulus (kgf/cm²)	Rigidity (kgf/cm²)
320	130	0.401	870	310
440	90	0.478	440	149
	160	0.424	1339	470
310		0.318	1240	470
570		0.457	1370	470
		0.426	6787	2380
1000	360	0.426	7541	2645
		0.426	6787	2380

Sample No.	Depth (m)	Method	Specific gravity	Natural water content (%)	Liquid limit (%)	Plastic limit (%)	Plasticity index (%)	Relative density (t/m³) Max.	Min.
1	0.55 1.00	P							
2	1.05 1.50	P	2.62	6.9	–	–	–	1.76	1.33
3	2.55 3.00	P							
4	4.05 4.50	P	2.62	24.4	–	–	–	1.76	1.30
5	5.05 5.50	P	–	20.3	–	–	–	1.74	1.39
6	6.55 7.00	P	–	19.7	–	–	–	1.74	1.39
7	8.05 8.50	P	2.65	18.6	–	–	–	1.78	1.40
8	9.55 10.00	P	–	18.2	–	–	–	1.74	1.39
9	11.05 11.50	P							
10	12.55 13.00 13.40	P							
11		R							
12	16.05 16.50	P	2.67	17.1	–	–	–	1.88	1.43
13	20.35 20.80	P							
14	22.00	P							
15	22.15 25.10	rock							

Note:

0 ~ 0.2	:	soft medium sand
0.2 ~ 0.4	:	sandy gravel (stabilized material)
0.4 ~ 0.5	:	single concrete slab
0.6 ~ 0.9	:	coarse to medium sand
22.15 ~ 22.25	:	thin layer of coke clincker with very compaction sand

P : sand ...... 1.8 g/cm³
backfill or gravel ...... 2.0 g/cm³
natural rock ...... 2.2 g/cm³

P : SPT
R : concrete or rock

Fig. II-2-14 (2) Boring Log at the Port of Valparaiso

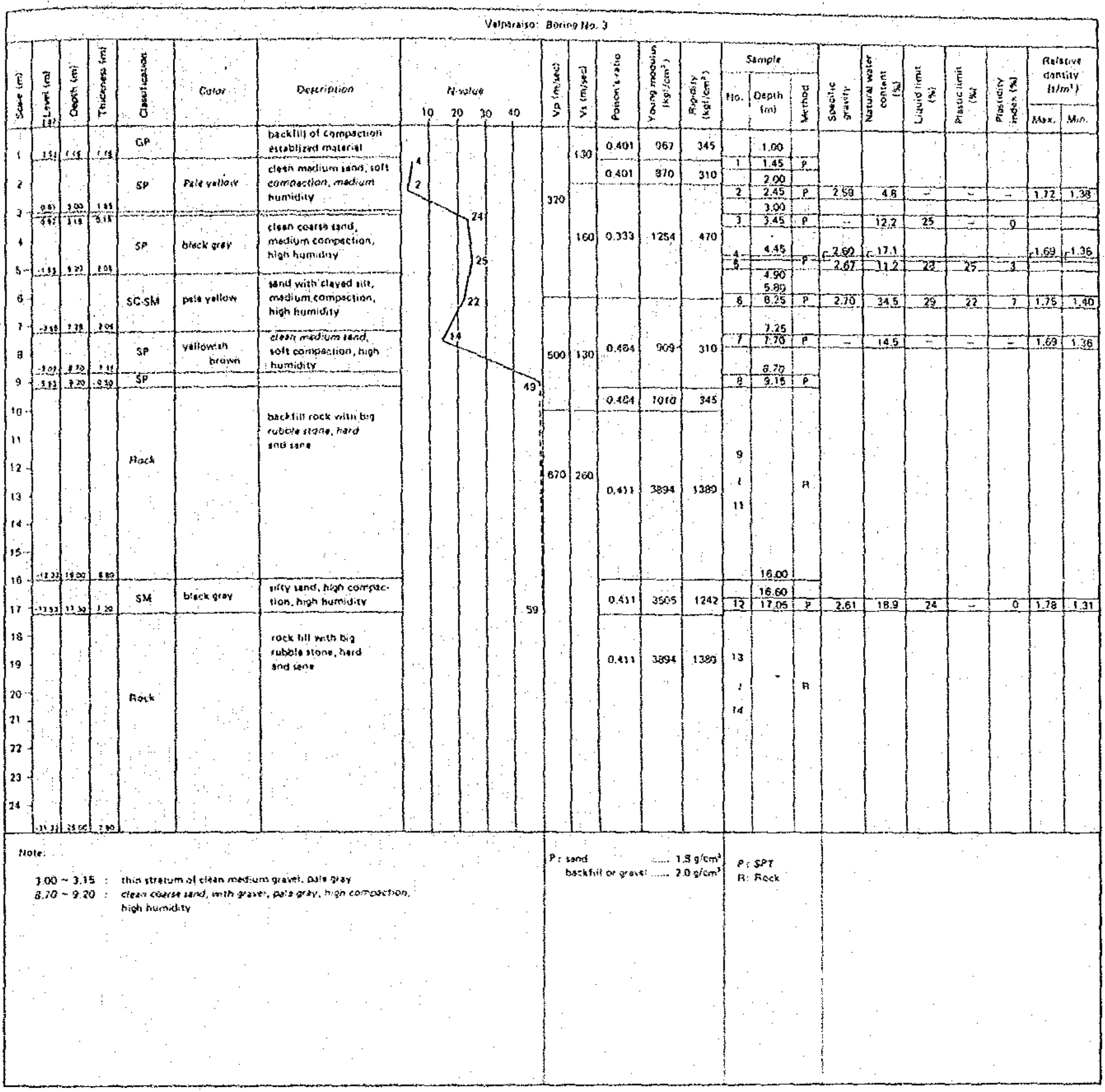

Valparaiso: Boring No. 3

Scale (m)	Level (m)	Depth (m)	Thickness (m)	Classification	Color	Description	N-value
1	[illegible]	1.15	1.15	GP		backfill of compaction establized material	
2–3	[illegible]	3.00	1.85	SP	Pale yellow	clean medium sand, soft compaction, medium humidity	4 2
3	[illegible]	3.15	0.15				
4–5	[illegible]	5.20	2.05	SP	black grey	clean coarse sand, medium compaction, high humidity	24 25
6–7	[illegible]	7.25	2.05	SC-SM	pale yellow	sand with clayed silt, medium compaction, high humidity	22
8	[illegible]	8.70	1.45	SP	yellowish brown	clean medium sand, soft compaction, high humidity	14
9	[illegible]	9.20	0.50	SP			49
10–16	[illegible]	16.00	6.80	Rock		backfill rock with big rubble stone, hard and sane	
17	[illegible]	17.30	1.30	SM	black gray	silty sand, high compaction, high humidity	59
18–24	[illegible]	25.00	7.90	Rock		rock fill with big rubble stone, hard and sane	

Vp (m/sec)	Vs (m/sec)	Poison's ratio	Young modulus (kgf/cm²)	Rigidity (kgf/cm²)
370	130	0.401	967	345
		0.401	870	310
	160	0.333	1254	470
500	130	0.404	909	310
		0.404	1010	345
670	260	0.411	3894	1389
		0.411	3505	1242
		0.411	3894	1380

Sample No.	Sample Depth (m)	Method	Specific gravity	Natural water content (%)	Liquid limit (%)	Plastic limit (%)	Plasticity index (%)	Relative density (t/m³) Max.	Min.
1	1.00 1.45	P							
2	2.00 2.45	P	2.59	4.8	–	–	–	1.72	1.38
3	3.00 3.45	P	–	12.2	25	–	0		
4	4.45	P	2.60	17.1				1.69	1.36
5	4.90		2.67	11.2	28	25	3		
6	5.80 6.25	P	2.70	34.5	29	22	7	1.75	1.40
7	7.25 7.70	P	–	14.5	–	–	–	1.69	1.36
8	8.70 9.15	P							
9 ~ 11		R							
12	16.00 16.60 17.05	P	2.61	18.9	24	–	0	1.78	1.31
13 ~ 14		R							

Note:

3.00 ~ 3.15 : thin stratum of clean medium gravel, pale gray
8.70 ~ 9.20 : clean coarse sand, with gravel, pale gray, high compaction, high humidity

P : sand ...... 1.8 g/cm³
backfill or gravel ...... 2.0 g/cm³

P : SPT
R: Rock

Fig. II-2-14 (3) Boring Log at the Port of Valparaiso

Valparaiso: Boring No. 4 (Baron pier)

Level (m)	Depth (m)	Thickness (m)	Classification	Color	Description
-11.10					
-11.55	0.45	0.45	SP	grey	coarse sand
-13.50	2.40	1.95	SM (ML)	light olive gray	silty very fine sand, low compaction, saturated humidity
-17.80	6.70	4.30	ML	black	silt, medium plasticity homogeneous, very low consistency, saturated humidity
-19.50	8.40	1.70	SM (ML)	very black gray	silty sand, low compaction high humidity
-23.50	12.40	4.00	SM	light olive gray	fine sand, homogeneous, high compaction, high humidity, with mica and shells
-30.50	19.40	7.00	SM	gray	medium to coarse sand, heterogeneous, high compaction, saturated humidity
-36.75	25.65	6.25	SM (ML)	black gray	silty fine sand, homogeneous, very high compaction, high humidity

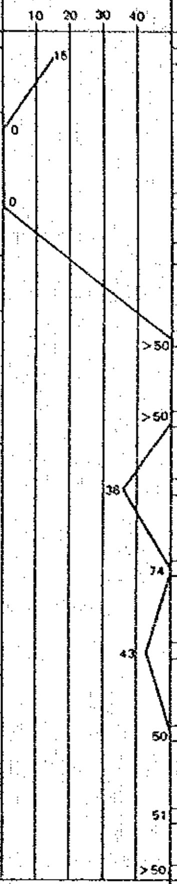

Sample			Specific gravity	Natural water content (%)	Liquid limit (%)	Plastic limit (%)	Plasticity index (%)	Relative density (t/m³)	
No.	Depth (m)	Method						Max.	Min.
1	0.45	P							
2	0.90	P	2.66	32.3	31	28	3	–	–
3	4.80 5.25	P							
4	6.30 6.90	T	2.69	35.8	34	25	9	–	–
5	8.93 9.40	P	2.74	18.5	–	–	–	1.72	1.29
6	11.40 11.85	P							
7	13.45 13.90	P							
8	15.95 16.40	P	2.69	17.0	29	–	0	–	–
9	18.45 18.90	P							
10	20.95 21.40	P	2.70	24.6	30	–	0	–	
11	23.45 23.90	P							
12	25.20 25.65	P							

Note:

This point is on the Baron pier.

P : SPT

T : Thin wall

Fig. II-2-14 (4) Boring Log at the Port of Valparaiso

Valparaiso: Boring No. 6

Scale (m)	Level (m)	Depth (m)	Thickness (m)	Classification	Color	Description
	+4.85 4.65	0.20	0.20			
1	3.25	1.60	1.40	SP	light yellowish brown	clean medium sand, heterogeneous, low compaction, *medium humidity*
2, 3	1.75	3.10	1.50	SP	pale yellow	clean fine sand, homogeneous, low compaction, medium humidity
4	0.25	4.60	1.50	SP	grayish brown	coarse sand with silty fines, heterogeneous, low *compaction, medium humidity*
5, 6	-1.15	6.00	1.40	SP	light gray brownish	coarse sand with gravels, heterogeneous, low *compaction, saturated humidity*
7, 8, 9	-5.00	9.85	3.85	SM	dark gray	silty sand, heterogensous, low compaction, high humidity, with some gravels
10	-5.20	10.05	0.20			
11, 12, 13	-8.45	13.30	3.25	SM	dark gray	silty medium sand, homogeneous, medium compaction, high humidity
14, 15	-10.95	15.80	2.50	SP	yellowish brown	*clean medium sand, homogeneous, very high* compaction, high humidity
16, 17, 18	-13.85	18.70	2.90	SM	gray	silty very fine sand, homogeneous, very high compaction, medium humidity, some micas and shells
19, 20, 21, 22, 23, 24, 25	-21.15	26.00	7.30	SM	black gray	silty fine sand, homogeneous, high compaction high humidity

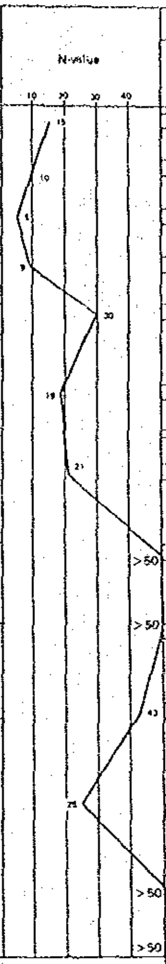

Sample		
No.	Depth (m)	Method
	0.20	
1	0.65	P
	1.65	
2	2.10	P
	3.10	
3	3.55	P
	4.55	
4	5.00	P
	6.00	
5	6.45	P
	8.45	
6	8.90	P
	9.85	
7		P
	10.05 10.50	
8	11.35	P
	13.35	
9	13.80	P
	15.80	
10	16.25	P
	18.25	
11	18.70	P
	21.05	
12	21.50	P
	23.55	
13	24.00	P
	25.55	
14	26.00	P

Note:

0.00 ~ 0.20 : *pavement of simple concrete*
9.85 ~ 10.05 : rubble stone

P : SPT

Fig. II-2-14 (5) Boring Log at the Port of Valparaiso

Table II-2-8 Cycle Triaxial Test Result

Boring No.	Number of Cycles Nℓ	Cycle Stress Ratio Rℓ	Relative Density Dr	Remarks
No.1	114.0	0.141	50	●$_1$
	32.0	0.211	50	●$_1$
	33.0	0.25	50	●$_1$
	23.0	0.313	50	●$_1$
	11.5	0.375	50	●$_1$
	53.0	0.201	50	▲$_1$
	38.5	0.246	50	▲$_1$
	18.5	0.312	50	▲$_1$
	56.0	0.179	70	○$_1$
	31.0	0.246	70	○$_1$
	7.5	0.424	70	○$_1$
No.2	8.0	0.15	50	●$_2$ Omit
	3.0	0.37	50	●$_2$ Omit
	4.0	0.20	50	▲$_2$ Omit
	2.5	0.30	50	▲$_2$ Omit
	31.5	0.20	70	○$_2$
	19.5	0.30	70	○$_2$
	5.5	0.56	70	○$_2$

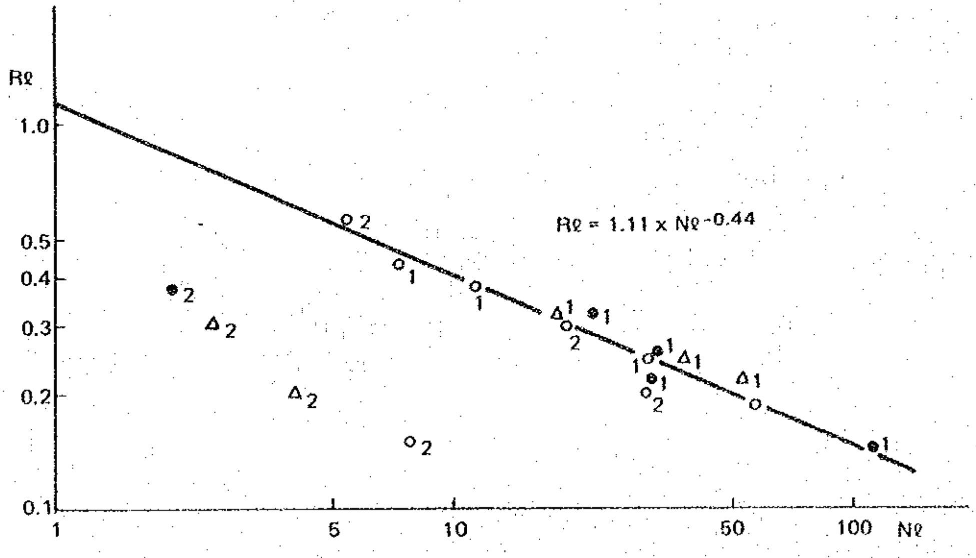

Cycle Stress Ratio vs. Number of Cycles

(3) The Port of San Antonio

1) Topography

Fig. II-2-15 shows San Antonio port which is embraced at the north by the hilley terrace of Co. El Centinela. There is sandy beach stretching south from the port and gently sloped hills to the east.

San Antonio port is protected from the west by a breakwater extended to the north from the southern part of the sand beach. The water region between the breakwater and Punta San Antonio forms the mouth of the port, which opens to the Pacific Ocean to the northwest.

The source of the sand deposits in and around San Antonio port is the Maipo River that lies approximately 2.5 km to the south of the port. The Maipo river has a large discharge of sandy sediment and the shoreline change at the river mouth is remarkable, resulting in the formation of lagoons as well as the sandy beach south of San Antonio.

Fig. II-2-16 shows the topographic map of San Antonio port and its hinterland prepared by the team through the field survey.

2) Seabed Topography

Fig. II-2-17 shows cross sections of the seabed topography at San Antonio port. The seabed topography shows deeps about 50 m in depth and 250 m wide running east to west at the north of the port. The deeps reach a water depth of around 110 m offshore of the port with the depth increasing towards the west. At approx. 1.5 km from the mouth of the port, the direction of the deeps changes to the north to pass by Punta Panul located 2 km away to the north of San Antonio where the deeps then fall into the deeps running along the coast of Chile.

The southern water area inside the port is shallow with a depth of not more than 10 m, with part of the water area showing a sandy beach. This sandy beach is assumed to have been formed by accretion of littoral draft sand before the construction of the breakwater.

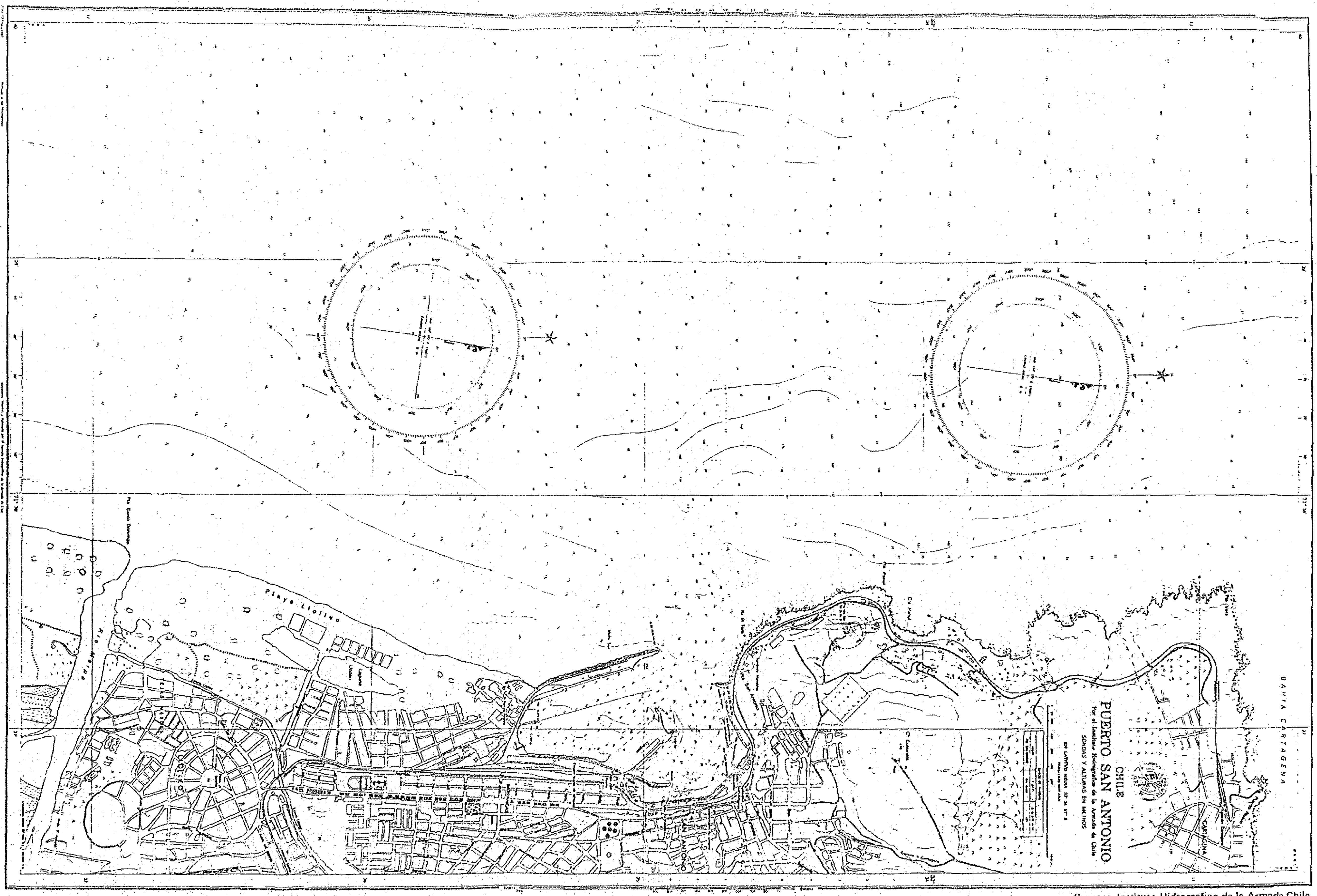

Source: Instituto Hidrografico de la Armada-Chile

Fig. II-2-15 Chart of San Antonio

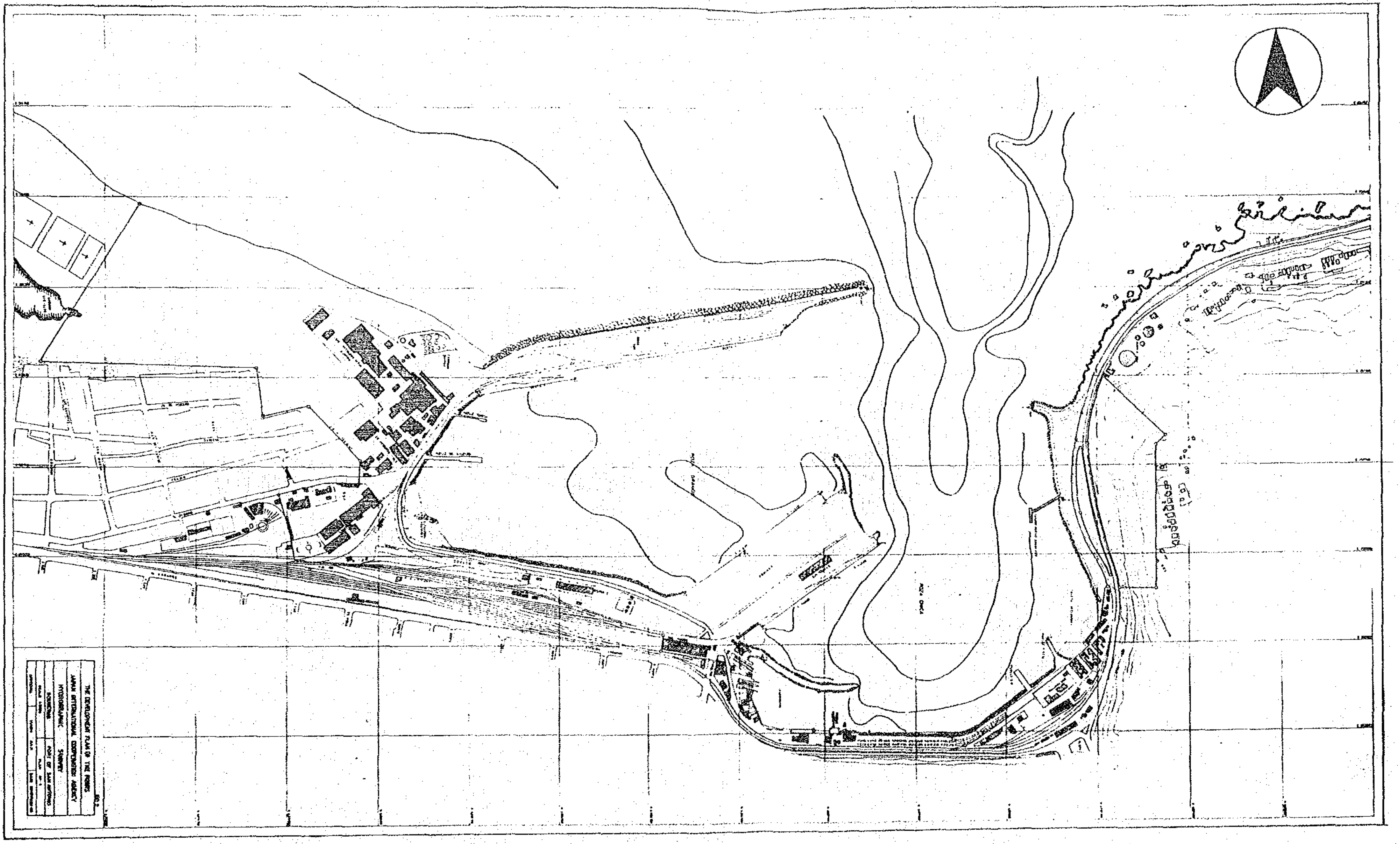

Fig. II-2-16 Topographic Survey Map of the Port of Valparaiso

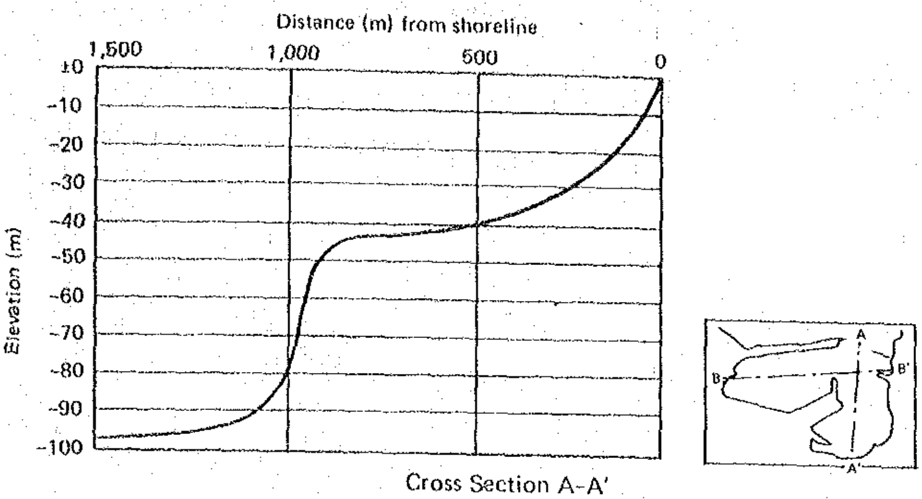

Cross Section A-A'

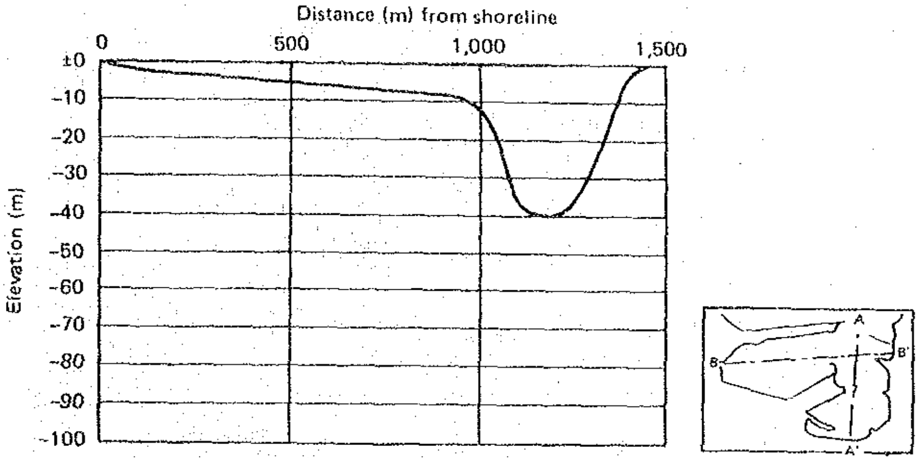

Cross Section B-B'

Fig. II-2-17 Seabed Cross Sections at San Antonio Port

3) Climate

(i) Temperature and Rainfall

Similar to Valparaiso, San Antonio is under the influence of the Peru Current. The climate at San Antonio is warm, having an annual mean temperature of 13.2°C, an annual mean maximum of 16.5°C and an annual mean minimum of 9.2°C.

The monthly mean temperatures and rainfall are shown in Table II-2-9 and Fig. II-2-18. The monthly mean temperatures are 10.2°C minimum and 16.6°C maximum; the temperature variation is very small - only 6.4°C. Moreover, the monthly rainfalls are almost the same as those at Valparaiso with the minimum of 1.4 mm falling in January, and a total rainfall of 448.7 mm.

Table III-2-9 Monthlv Temperatures and Rainfall

	Jan.	Feb.	Mar.	Apr.	May	Jun.	Jul.	Aug.	Sep.	Oct.	Nov.	Dec.
(°C) Max. Temperature	18.0	19.6	17.3	17.5	16.3	14.7	14.1	14.3	15.1	15.9	17.1	18.6
(°C) Mean Temperature	15.2	16.6	14.3	13.8	13.3	10.6	10.2	10.7	10.9	11.9	14.0	15.1
(°C) Min. Temperature	12.1	13.3	10.8	9.7	10.1	6.4	6.2	7.0	6.3	7.6	10.5	10.9
Rain fall (mm)	1.4	5.4	6.1	20.3	80.9	12.3	98.0	71.0	24.4	14.7	4.4	2.3

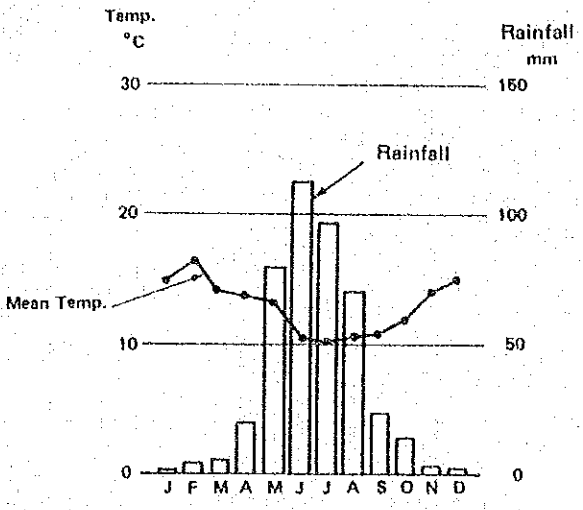

Fig. II-2-18 Mean Temperature and Rainfall at San Antonio

Source: Instituto Hydrografico de la Armada-Chile

(ii) Winds

The frequency of wind direction in Table II-2-10 and Fig. II-2-19 cleary indicates that southwesterly winds are the most common in all months, but their occurrence is not as large as at Valparaiso. In the winter season, winds from directions other than the northeast and north occur at about the same frequency. The mean wind velocity is around 5 to 10 knots with the exception of northeasterly winds and the southerly to southwesterly winds which prevail throughout the year.

The maximum wind velocity observed up to the present is 28 knots southwesterly in January, 1970. The annual mean frequency of occurrence of winds over 20 knots is 23 days. The comparison with Valparaiso indicates relatively weak winds at San Antonio, presumably because of the further inland location.

All the wind data so far mentioned were observed at the inland station. Although no clear relationship between the inland and sea wind pattern is obtainable due to the lack of coastal winds, the wind velocities over the sea would be at least 1.5 times those inland.

Table II-2-10 Wind Data at San Antonio

MONTH		N	NE	E	SE	S	SW	W	NW	Calm
Jan.	D	5.6	1.4	1.4	5.3	15.8	24.6	12.3	19.3	14.4
	V	5	5	5	13	10	10	7	8	
Feb.	D	3.5	1.6	2.7	8.2	17.3	29.8	9.8	13.7	13.3
	V	4	6	3	12	10	10	7	5	
Mar.	D	4.6	3.2	4.5	10.7	11.0	23.5	11.4	12.5	18.5
	V	5	4	4	8	10	9	7	7	
Apr.	D	3.5	2.1	3.5	8.4	10.5	18.1	9.4	14.6	30.0
	V	3	3	5	5	8	7	7	7	
May	D	7.6	3.2	3.9	10.7	15.0	13.9	10.4	12.1	23.2
	V	10	10	8	9	10	10	8	7	
Jun.	D	9.3	3.4	7.8	12.3	12.7	14.9	10.4	11.2	17.9
	V	8	4	8	8	10	10	8	7	
Jul.	D	7.2	2.5	5.7	11.1	12.2	14.7	8.6	12.9	25.1
	V	9	3	7	5	8	6	8	7	
Aug.	D	3.5	2.1	2.8	14.8	5.7	19.4	12.7	9.2	29.7
	V	6	4	8	7	10	8	7	7	
Sep.	D	2.8	2.1	3.5	9.9	9.2	21.5	13.4	10.2	27.5
	V	14	4	3	7	10	10	7	10	
Oct.	D	3.2	2.5	3.9	10.4	16.1	34.6	6.1	3.9	19.3
	V	6	5	3	7	10	10	8	6	
Nov.	D	5.3	1.8	4.2	5.6	14.1	22.9	11.6	15.5	19.0
	V	5	4	4	7	10	10	8	10	
Dec.	D	2.5	1.8	1.8	2.2	21.9	30.5	13.6	16.8	10.0
	V	6	3	3	6	10	10	8	8	

D: Frequency (%) of wind diection

V: Mean velocity (knots)

Total Observationes: 3332 (about three years)

Source: Instituto Hydrografico de la Armada-Chile

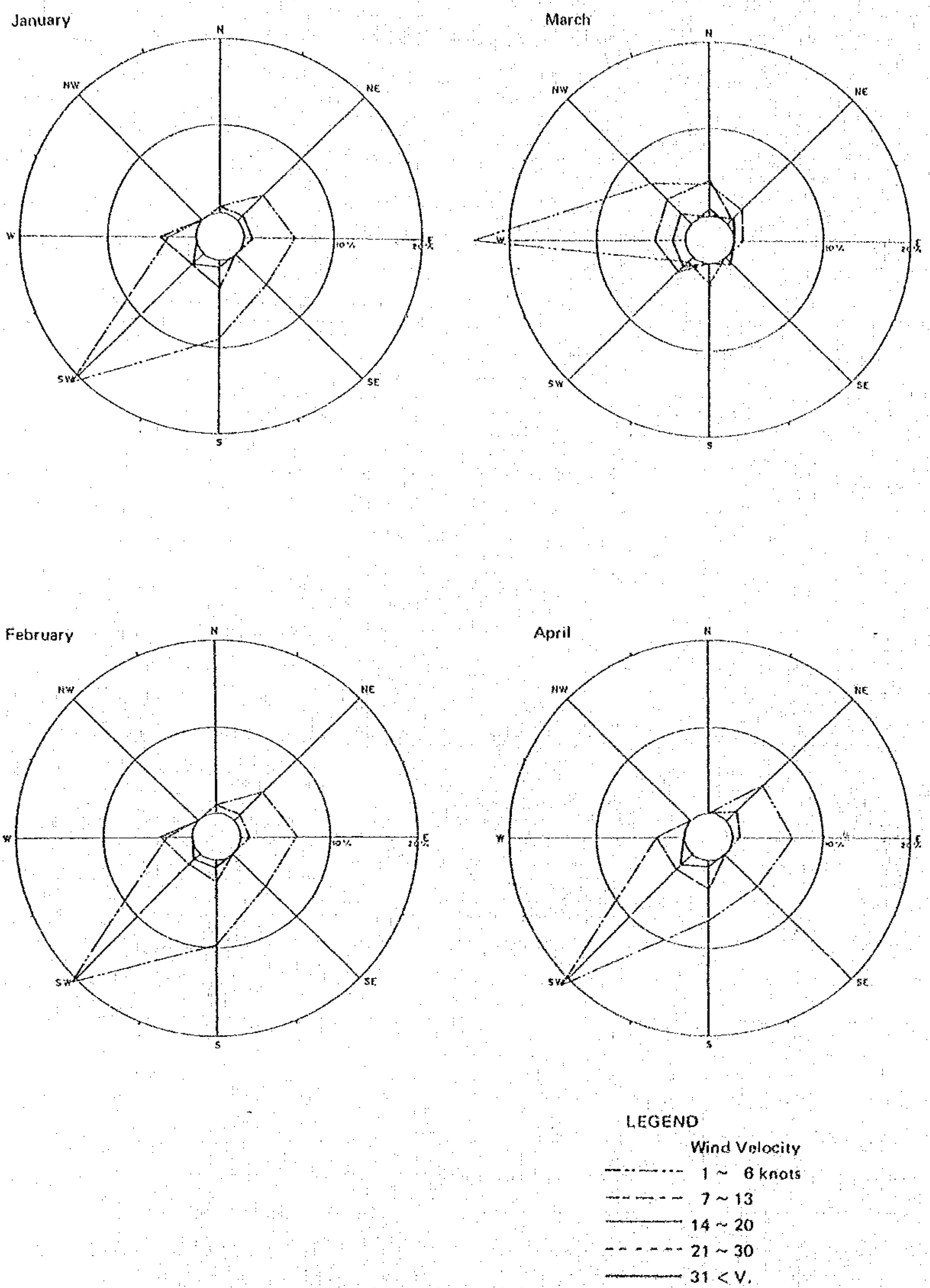

Fig. II-2-19 (1) Monthly Wind Rose at San Antonio (1981)

Source: Institute Hidrografico de la Armada – Chile.

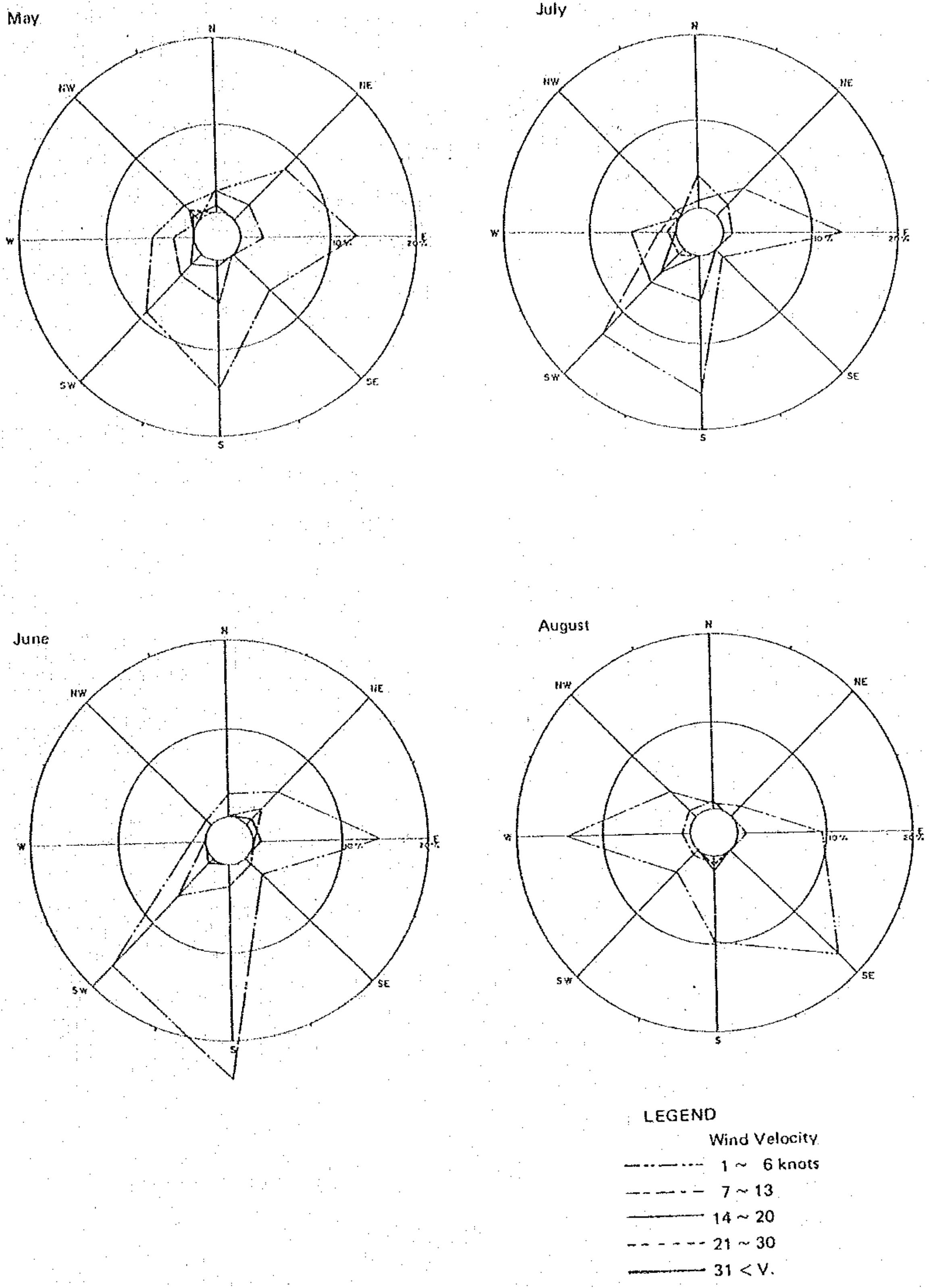

Fig. II-2-19 (2) Monthly Wind Rose at San Antonio (1981)

Source: Institute Hidrografico de la Armada – Chile.

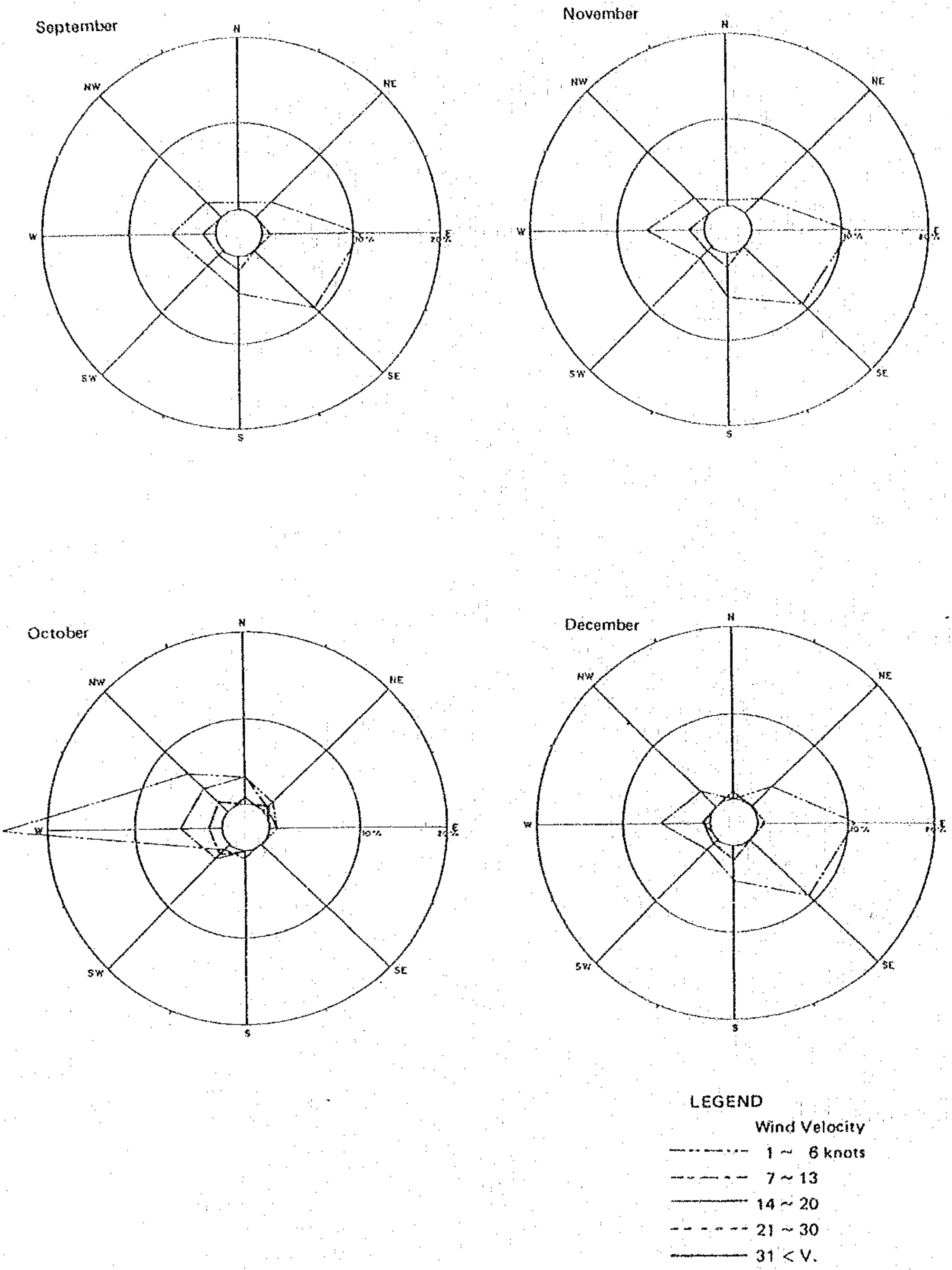

Fig. II-2-19 (3) Monthly Wind Rose at San Antonio (1981)

Source: Institute Hidrografico de la Armada – Chile.

4) Sea Conditions

(i) Offshore Waves

Extremely high waves at San Antonio are those from the northwest to the southwest. San Antonio port is located approximately 50 km from Valparaiso but the offshore wave data at Valparaiso can be used practically in the case of northwesterly waves. Because of the lack of statistical data on southwesterly waves, the weather charts of the southern hemisphere are used to hindcast the offshore waves at the port of San Antonio.

The weather charts used for the offshore wave hindcasting are for a period of 12 years: in 1970 and from 1972 to 1982. The wave hindcasting is made by adopting the relationship between the fetch and the continuation time of wind blow and/or by using Wilson's method. The hindcast waves are plotted on Gumbel extreme probability paper as shown in Fig. II-2-20. Waves 11.2 m high or of 15.2 sec period from the WSW-SW will probably occur once in 50 years.

The west-southwesterly and northwesterly wave refraction diagrams are drawn as shown in Fig. II-2-21. According to these diagrams, design wave hights for the San Antonio breakwater are calculated as follows.

① Waves of WSW, $H\ 1/3 = 11.2\text{m}$, $T = 15.0$ sec

Design wave height $H_o' = Kr1 \times Kr2 \times H\ 1/3$

$= 0.93 \times 0.65 \times 11.2$

$= 6.7$ m

where Kr1: refraction coefficient to the water depth of 40 m

Kr2: ditto, but from the 40 m water depth

② Waves of NW, $H\ 1/3 = 9.2$ m, $T = 11.0$ sec

Design wave height $Ho' = Kt \times Ko \times H\ 1/3$

$= 0.65 \times 0.88 \times 9.2$

$= 5.3$ m

where Kr: refraction coefficient

Ko: diffraction coefficient

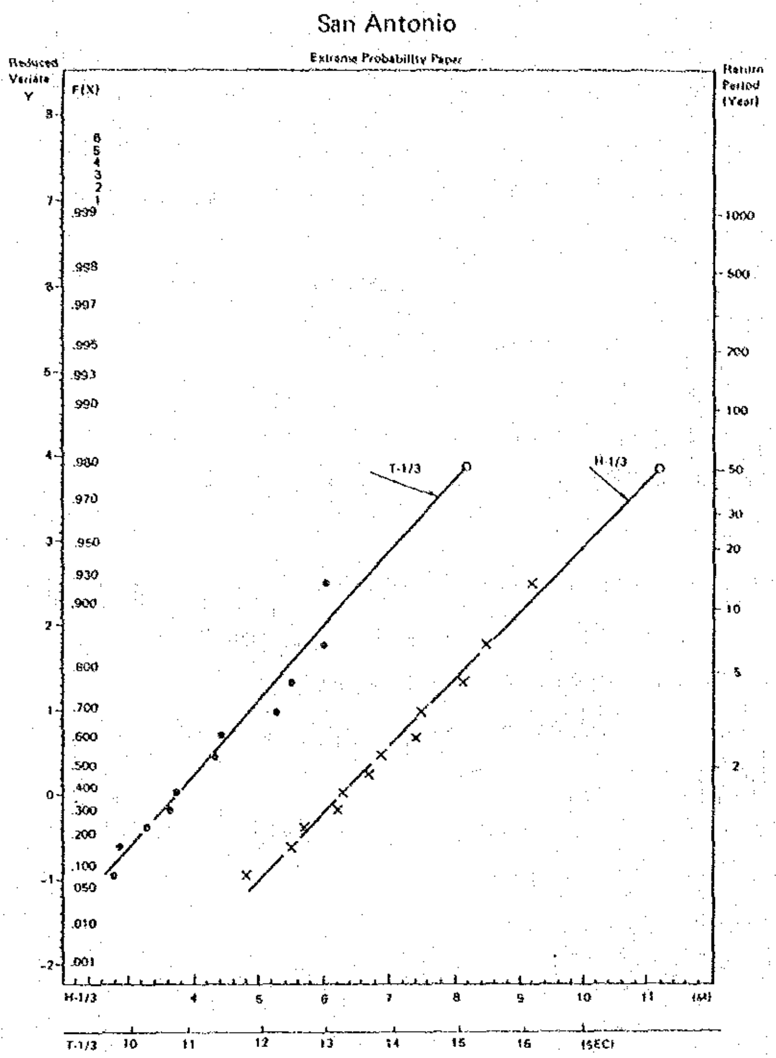

Fig. II-2-20 Max. Wave Height and Return Period at San Antonio

(ii) Tide Levels

The datum and tide levels for the port of Valparaiso are also adopted for the port of San Antonio as follows.

- Mean High Water	+ 1.80
- Mean Water	+ 0.91
- Mean Low Water	+ 0.15
- Lowest Low Water (Port datum of tide table)	± 0.00

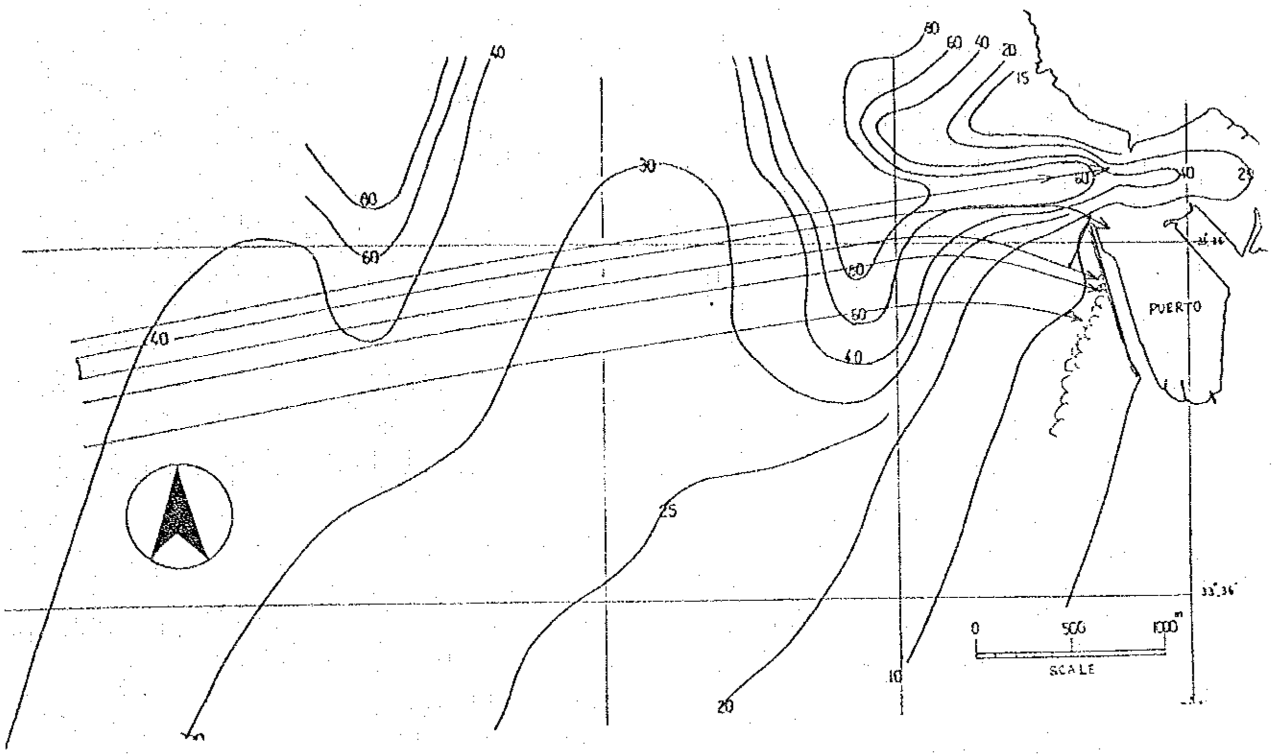

(1) Wave Direction WSW, Period 15.0 sec.

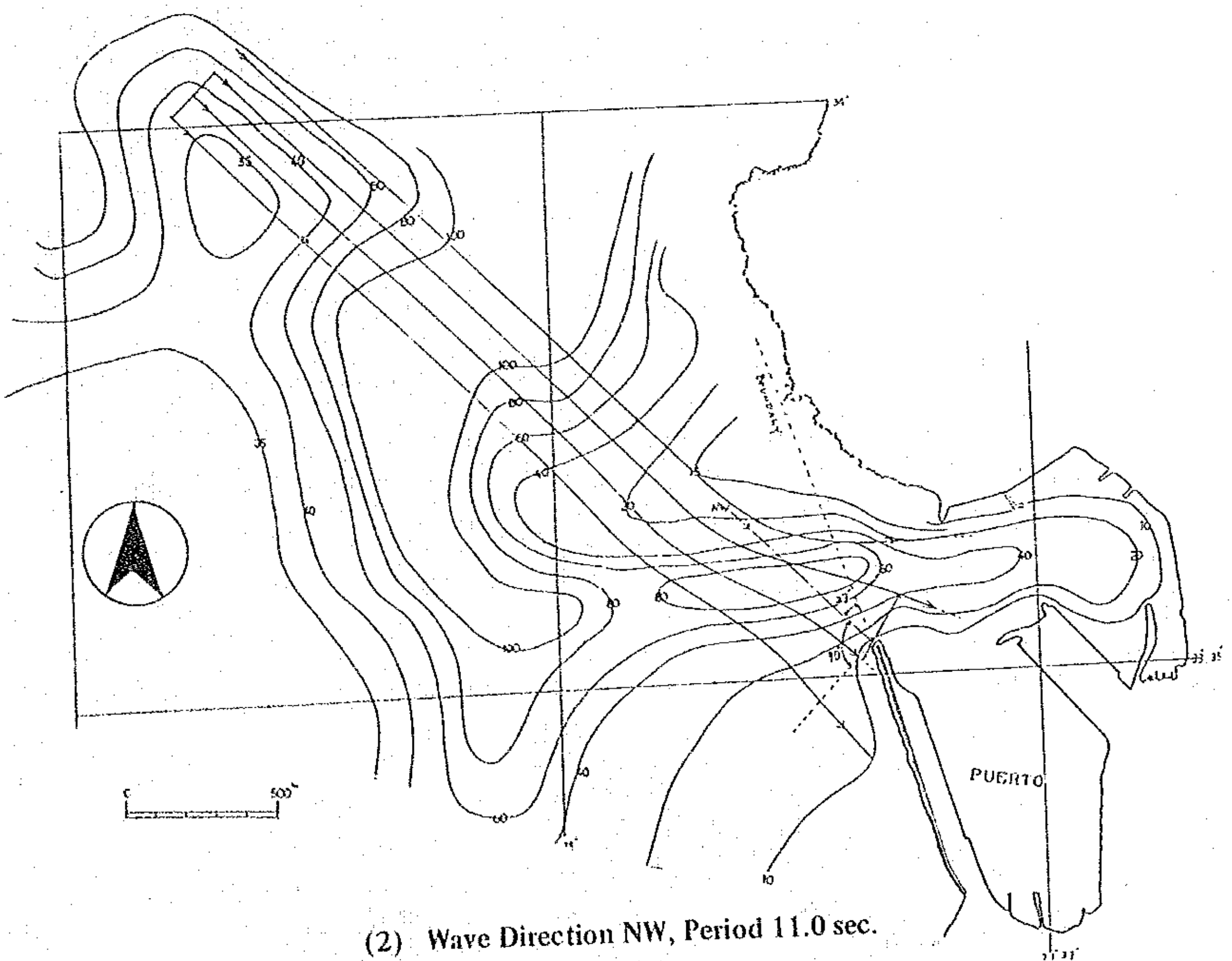

(2) Wave Direction NW, Period 11.0 sec.

Fig. II-2-21 Ware Refraction Diagram at San Antonio

(iii) Current

The current observation was performed using a current meter and float tracking at the locations in the port as shown in Fig. II-2-22. The observation was made during spring tides from Oct. 31 to Nov. 2, 1985. The current meter was set in two depths of water, 3 m beneath the surface and 5 m above the sea bed. This observation was continously carried out for 25 hours.

Fig. II-2-23 shows the northerly and easterly component of the current velocity at 3 m water depth of locations 1 and 3. The results show a variable flow in direction, but no apparent relationship between the current and tide was observed. This may be due to the stronger influence of winds and longshore current induced by waves to the shoreline around the port. It is also noted that the difference of the current velocity recorded is not so great between the surface flow and the seabed.

The results of the float tracking show a complex movement of the current inside the harbour, and no clear relationship with the tidal variations is obtained. The maximum velocity of flows are 0.15 knots at location 1, 0.25 knots at location 2 and 0.48 knots at location 3.

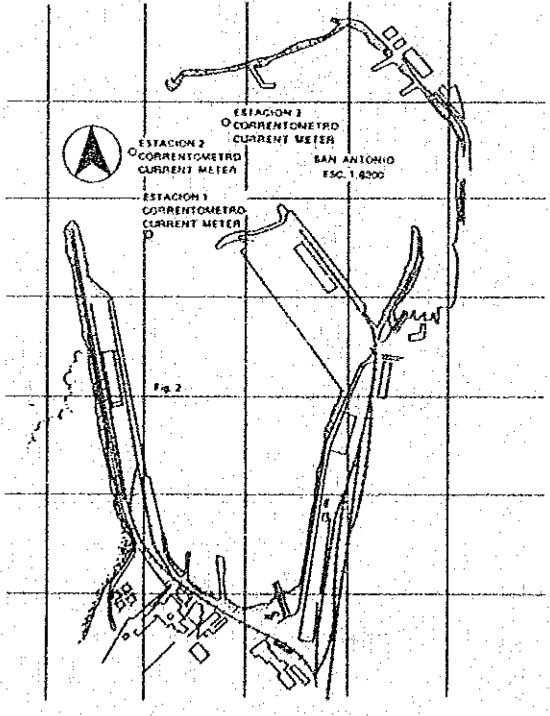

Fig. II-2-22 Location of Current Observation

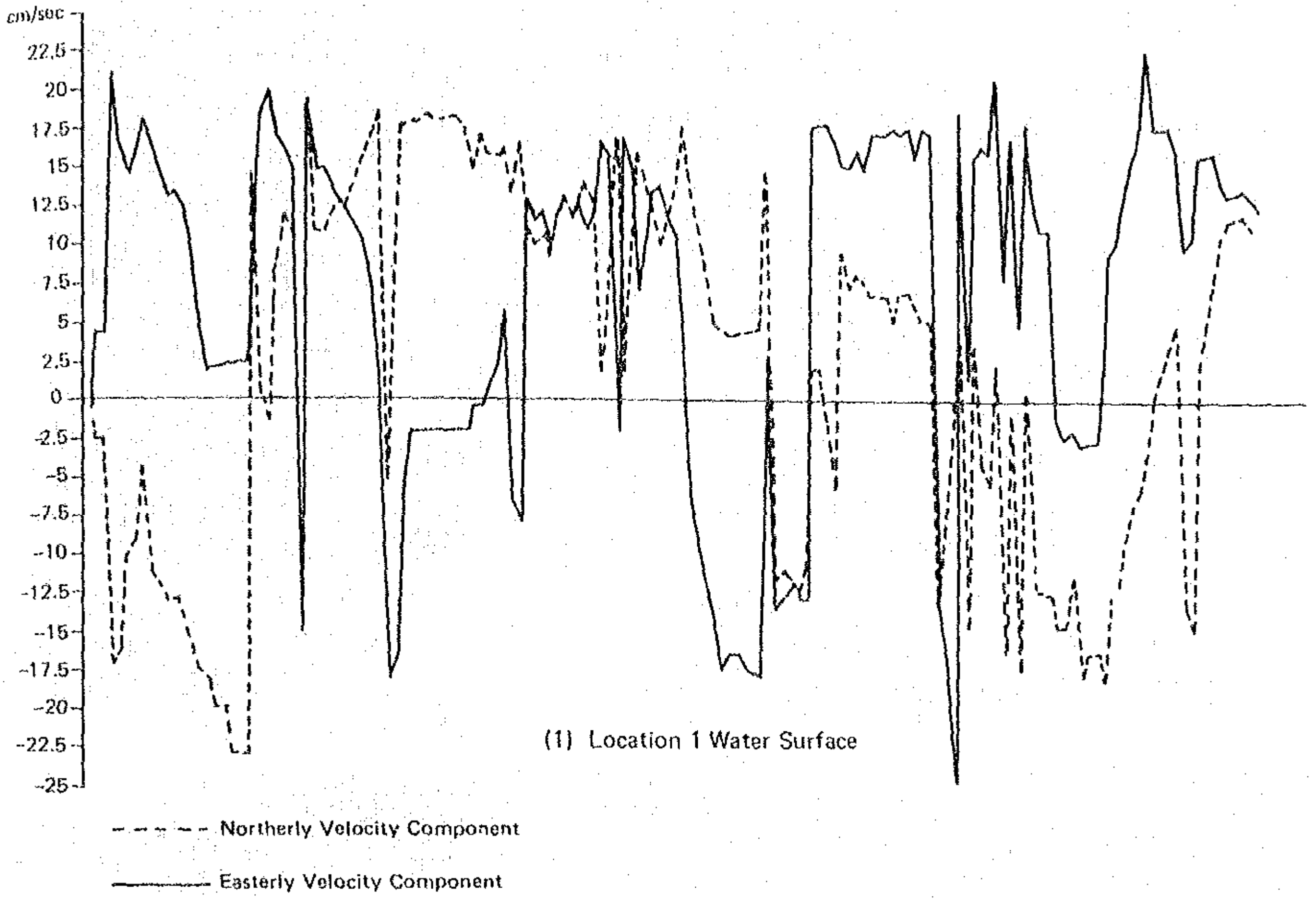

(1) Location 1 Water Surface

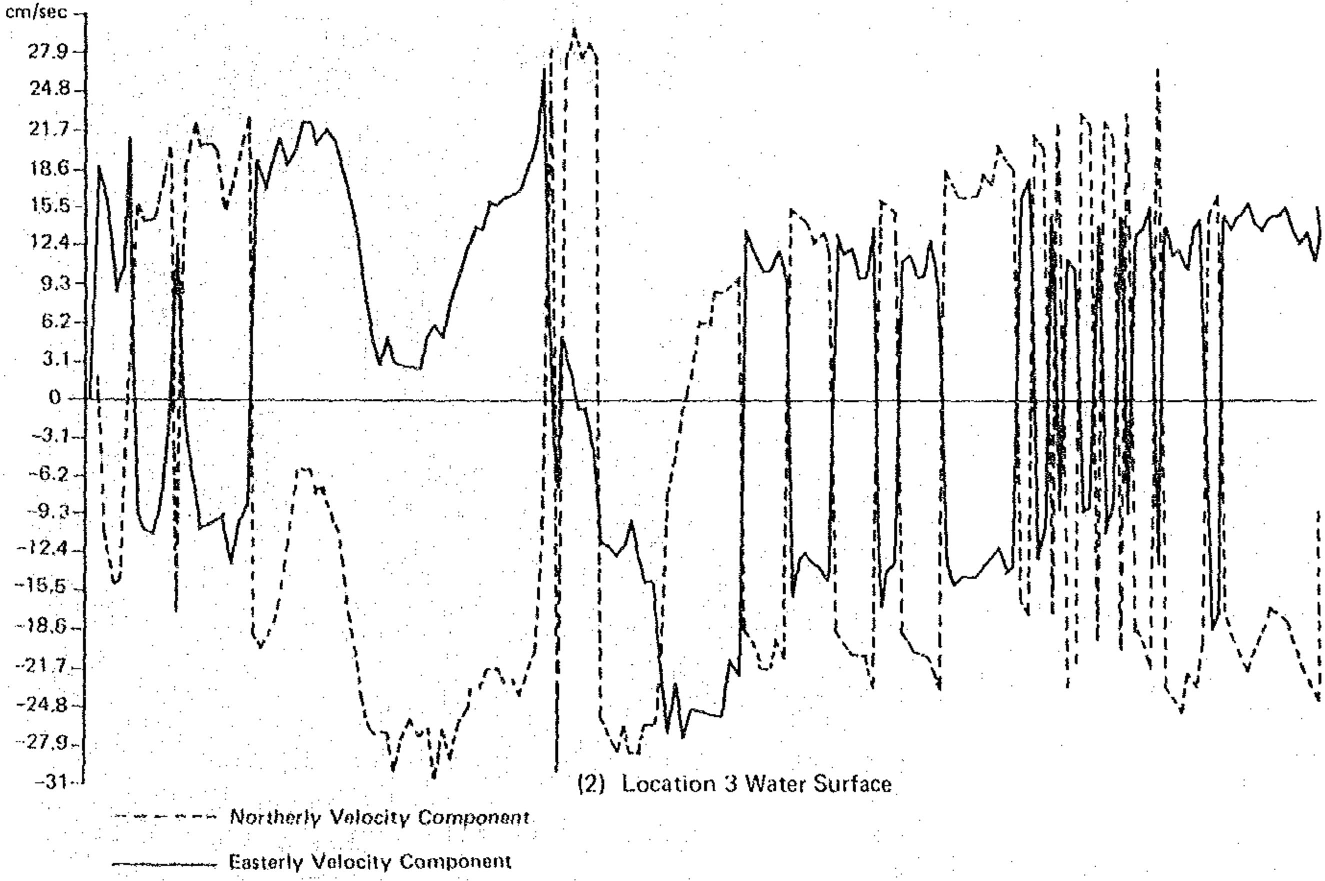

(2) Location 3 Water Surface

Fig. II-2-23 Northerly and Easterly Current Velocity Component at San Antonio

5) Geological and Subsoil Conditions

(i) Geological Features Surrounding the Port

Fig. II-2-24 shows the geological map in the vicinity of San Antonio. The geological features at the port of San Antonio reflect the topography of its vicinity. The deeps running east to west at the north of the port indicate the concave along the geological fault.

Co. El Centinela at the north of the port is a 180 m high hill possibly of Quarternary rock. In contrast with the north, the coastal area south of the port is mainly flat, and alluvial deposits are observed up to the month of the Maipo river and along the river banks. Rock terraces of Quarternary and Paleozoic ages are located extensively behind the port zone.

Qal: Depósitos aluviales y duras
Qt: Remanentes de terrazas con a sin cubierta depositos de terrazes
TTm: Rocas sedimentarias marinas. Incluye Formación Navidad (Mioceno) y estratos del Plioceno
Pzq: FOMACION QUINTAY (Basament Metamorfico) Principalmente anfibolitas y gneises
Pzt: BATOLITO DE LA COSTA Principalmente granodioritarito; tambien tonalita y adamelita

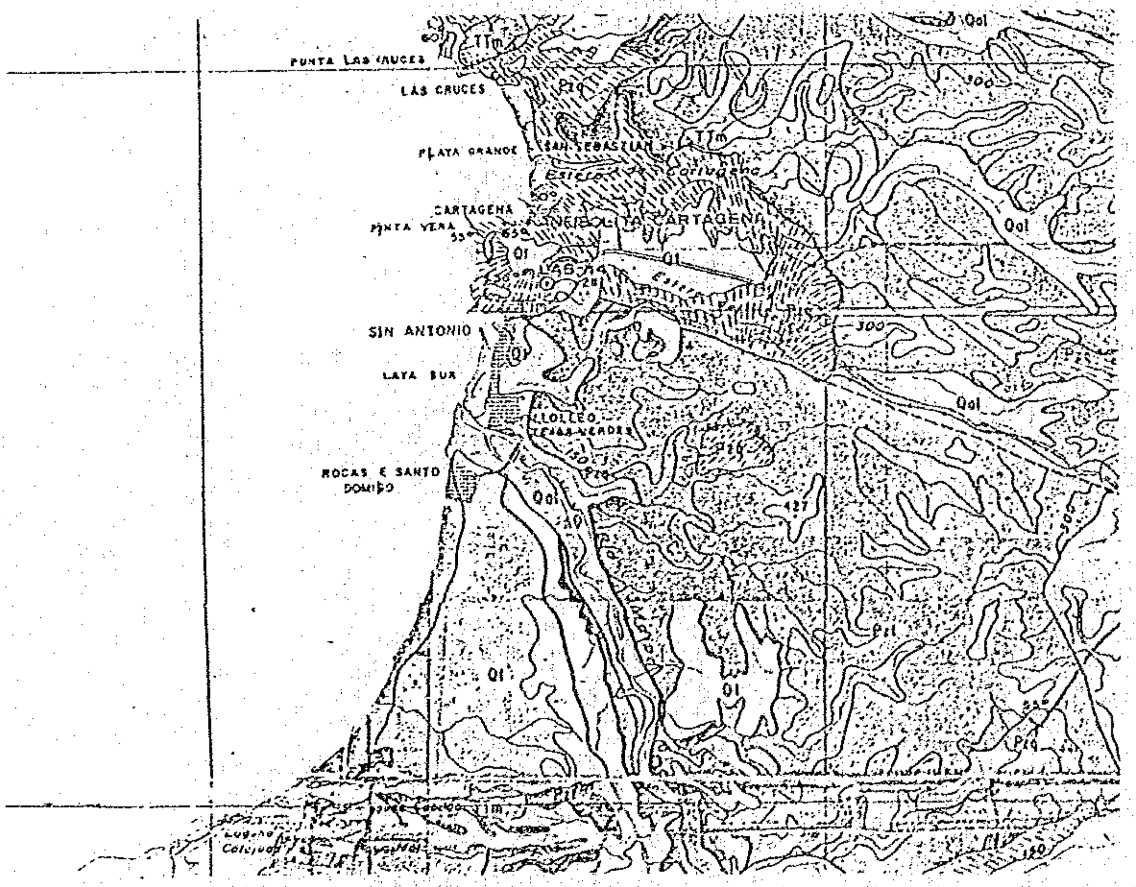

Fig. II-2-24 Geological Map of San Antonio and Its Vicinity

Source: Institute de Investigationes Geologicas-Chile, Mapa Geologico de la Hoja Valparaiso-San Antonio

(ii) Subsoil Conditions

The on-land boring works supplemented by geological exploration at the water area of the port were carried out at locations shown in Fig. II-2-25.

Fig. II-2-26 shows the subsoil profile at the port of San Antonio obtained through the boring works which were carried out by the Chilean Government. The geological formation in the port area of San Antonio can be summarized as follows.

Table II-2-11 Geology of the San Antonio Area

Symbol	Geological Period	Subsoil Classification	Description
S_1	Quarternary to the Recent	Silty or Clayey Soil	Marine or alluvial sediments of 3 - 15m depth for (S_1) and not less than 7m for (S_2)
S_2		Sand and Gravel	
B_1	Quarternary or	——	no data
B_2	Paleozoic	——	

The subsurface layer (S_1) is uniformly distributed over the port area and consists of fine sand deposits at the upper layer and clayey deposits at the lower layer. The lower clayey soil with a thinner sandy layer is dominant at the onshore side of the port as shown in the boring logs of Br. Nos. 3 and 4, while the upper sandy soil with a thinner clayey layer is notable at the offshore side near the breakwater as shown in Br. Nos. 1 and 2. The upper sands of 20 N-value in SPT are deemed to be sediments of littoral sand drift from the Maipo river. The lower clayey layer is hard, having an N-value in SPT of 15 to 20. The thickness of this clayey layer is around 10 m at Br.No.4.

The second layer (S_2) is very dense sand or gravel. Technically, this stratum is regarded as the bearing layer for structural foundations for port facilities due to its hardness of not less than 50 N-value. The layer was found at the depth of approx. -19 m. at Br. 1 and 2, -24 m at Br. 3 and -16 m at Br. 4. The upper boundary with the S_1 layer varies by location, indicating marine abrasion in the past.

The layers B_1 and B_2 are not explored by the boring work. The reflection pattern of the B_1 layer shows a slant and disconnected boundary. This indicates the presence of faults. The presence of these faults were observed in survey lines 3 to 6. These faults run east to west along the deeps intruding into the onshore area of the port. Both B_1 and B_2 layers are considered very hard strata due to a weak reflection in the recorded profiles.

Fig. II-2-27 show the subsoil profiles of the port of San Antonio obtained by the geological exploration. The boring logs with the results of laboratory tests on subsoil samples and PS prospecting at boreholes Nos. 1 to 3 are shown in Fig. II-2-28.

Disturbed backfilled sands taken from boreholes Nos. 1 to 3 were used to the cyclic triaxial tests. The test results are shown in Table II-2-12.

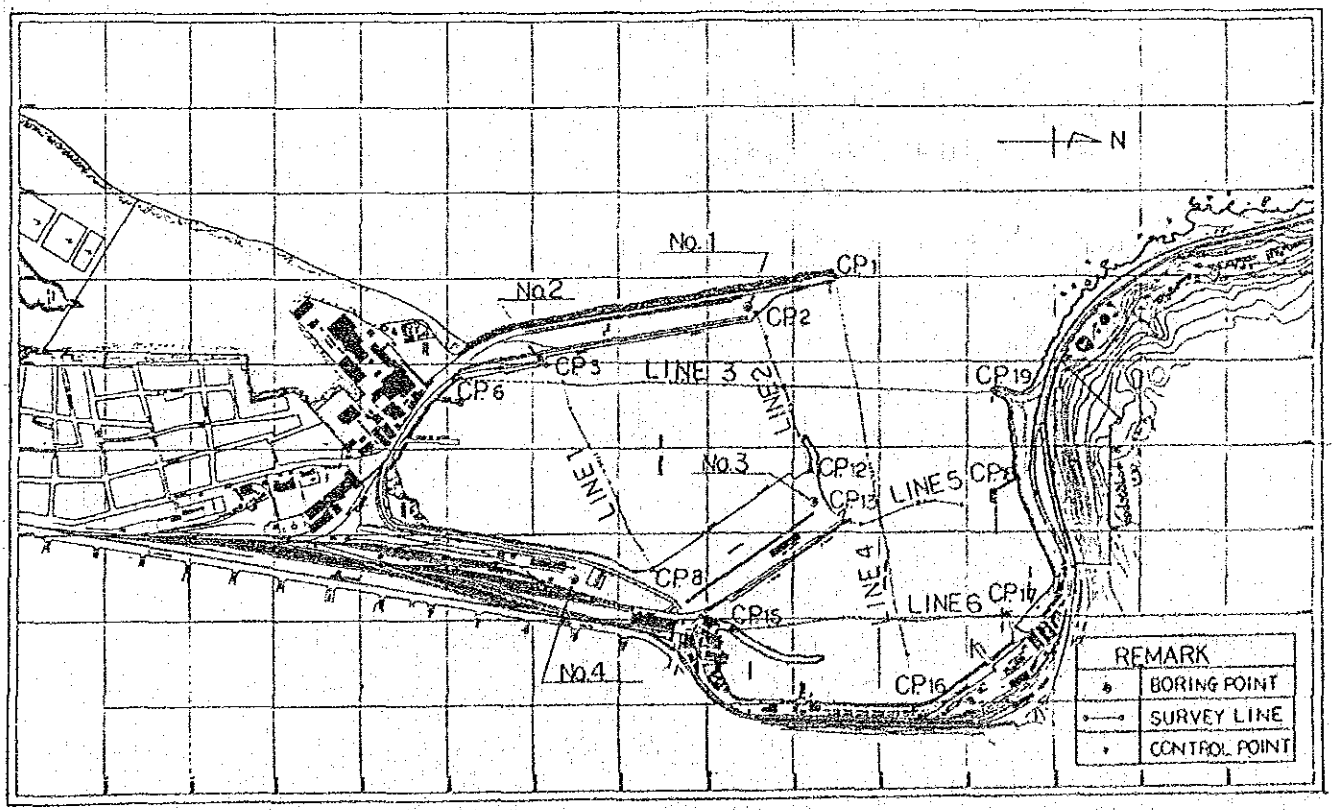

Fig. II-2-25 Location of Soil Investigation at the Port of San Antonio

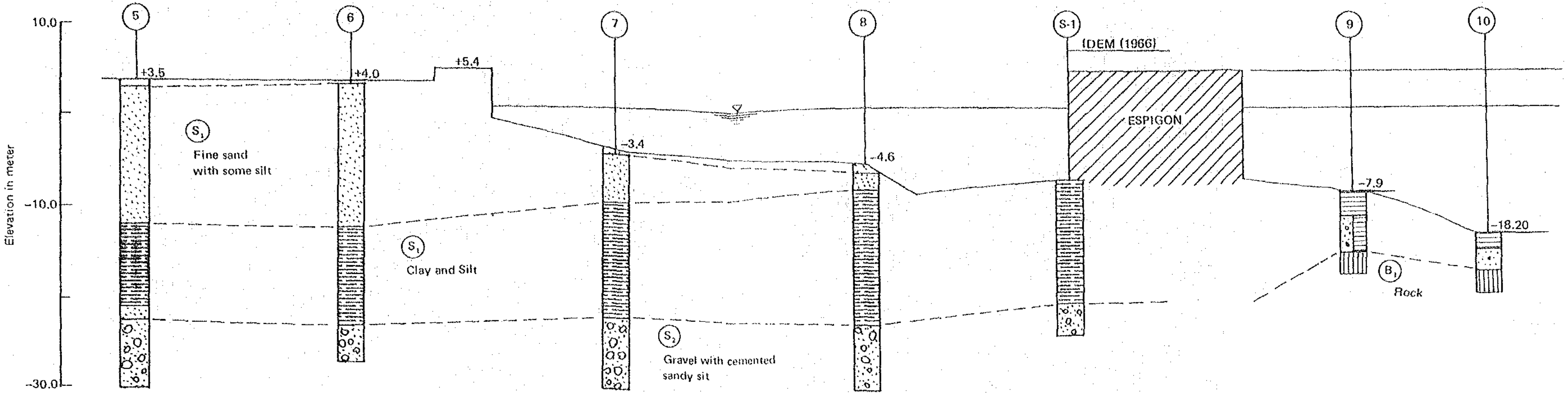

Subsoil Profile along A-A Line

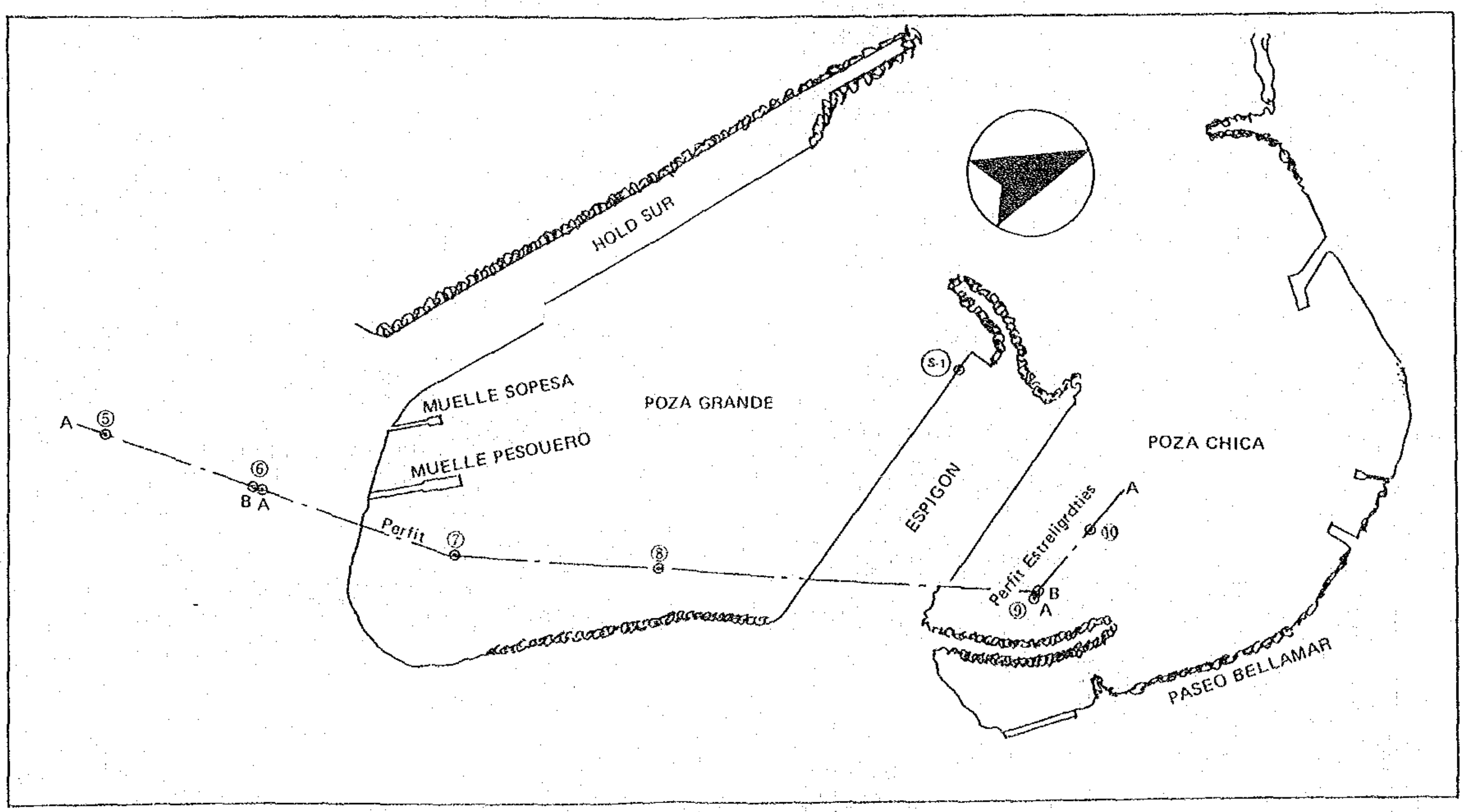

Location of Boring Works

Source: Proyecto Reparacion y Reposicion Puerto de San Antonio – X parte
Sondeos Geotecnicos Volumen 1; Direccion de Obras Portuarias,
Ministerio de Obras Publicas, Abril – 1986

Fig. II-2-26 Subsoil Conditions at the Port of San Antonio

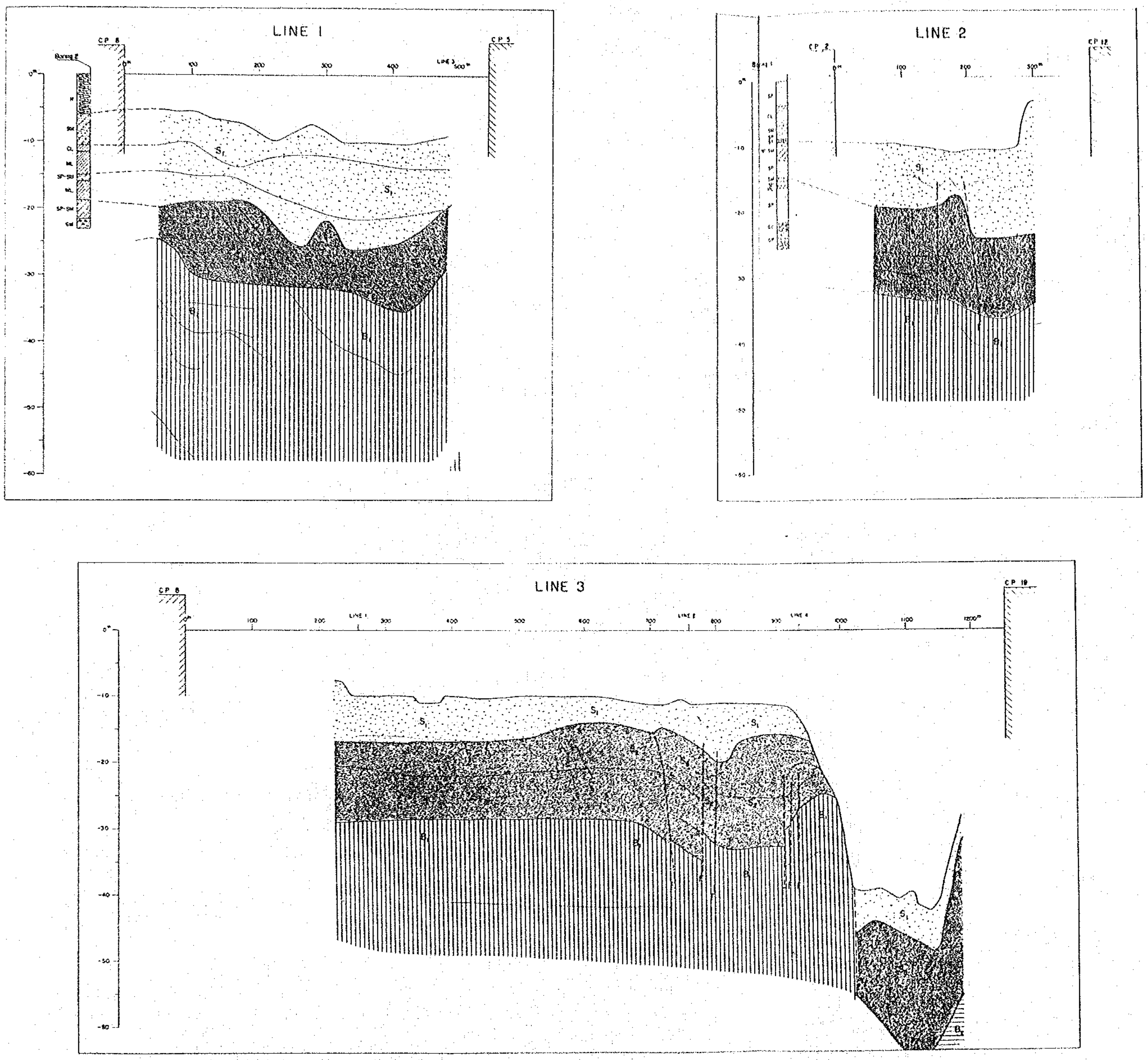

Fig. II-2-27 (1) Cross Section of Geological Profiles in the Port Area of San Antonio

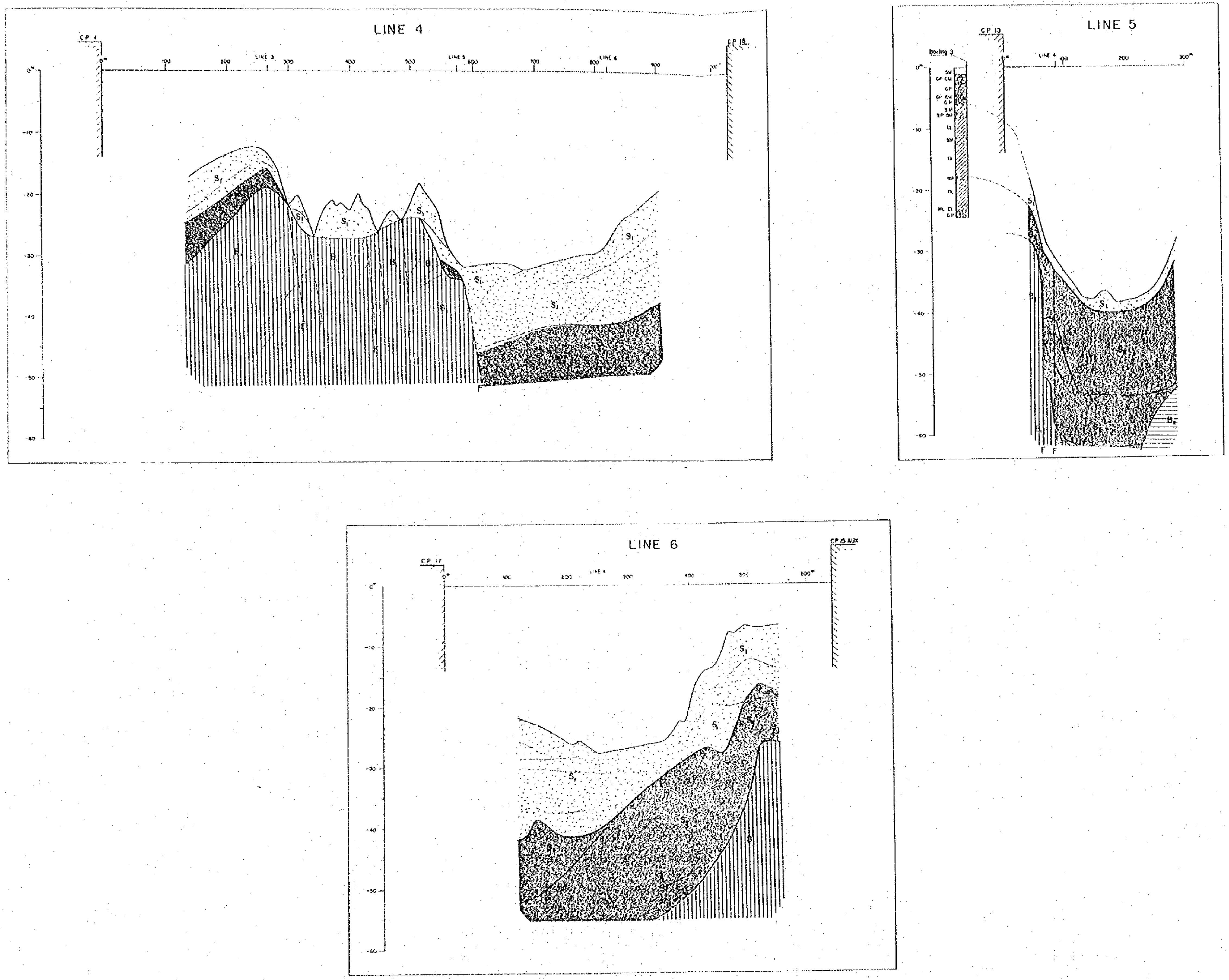

Fig. II-2-27 (2) Cross Section of Geological Profiles in the Port Area of San Antonio

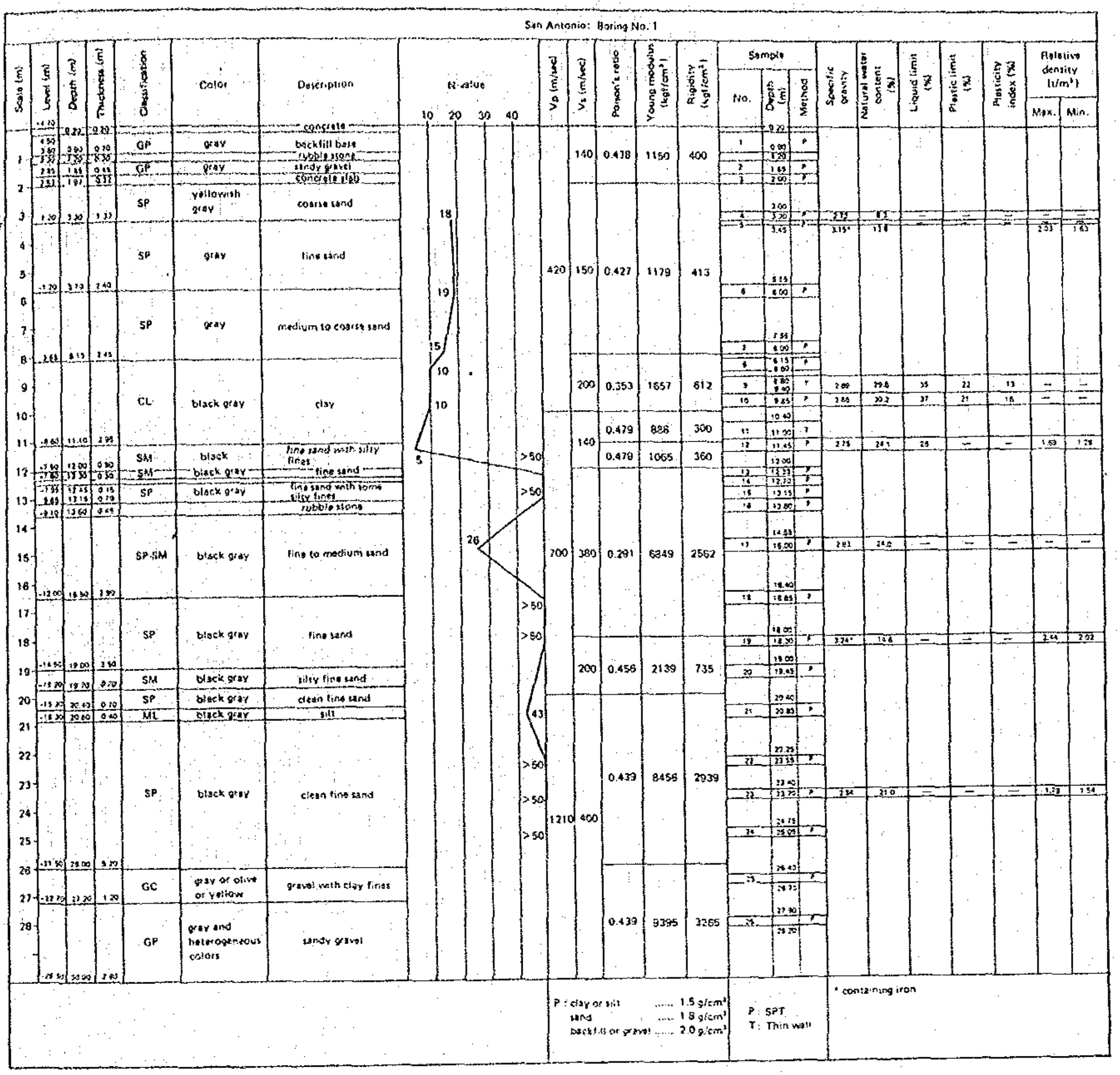

Fig. II-2-28 (1)   Boring Log at the Port of San Antonio

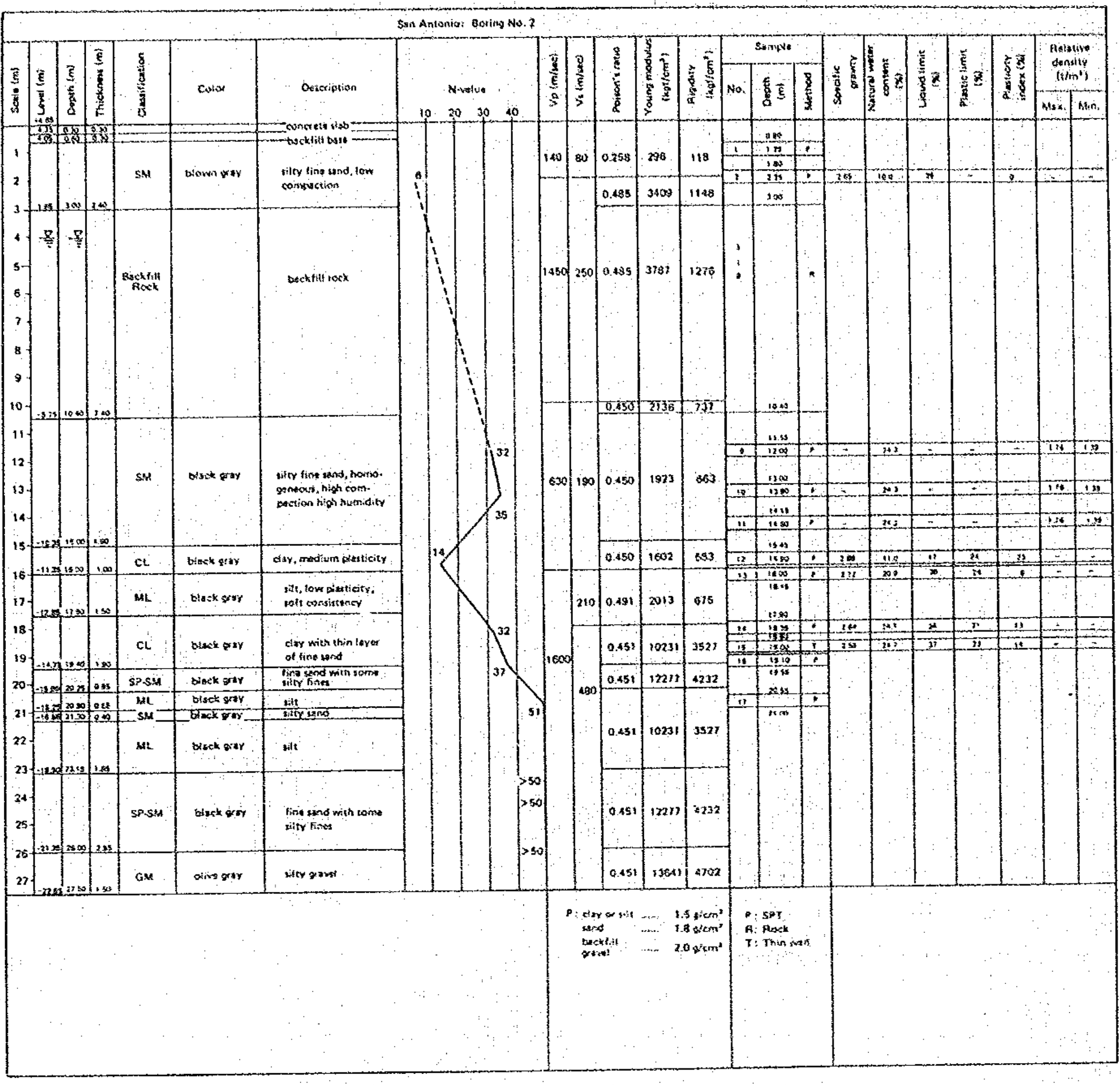

Fig. II-2-28 (2) Boring Log at the Port of San Antonio

San Antonio: Boring No. 3

Level (m)	Depth (m)	Thickness (m)	Classification	Color	Description
4.84					
4.64	0.20	0.20			
4.44	0.40	0.20			
2.14	2.70	2.30	SM	pale yellowish brown	silty sand
1.94	2.90	0.20	SP		
0.54	4.30	1.40	SM	pale brown gray	fine sand with of silty fines
-0.91	5.75	1.45	SM	black gray	fine sand with clots of silty fines
-2.36	7.20	1.45	GP-GM	yellowish brown	gravel with silty fines
-4.06	8.90	1.70	GP	pale brown gray	sandy gravel with some of silty fines
-5.06	9.90	1.00	GP-GM	yellowish brown	similar layer 5.75 ~ 7.20
-5.71	10.55	0.65	GP	pale brown gray	similar layer 7.20 ~ 8.90
-5.81	10.65	0.10			
-7.16	12.00		SM	black gray	fine sand with clots of silty fines
-7.86	12.70	0.70	SP-SM	gray	medium sand
-11.11	15.95	3.25	CL	black grey	clay
-12.16	17.00	1.05	SM	black gray	silty very fine sand
-17.46	22.30	5.30	CL	gray	clay
-17.96	22.80	0.50	SM	black gray	silty very fine sand
-22.16	27.00	4.20	CL	black gray	clay
-22.96	27.80	0.80	ML-CL	black grey	clayed silt
-24.16	29.00	1.15	GP	gray or green	clean gravel

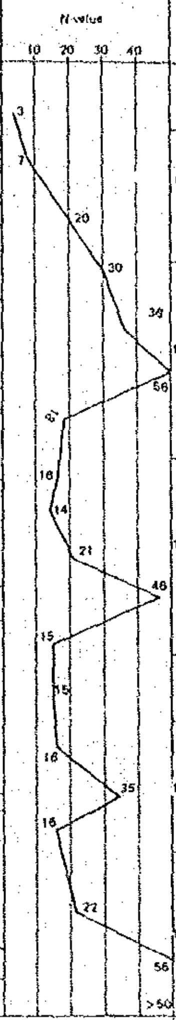

Vp (m/sec)	Vs (m/sec)	Poisson's ratio	Young modulus (kgf/cm²)	Rigidity (kgf/cm²)
230	120	0.313	695	264
650	180	0.458	1736	595
1000	220	0.475	2913	988
		0.475	2622	889
1500	310	0.478	5217	1765
		0.478	4347	1471
	210	0.490	2414	810
		0.490	2012	675
670		0.446	1951	675
1140	360	0.438	6354	2210
		0.438	7625	2651
		0.438	6354	2210
1600	450	0.457	9032	3099
		0.457	12043	4133

Sample			Specific gravity	Natural water content (%)	Liquid limit (%)	Plastic limit (%)	Plasticity index (%)	Relative density (t/m³)	
No.	Depth (m)	Method						Max.	Min.
	0.90								
1	1.25	P							
2	1.75	P	2.78	11.8	26	22	4	–	–
	2.45								
3	3.00	P							
	3.90								
4	4.35	P	2.64	15.8	–	–	–	–	–
5, 6	4.55	P	2.78	21.2	–	–	–	1.81	1.45
	5.60								
7	6.05	P							
8	6.50	P							
	7.80								
9	8.25	P							
	9.05								
10	9.50	P							
	10.10								
11	10.55	P							
13		P	2.64	29.3	–	–	–	–	–
	11.00								
	12.30								
14	12.75	P							
	13.35								
15	13.80	P	2.87	36.1	47	23	24	–	–
	14.20								
16	14.80	T	2.66	38.1	83	26	37	–	–
17, 18	15.25	P							
19	15.95	T							
20	16.40	P							
	17.40								
21	17.85	P							
	18.20								
22	18.80	T	2.66	36.8	58	25	31	–	–
23	19.25	P							
	20.55								
24	21.00	P							
	22.05								
25	22.50	P							
26	22.80	P							
27	23.05	P							
	23.50 23.80								
28	24.40	T							
	25.60								
29	26.05	P							
	27.00								
30	27.45	P							
	28.15								
31	28.60	P							

Note:

0.00 ~ 0.20 : concrete slab

0.20 ~ 0.40 : backfill of pavement base material

2.70 ~ 2.90 : thin layer of clean fine sand, brown gray, soft compaction

10.55 ~ 10.65 : thin layer of very fine silty sand, medium compaction

P: clay or silt ...... 1.5 g/cm³

sand ...... 1.8 g/cm³

gravel ...... 2.0 g/cm³

P: SPT

T: Thin wall

Fig. II-2-28 (3) Boring Log at the Port of San Antonio

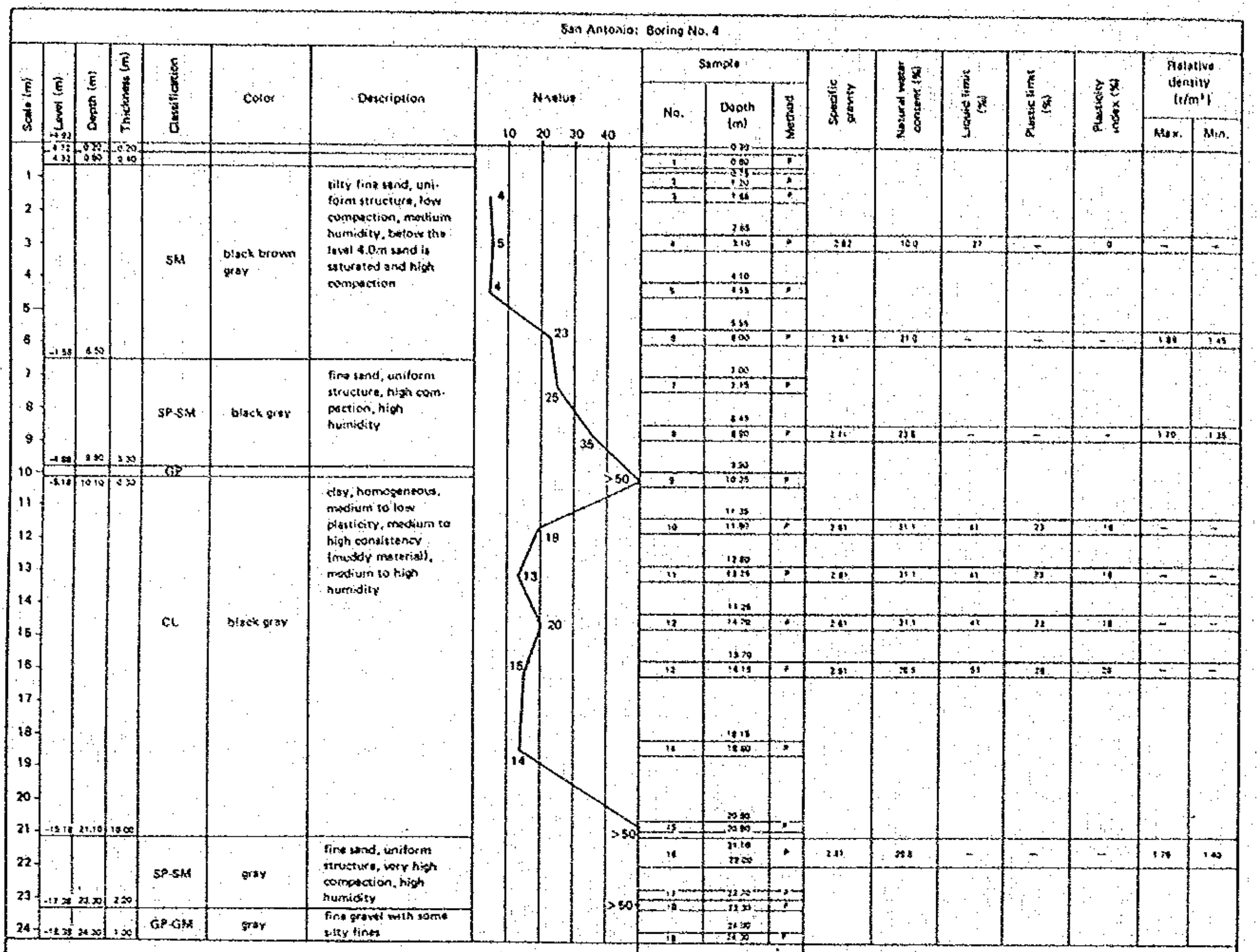

Note:

0.00 ~ 0.20 : concrete slab
0.20 ~ 0.80 : material of pavement base
9.80 ~ 10.10 : thin layer of sandy gravel with clayed fines of low plasticity

P : SPT

Fig. II-2-28 (4) Boring Log at the Port of San Antonio

Table II-2-12 Cycle Triaxial Test Result

Boring No.	Number of Cycle Nℓ	Cycle Stress Ratio Rℓ	Relative Density Dr	Remarks
No.1	61.0	0.14	50	●$_1$
	21.0	0.20	50	●$_1$
	1.0	0.25	50	▲$_1$ Omit
	6.5	0.25	65	▲$_1$
	1.0	0.31	68	○$_1$ Omit
	0.5	0.42	68	○$_1$ Omit
No.2	78.0	0.15	50	●$_2$
	4.5	0.37	50	●$_2$
	26.5	0.25	50	▲$_2$
	12.0	0.31	50	▲$_2$
	38.5	0.23	68	○$_2$
	14.5	0.30	68	○$_2$
	4.0	0.40	65	○$_2$
No.3	14.0	0.15	50	●$_3$
	2.0	0.37	50	●$_3$
	5.0	0.25	50	▲$_3$
	5.0	0.30	50	▲$_3$
	13.5	0.20	67	○$_3$
	6.0	0.30	60	○$_3$
	1.0	0.40	67	○$_3$ Omit

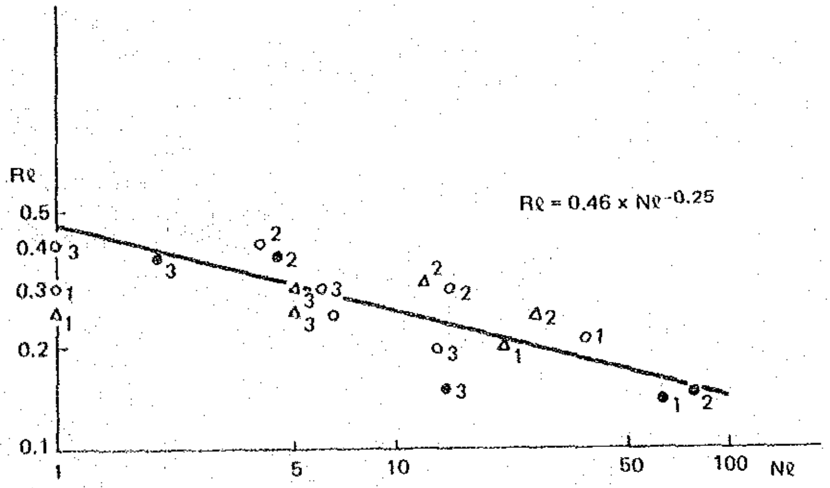

Cycle Stress Ratio vs. Number of Cycles